MSC thesis in Sustainable Energy Technology

The Potential of Thermal Energy Storage in combination with District Heating to deliver Winter Peak Load

Jessy van Eesteren
2022

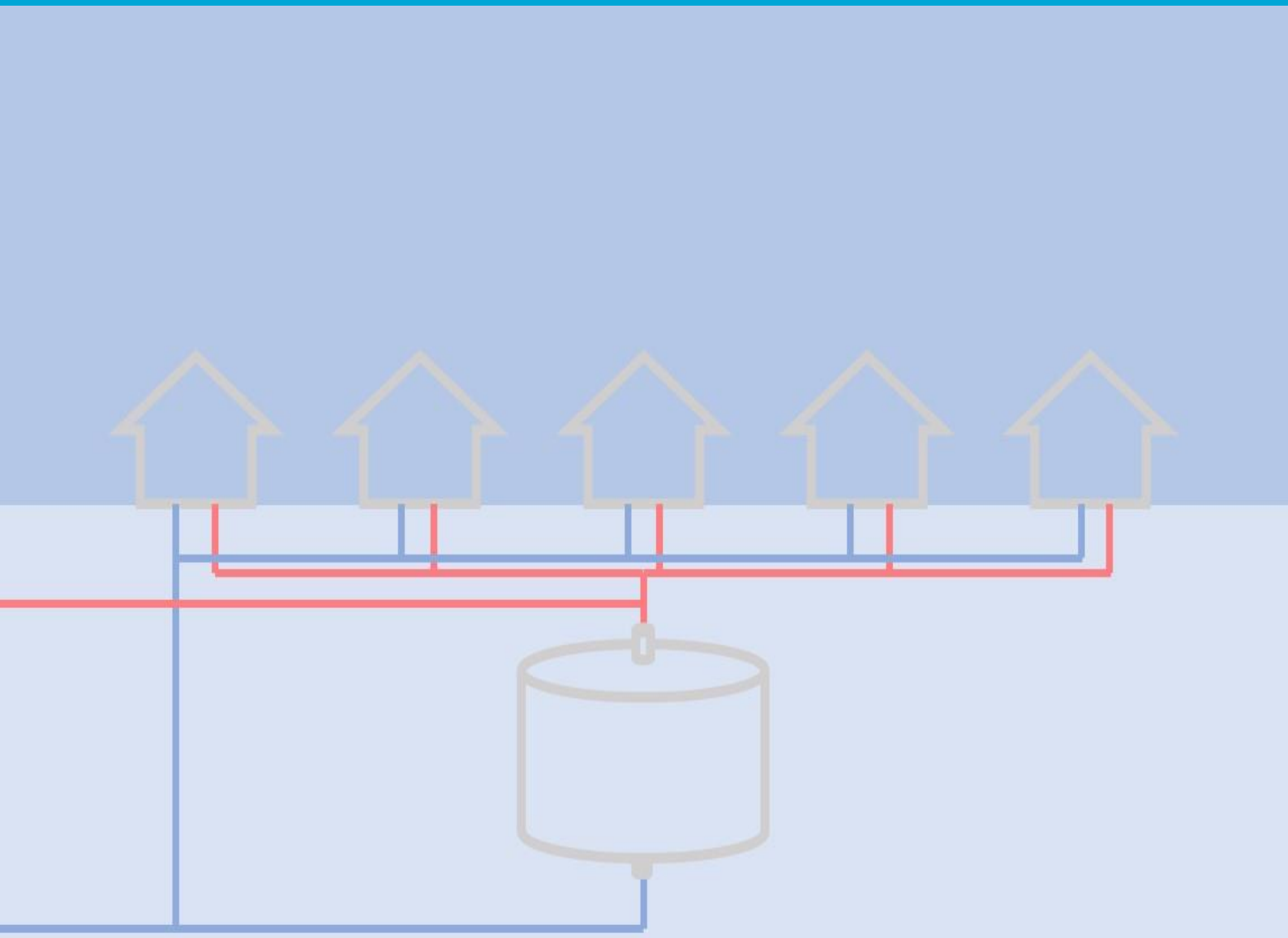

TU Delft

EQUANS

MSc thesis in Sustainable Energy Technology

The Potential of Thermal Energy Storage in combination with District Heating to deliver Winter Peak Load

Jessy van Eesteren

April 2023

A thesis submitted to the Delft University of Technology in partial fulfillment of the requirements for the degree of Master of Science in Sustainable Energy Technology

The Potential of Thermal Energy Storage in combination with District Heating to deliver Winter Peak Load

Thesis report

by

Jessy van Eesteren

Thesis committee:

Chair:	Dr. E.M.Kelder
Supervisors:	Dr. M. Bloemendal
	Prof. T. Vlugt
External Supervisor:	Ir. Sanne Buisman
Place:	Faculty of Electrical Engineering, Mathematics and Computer Science, Delft
Project Duration:	September, 2022 - April, 2023
Student number:	4468554

Abstract

District heating networks (DHN) in the Netherlands have the potential to supply sustainable heat but are currently designed to deliver around 80 % of the heat from a sustainable source. The peak demand is delivered with a gas boiler because of flexibility and costs. With the share of DHNs increasing in the Netherlands and the goal to be CO_2 neutral by 2050, a replacement for gas boilers in DHNs has to be found. This research evaluates the potential of seasonable thermal energy storage to supply the peak load in small-size DHNs in the Netherlands.

The research consists of 3 steps. First, the key performance indicators (KPIs) of the implementation of STES in DHNs are determined and the technologies with the most potential per seasonal thermal energy storage (STES) category (sensible heat storage (SHS), latent heat storage (LHS) and thermo-chemical energy storage (TCES)) are determined. Then a Matlab model is developed to determine the volume, storage losses and total efficiency of the three selected technologies. Multiple scenarios are defined to evaluate the technical and financial potential of STES in different situations and configurations. Lastly, the STES are assessed on their potential to be integrated into a DHN to supply peak demand by analyzing investment costs, operating costs, volume, storage losses, and total efficiency. Throughout the research, a gas boiler is used as the reference scenario.

The models developed in the research are validated and can be used in specific case studies to determine the necessary volume of the STES, temperature profile throughout the year in the STES, mass flows and temperature of the supply HTF to the DHN, and the total losses of the STES, using the heat demand of the DHN, the HTF, the PCM, the reactant, the shape of the tank, the insulation thickness an material and the heat supply of the source. With the outputs of the developed models, the costs can be calculated. The output of the model and the costs can be used to select the optimal STES to be implemented in the DHN of that specific case study.

This research shows that SHS is most feasible to be integrated into a small-size district heating network to deliver winter peak load in the existing built environment regarding volume, CO2 emissions, and costs.
A buried tank with water as the storage medium and heat transfer fluid (HTF) is selected as the technology with the most potential within SHS. For LHS, Paraffin is selected as phase change material (PCM) and water as HTF. For TCES, potassium carbonate is selected as the reactant.

Preface

This research was written to fulfill the graduation requirements to obtain the degree of Master of Science in Sustainable Energy Technology at the Delft University of Technology. This study was performed in collaboration with Equans and the TU Delft.
First I would like to thank Sanne Buisman, my supervisor from Equans. I enjoyed our meetings in which she helped me with valuable input for the approach and finishing of the research problem.
Second, I want to thank Martin Bloemendal for our weekly meetings in which he helped me with critical input on the content of my research and thesis process.
Furthermore, I want to thank Erik Kelder for his supervision and guidance.
Lastly, I want to thank Thijs Vlugt for being part of my thesis committee and for their interest in my work.

Contents

List of Figures

List of Tables

Acronyms

ATES Acquifier Thermal Energy Storage
BTES Borehole THermal Energy Storage
CAPEX Capital Expenditure
COP Coefficient of Performance
DHN District Heating Network
HP Heat Pump
HTF Heat Transfer Fluid
KPI Key Performace Indicator
LCOE Levelized Costs of Energy
LHS Latent Heat Storage
OPEX Operational Expenditure
PCM Phase Change Material
RES Renewable Energy Source
SHS Sensible Heat Storage
STES Seasonal Thermal Energy Storage
TCES Thermo-chemical Energy Storage
TES Thermal Energy Storage
TRL Technology Readiness Level
TTES Tank Thermal Energy Storage

1 Introduction

In 2015 the Paris Agreement was signed by the United Nations with the goal to "limit global warming to well below 2, preferably to 1.5 degrees Celsius, compared to pre-industrial levels" [3]. The legally binding international treaty determined this maximum temperature rise in order to achieve a climate-neutral world by reducing the emission of CO_2. A climate-neutral world is necessary in order to mitigate climate impacts, which have proven to be caused by "anthropogenic carbon dioxide emissions and consequent global warming" [1]. Climate impacts related to temperature rise are extreme weather events, reduced water availability, reduced agricultural yields, sea-level rise and risk of coral reef loss [59]. Climate impacts will increase when the temperature rise will continue [2].

The Netherlands has established agreements about reducing greenhouse gasses (GHG) in the climate agreement. This agreement states that Dutch households must be energy neutral by 2050 [4] while the expected primary energy use will grow by 48 % by 2040[57]. In the Netherlands, the built environment accounts for one-third of the total energy consumption of which 70% of the energy is used for heating [40]. This means 25 % of the total energy use is necessary for the heating of the built environment. Currently, Dutch households have natural gas as the main source of heating which equates to nine percent of the emission of GHG in the Netherlands [5]. District heat networks (DHN) can provide heat from sustainable heat sources to households eliminating natural gas as the main heating source. These sustainable heat sources are scaled to provide 80 % of the heating demand because it is not economically efficient to also provide the peak demand with these sources. The most important source of remaining GHG emissions in such networks in order to provide heating for the peak loads is the burning of natural gas, which can lead to 70 % of the emissions of the total system [24]. While the peak load in this system accounts for 20 % of the system's total energy. Various studies show that at this moment multiple possibilities for sustainable DHNs are developed [69][56][41][29][42][62][24]. These studies focus on base loads. The possibilities to replace the usage of natural gas to cover the peak load are also researched, but not one clear alternative is yet discovered [13] [35] [55].

1.1 Research Objectives

The aim of the research is to assess the technical feasibility of a seasonal thermal energy storage (STES) system integrated into a DHN in order to supply the heat demand during peak load in combination with a sustainable energy source. The integration of STES to supply the peak load of DHN charged with a sustainable energy source can reduce 70% of the total GHG emissions of the system compared to the base scenario where the peak load is supplied with a gas boiler. The scope of the research is a small-size DHN, which consists of 200-1000 households with houses in the existing built environment and therefore having a medium level of insulation. Equans expects the number of these types of DHNs to increase most in the near future. The supply temperature of the DHNs consisting of houses with

little insulation is 70 °C and the return temperature is 40 °C. The main research question is:

- What seasonal thermal energy storage technology is most feasible to be integrated into a small-size district heating network to deliver winter peak load in the existing built environment regarding volume, CO_2 emissions, and costs?

In order to answer the research question, sub-research questions have been formulated as follows:

- What seasonal thermal energy storage technology categories have the most potential to be implemented in a small-size district heating network to supply winter peak load in the existing built environment?
- What are the important characteristics of the selected seasonal thermal energy storage technologies and how can this be modeled?
- What is the optimal design for the selected seasonal thermal energy storage technologies in the base scenario?
- What are the volumes and costs of TES to deliver peak load in a DHN with 200 households?
- What is the influence of demand, height, insulation, maximum storage temperature, the absence of a heat pump and interim charging on the volume of the seasonal thermal energy storage technologies?

1.2 Outline of the Report

In order to answer the research questions, the report is organized as follows. First, a literature review is executed in Chapter 2 in order to determine the possible STES technologies that can be integrated into a small DHN. Many STES systems exist that are based on different storage technologies and that have different advantages and disadvantages when used in certain applications. It is, therefore, necessary to first conduct a broad review of all the STES that exist and select which technologies can be applied in combination with a DHN. From the literature review, the KPIs (key performance indicators) of STES integrated into a small DHN will be selected in Section 2.4 and the technologies with the most potential will be determined in Section 3.2.1, Section 3.2.2 and Section 3.2.3. Secondly, the KPIs are important to select in order to narrow the selection of suitable STES technologies and to determine what parameters affect the design of the STES in the models. An optimal basis design will then be made per STES technology selected of which a model will be made in Section 3.3.3, Section 3.3.2, and Section 3.3.4. The STES systems selected from the literature review vary in working principles but will be modeled with the same base model, described in Section 3.3.1, in order to be able to compare the results. All models consist of a tank that can function as a storage tank or a plug-flow reactor.
The models will be validated in Section 3.4 and then the description of the scenarios that will be simulated are given in Section 3.5.
Chapter 4 will provide the results of the simulations of the described scenarios. First, the GHG emissions, energy supply, and operating costs for the base scenario where peak load is provided with a gas boiler will be determined in Section 4.1. Then, with the models, the volume, losses, efficiency, and heat supply to the STES technologies will be calculated for

the base scenario in Section 4.2. The base scenario consists of the STES with the ideal design determined in Section 3.3.3, Section 3.3.2, and Section 3.3.4 and the load from a DHN with 200 households in the existing built environment from Section 3.1. After that, the influence of an increase and decrease in load on the volume of the STES technologies will be modeled in Section 4.3.1. The effect of a maximum and minimum height on the design and the volume will then be modeled in Section 4.3.2. After this, the effect on the volume of charging in between loads will be determined in Section 4.3.3. The effect of a decrease and an increase in maximum storage temperature on the volume will be determined in Section 4.3.4. The increase and decrease in insulation are evaluated in Section 4.3.5. Lastly, the effect of the absence of a heat pump on the total volume will be given in Section 4.3.6.
The influence of the scaling of the parameters on the costs is evaluated in Section 4.4.
From these scenarios, the potential of the integration of STES into a DHN with a sustainable heat source to deliver winter peak load in the existing built environment regarding volume and operating costs will be determined.
After the results, an evaluation and discussion of the results with further recommendations will be provided in Chapter 5. Lastly, a conclusion will be given in Chapter 6.

2 Literature Review

2.1 District Heating Networks

The objective of this section is to describe the working principles of DHNs and to determine the boundary conditions of heat sources connected to small-scale DHNs for the existing build environment. A small-scale DHN consists of 200-1000 households. The research is focused on small-scale DHNs because most growth in the development of these size networks is expected in the existing built environment by Equans. The existing built environment consists of houses with little insulation resulting in high peak heat demand, a supply temperature of 70 °C, and a return temperature of 40 °C.

2.1.1 Background Information

DHNs are systems that distribute heating or cooling from one central source to multiple users. The system is built up of pipes that deliver heat by circulating liquid water or low-pressure steam. The receivers can be industrial, commercial, or residential users, but they need to be located in a relatively small area. The reason for the necessity of the receivers to be close to each other is the losses in the DHN that make the system inefficient if the distance that the heat needs to be transported becomes too large.

DHNs in Europe all have different heat capacities, pipeline lengths, ancillary equipment, and sources. The networks are all designed with different design demands, resulting in different operating pressure, temperature, ancillary equipment like heat pumps, efficiencies, insulation, heat source, and direct or indirect system designs. In Europe 10 % of the heating demand is delivered by heating networks with 4174 systems. In Denmark and Sweden more than 50 % of the heating demand is provided with heating networks [43]. In the Netherlands currently, only 4 % of the households are connected to heating networks [67].

DHNs can have different sizes. Small DHNs, often in rural areas, can be a couple of kilometers long providing heat by using biogas or wood in combination with a combined heat and power plant. Large systems are often situated in cities and consist of a maximum of hundred kilometers. These systems often do need substations to provide extra heating. Micro heating systems are also built. These systems often have a heat pump that needs a stable heat source.

The temperature in a heating network can vary from 30 °C to 150 °C. Traditionally high temperature heating networks run on fossil fuel heat sources and have temperatures from 120 °C to 150 °C. The advantages of these networks are the possibility to directly supply heat to consumers without extra equipment to upgrade the temperature and the necessity of only a few heat sources with high capacity instead of more heat sources with lower capacity. The reason for the high temperatures was the possible increase in efficiency and decreased operating costs. The disadvantage of high-temperature networks is the higher thermal losses and

the higher installment costs of the pipe network. The temperature in these heating networks would be 120-150 °C in a steam-based system. Pressurized high or medium-temperature water systems have been developed later and can have temperatures of respectively more than 100°C or less than 100°C. The last developed DHNs have temperatures from 30-70°C. These systems have fewer losses and are often combined with low-grade and RES in combination with heat pumps. Low-temperature DHNs, which have a supply line temperature of 50-55°C or 60-70°C with return temperatures of 25-40°C, can be used to supply heating and tap water in new, well-insulated buildings[58].

Different heat sources can supply the DHN with different temperatures. Figure 2.1 gives an overview of different heat sources for DHNs and their working temperatures. Figure 2.1 shows that low-temperature DH can be combined with more RES. Low-temperature DHNs also have less high pressure to endure within the pipelines, making their use more durable.

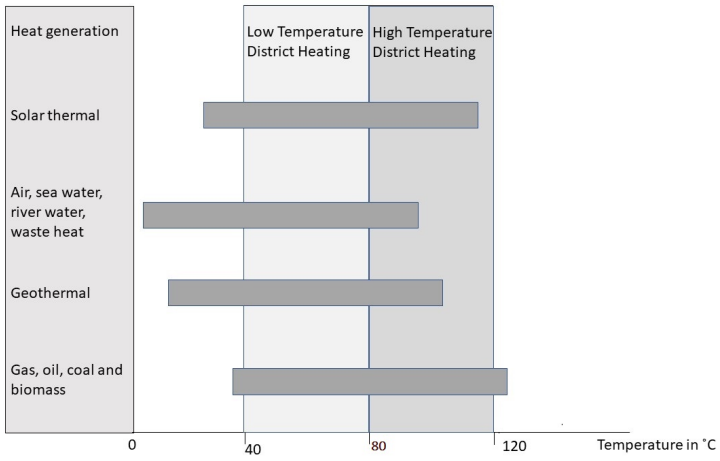

Figure 2.1: *The temperature range of different heat sources related to the operating temperatures of district heating networks[58]*

2.1.2 Sustainability of District Heating Networks

The sustainability of a DHN highly depends on the source of the heat that supplies the network. There are multiple sources possible to supply the heat for a low-temperature DHN:

- nuclear power [64]
- cogenerated heat[36]
- biomass gassification [69]
- a plant using fossil fuels [58]
- renewable thermal energy including solar thermal energy[29]
- geothermal energy [24]

- waste heat from industry [62]
- waste heat from data centers or burning waste[42]

The sources of heat for DHNs are divided into renewable energy sources (RES), fossil fuels, and hybrid sources. At this moment natural gas is a common energy source for DHNs because it is cheaper and has relatively low emissions compared to other fossil fuels. However, the share of renewable heat sources in heating networks is increasing. A technology that shows a lot of potential is biomass gasification. In combination with producing heat, it produces feedstocks and downstream fuel alternatives like methanol, synthetic natural gas (SNG), and Fischer–Tropsch diesel. Wetterlund et al. explain that in these processes so much extra heat is generated that a DHN could be connected to increase the overall efficiency[69]. Another technique that is used more and more is cogeneration (CHP), which has a fuel efficiency of at least 90 percent because of the co-production of electricity and usable heat[36]. DHNs can greatly reduce the production of greenhouse gasses when a sustainable heat source is used. When geothermal energy is used in comparison with a boiler the CO_2 production is ninety percent lower[24]. Furthermore, DH can replace less efficient equipment for individual heating systems. This, combined with a sustainable heat source, has so many environmental benefits that Rosen states it is a reason to pursue DHNs [56]. The high amount of energy demand divided over a lot of consumers gives DHNs a lot of opportunity to increase efficiency, reduce maintenance, reduction of greenhouse gas (GHG) emissions, and safe energy compared to the original heat supply[58].

2.1.3 Peak loads in District Heating Networks

DHNs have numerous advantages such as flexibility in source, availability for heating and cooling, contribution to reducing fossil fuels and therefore emitting fewer greenhouse gasses, efficiency, and environmental and economic benefits when applied correctly. As Rezaie states: ”District energy can provide efficiency, environmental and economic benefits to communities and of energy consumers”[55]. However, their disadvantage is that they must often be used in combination with ancillary equipment like heat pumps or absorption chillers used for air conditioning and with other systems to supply the peak load[24]. Figure 2.2 displays the load profile of a typical residential consumer in a DHN. HP means heat pump in this case but can be replaced for any type of base load-producing technique such as geothermal heat or waste heat from data centers for example. It is visible that in winter only part of the load can be supplied by the source. This is the case because the heat source for DHNs is built to provide around 80 % of the total energy demand of the consumer. The capacity is not large enough to provide heat during the peaks because designing a system that has the capacity to supply the peaks would be too expensive. The peaks account for around 20 % of the total heating energy but the capacity needed to supply these peaks could be several times the designed capacity. Therefore the peak demand is still provided by gas boilers.

Another factor that plays a role in the mismatch of the energy supply in the system and the energy demand pattern is the abundance of RES in summer as is visible in Figure 2.2. This energy can be used in winter if long-term storage would be applied. Lund states: that the combination of low-heat sources such as waste heat, waste incineration, power plant waste heat, and geothermal energy with Thermal Energy Storage (TES) can be applied to low-energy buildings. [41]

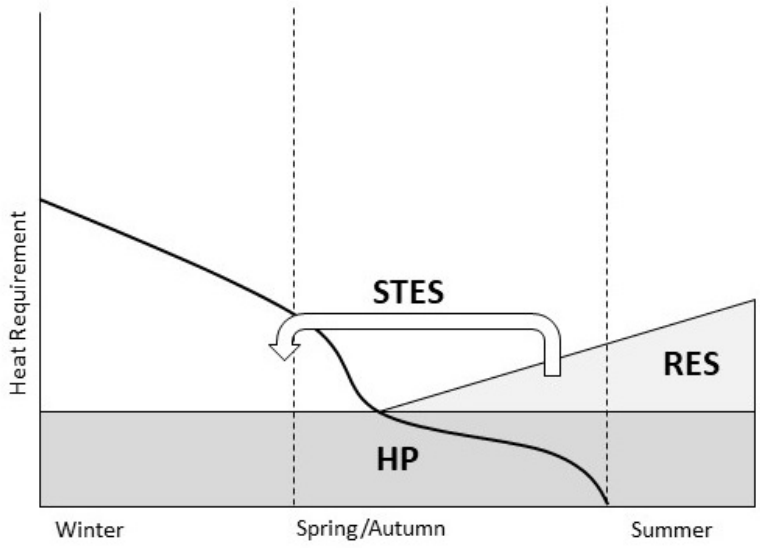

Figure 2.2: *Working principle of Seasonable thermal energy storage in district heat networks with a heat pump and renewable energy sources.[58]*

2.1.4 Economical Aspects of District Heating Networks

Economically DHNs can be competitive with independent heating systems, but only in certain business cases. As stated by Rezaie: "Providing energy services with renewable energy via such a central system can be simpler and less expensive compared to utilizing renewable energy directly in each individual residential building." [55] Without taking the externalities of heating systems into account, DHNs can compete economically if the heat demand is high and centralized in a small area. When externalities are taken into account with for example fossil fuel taxation or a CO_2 tax, DHNs are financially profitable without government support.

2.1.5 District Heating and Thermal Energy Storage

Energy storage can be seasonal or diurnal[25]. Both are necessary to cover peak demand in DHNs in order to cover the daily variations and the seasonal shortages and abundances. The principle of diurnal and seasonal storage is the same, however seasonal storage is more complex and therefore costly. Another difference is the storage temperature. Short-term storage often can be executed at a high temperature making it suitable for direct use in combination with a DH while long-term storage has lower temperatures and therefore needs extra equipment to upgrade the temperature before it can be used in a DHN. TES is at this moment mostly used in combination with solar thermal systems. Another application such as TES is the thermal mass of building structures[34]. However, the greatest potential for the usage of TES in the energy transition lies in the combination of TES and DHNs. DHNs and TES can be used in combination with heat pumps, hybrid systems, and energy management

software in order to reduce energy consumption, increase energy efficiency, energy security, reduction of costs, and benefit the environment by the reduction of GHG emissions.

DHNs can play an important role in the energy transition by implementing RES such as solar, and geothermal energy in combination with heat pumps, waste heat, and CHP plants and connecting prosumers and consumers into the heating network. However, DHNs have two shortcomings. The first shortcoming is the mismatch between supply and demand and the second shortcoming is the physical distance between supply and demand creating losses. TES can be used to equal the supply with the demand by making the system more flexible and therefore increasing efficiency. [35]

The demand varies daily and annually. Furthermore, renewable energy production also has an intermittent pattern. TES can absorb energy when the production is higher than the energy demand and emit energy when the demand is higher than the energy supply. TES must therefore be able to store energy for short-term variations and long-term variations.

Advantages and Disadvantages of the integration of District Heating and Thermal Energy Storage

The integration of TES into DHNs has physical, energetic, economic, and environmental advantages. The first example of a physical advantage is that TES increases the flexibility of the system to react to unexpected changes in energy demand. Furthermore, the integration of RES into energy production becomes easier because these sources are intermittent and therefore the energy produced needs to be stored in order to match the energy demand pattern. Another advantage of TES is the decrease in the installation of generation facilities. The generation capacity does not have to match the maximum load because the peak load can be covered with TES. When the DHNs function more efficiently because of TES, smaller transport pipes are necessary and the size of the network can increase. TES decreases the use of boilers and chillers because they can rapidly react to demand changes.

Energetic advantages lay in the improved efficiency of the system. First, the system can make use of the production units with the highest efficiency. Furthermore, since the efficiency of the system is improved and the transport pipes are smaller, the pumping efficiency is also higher. Lastly, energy security is higher because failures in the production system can be solved with the storage medium.

Economically there are also multiple advantages. First, there are lower user costs because of the higher usage of RES which has free supply. Furthermore, there are higher selling margins because of the possibility to store energy when there is an abundance and selling energy when there is a shortage. The is a decrease in investment cost for generation units because there are fewer generation units needed as described above. Pumping costs are lower because of the lower pumping efficiency. Maintenance costs for users are lower because there are no individual heating systems necessary anymore.

There are also environmental benefits of the combined system. The first environmental benefit is the reduction of emissions because of the increase in the usage of RES sources. Furthermore, there are fewer production units and fewer pumping units necessary which also decreases the emission of GHG. Lastly, chillers and boilers will not be necessary anymore which will also reduce the emission of GHG.

The integration of DHNs and TES also has some drawbacks. The TES investment costs are high. At this moment there is a lack of supportive legislation. Furthermore building the

storage facility does require space and the thermal losses during the storage of heat are also not negligible. Lastly, the design of the system is more complex than that of current systems.

Table 2.1 gives an overview of the advantages and disadvantages of the integration of DH and TES.

Table 2.1: *Advantages and disadvantages of the integration of thermal energy storage into district heating networks.*

Physical	**Energetic**	**Economic**	**Environmental**
Advantages			
Integration of RES into DHN	Higher production efficiency	Lower user cost	Reduction emissions because of integration of RES sources
Increase flexibility of the system	Higher pumping effficiency	Higher selling margins	Reduce emissions because of less production units
Decrease generation facility	Higher energy security	Reduce investment costs (generation units)	Reduce emissions by decreasing pumping
Smaller transport pipes		Reduce pumping cost	Less emissions by boilers and chillers
Increase size of DHN		Reduce maintanence cost for users	
Less use of boilers and chillers			
Disadvantages			
Volume of the storage facility		High investment cost for TES	
Thermal losses during storage		Lack of supportive legislation	
System complexity			

Advantages and Disadvantages of TES compared to other Storage

Other types of storage possible in combination with DHNs are for example electricity or hydrogen storage that can later be used to generate heat. There are multiple advantages of TES compared to other types of storage such as batteries, compressed air energy storage (CAES) and pumped hydroelectric energy storage (PHES). TES is less expensive than the average electrical storage system. TES has investment costs between 0.5 to 3 €/kW while an average electrical storage system has investment costs of around 170 €/kW. Another advantage is that TES does not have round-trip losses which hydrogen, PHES and CAES do have. Their round-trip efficiencies are 85 % and 65%. TES also has a longer lifetime and a more stable capacity compared to electrical storage. However, electrical and hydrogen storage do not have thermal losses.

2.1.6 Conclusions on District Heat Networks and the integration of Thermal Energy Storage into District Heating Networks

DHNs can supply heating to different types and amounts of consumers with different specifications. In this research, a small DHN (200-1000 households) will be researched in the existing build environment.

The temperature in a DHN depends on the type of consumers and the type of buildings. Industry requires higher temperatures than households. Furthermore, old buildings with less insulation require higher temperatures than new buildings. The industry needs supply temperatures of more than 100 ° C, while households require temperatures from 50-90 ° C depending on their insulation. The DHNs considered in this research have temperatures of 70 ° C. This is high enough to supply houses in the existing built environment that have medium insulation, but it is not too high because higher temperatures mean more losses.

The combination of seasonal thermal energy storage (STES) with a renewable energy source to supply heat in a DC network has the potential to play an important role in the energy transition by reducing carbon emissions and increasing energy efficiency. Many different sources in combination with DHNs are possible and some examples are geothermal energy, combined heat and power plants, solar thermal energy, biomass plants, or waste heat from different sources. The renewable heat source is usually built to cover 80 % of the heating demand in order to make the system economically viable. The peak demand, which accounts for the remaining 20 % of the energy is still supplied with gas boilers. When DHNs are fed with a renewable energy source the STES can absorb energy when there is abundance and supply energy when there is a shortage, resolving the mismatch in supply and demand. DHNs and TES can be used in combination with heat pumps, hybrid systems, and energy management software in order to reduce energy consumption, increase energy efficiency, energy security, reduction of costs and benefit the environment by the reduction of GHG emissions. At this moment no economically favorable concept has been developed to replace these gas boilers, but research shows STES has potential. The potential of the implementation of different STES technologies in combination with a DHN differs per situation and the selection of the suitable STES technology is therefore very important.

2.2 Seasonal Thermal Energy Storage

This chapter will provide background information on the duration of storage of STES, the applications of STES in combination with DHNs, and the types of STES and their parameters.

TES is the capture and storage of energy in the form of heat in order to be released and used at a later moment in time. Different technologies can be used to store thermal energy. Examples of these technologies are water tanks, material mass in combination with heat exchangers, boreholes, aquifers, eutectic systems, phase change materials, and chemical reactions. TES can be used in different time scales, from hours to seasons. TES is considered to have the potential to play an important role in balancing production and demand in the renewable electricity market and heating systems. TES can help to balance energy demand and supply on a daily, weekly, and even seasonal basis, presented in thermal systems. The advantages of TES, displayed in Table 2.2, are low energy demand, low carbon footprint, low cost, low maintenance cost, low GHG emissions, flexibility in operation, and high storage capacity per kg. [22] Disadvantages are relatively low efficiency, relatively slow response time, and thermal losses in standby mode (during storage time). [31]

Table 2.2: *Advantages and Disadvantages of thermal energy storage [27] [35]*

	Advantages	**Disadvantages**
Sensible heat storage	-High temperature range (50°C to 400 °C) -Long life span -Low cost materials -Available materials -Thermally stable at high temperatures	-Short storage period (losses) -Reduced storage density -No stable temperature during charge and discharge
Latent heat storage	-Non toxic material -Stable temperature during charge and discharge -High specific heat of materials	-Low temperature range (20°C to 80°C) -Short storage period (losses) -Medium storage density -Short life span -Low thermal conductivity -Organic phase change materials are flammable -Inorganic phase change materials are corrosive
Thermo-chemical heat storage	-High temperature range (20°C to 200 °C) -Long storage period -High storage density -No thermal loss	-Short life span -High cost -Low reliability -Possible toxicity -Recycling is difficult

2.2.1 Thermal Energy Storage Applications in the Energy Transition

One possible important application for TES is the management of peaks in DH. The share of renewable energy in energy production is increasing.[38] This leads to the necessity for more storage systems as renewable energy often has intermittent sources that can't be controlled and which pattern does not match the demand pattern of the energy consumer. The energy transition from controlled energy production with fossil fuels to renewable energy causes mismatches between demand and supply. As half of the total energy use can be ascribed to heat [50], TES can play an important role in the energy transition. When TES is used no extra heat production systems have to be installed or used in combination with DHNs making the system financially more interesting and more environmentally friendly. TES can also be used to incorporate solar and wind energy into the production of heat or cold in combination with heat pumps and electric boilers. To conclude, TES can also reduce peak demand, energy consumption, CO2 emissions, and costs; while also increasing the overall efficiency of energy systems." [25]

2.2.2 Duration of Storage

Another important parameter for TES is the duration of the storage. TES can be used for short-term or for seasonal storage. Short terms storage is used in DHNs for daily balancing and examples of short-term storage are tanks storing a liquid with different temperatures and thermal inertia of buildings. Short-term TES can be divided into pressurized and atmospheric TES. Pressurized TES is mostly used in combination with high-temperature and large DHNs. The storage and the pipeline network function at the same pressure level in such a system and the TES system can be used as a pressurization vessel. Pressurized TES is an easier system than atmospheric TES. Atmospheric TES is mainly used for low-temperature DHNs and can also handle a lower temperature gap. Pressurized TES can handle a temperature gap of 50 ° C while atmospheric can only handle a temperature gap of 30 to 40 ° C. Since the TES medium and the pipelines do not have the same pressure, the system is connected indirectly. Pumps and valves are necessary to regulate the system. Atmospheric TES has lower investment costs than pressurized TES.

Long-term storage is necessary to account for seasonal demand changes. Solar energy is often combined with long-term storage to use the surplus of solar energy in summer to provide energy in the winter. Other possible combinations with long-term storage are waste heat and biomass plants. Long-term TES has two categories; direct usage and indirect usage. TES for direct usage has one medium that is used for heat transfer and storage and operates in low-temperature DHNs and with high storage temperatures. Indirect usage TES uses low-temperature storage in combination with ancillary equipment to upgrade the temperature such as a heat pump. Indirect usage TES is used on high-temperature DHNs.

Long-term TES systems are usually expensive to build, but they have a long lifetime of up to thirty years. Examples of long-term energy storage are tank and pit thermal energy storage (TTES and PTES), borehole thermal energy storage (BTES), aquifer thermal energy storage (ATES), Cavern Thermal Energy Storage (CTES), LHS. Storing biomass and other fuels can also be seen as long-term storage.

2.2.3 Centralised or Decentralised Thermal Energy Storage

TES can be centralized or decentralized. Centralized TES is used for large applications such as industrial plants, CHP plants, and renewable energy plants in combination with for example DHNs. Decentralized TES is used for small applications in domestic and commercial buildings.

2.2.4 Thermal Energy Storage Parameters

TES can be divided into three categories: sensible heat storage (SHS), latent heat storage (LHS), and thermo-chemical energy storage (TCES). SHS is the storage of energy in the mass of a material by increasing or decreasing its temperature while the material stays in the same phase. LHS is the heat released or taken up during the phase change of a material while the temperature of the material stays equal. TCES storage with or without sorption is the energy stored in chemical bonds on the surface of materials.

Parameters that are important to describe TES are the operating temperature, capacity, power, efficiency, cost, and storage time[27]. Table 2.3 gives an overview of the TES categories and important parameters. The operating temperature can be high or low, ranging from -18°C to over 175°C.

Table 2.3: *Parameters of sensible, latent and thermo-chemical energy storage[57]*

	Unit	SHS				LHS	TCES
Type	-	Water Tank	Pit	Borehole	Aquifier		
Container	-	Tank	Tank	-	-	Tank	Tank
Insulation	-	Yes	No	No	No	Yes	No
Storage Medium	-	Water	Water	Ground	Ground	PCM	Reactants
HTF	-	Water	Water	Water	Water	Water	Air or water
Heat Exchanger	-	No	Yes/No	No	No	Yes/No	Yes
Storage Denisity	kWh/m3	50	30-50	15-30	30-40	40-150	60-130
Costs	€/m3	30-500	30-500	50-150	40-100	50-500	100-5000
Costs	€/kWh	0.1-10	1-10	4-10	1-10	1-50	2-500
Power	MW	0.001-10	0.001-10	0.001-10	0.001-10	0.01-10	0.01-1
Efficiency	%	50-90	50-90	50-90	50-90	75-90	75-100
Storage Period	-	days-months	weeks-months	weeks-months	weeks-months	weeks-months	weeks-months

2.2.5 Sensible Heat Storage

SHS is used mostly for daily storage, but it can also be used for long-term storage. Different materials can be used for SHS, which are selected with the following parameters: heat capacity, density, and thermal conductivity. SHS is at a further research state, cheaper, and has been used a lot more than LHS or chemical storage. Furthermore, the advantages of SHS are that the method is cheap and does not involve toxic materials. However, the disadvantages

of SHS are the high volume, costly insulation layer, and possibly the pressurization system necessary.

SHS uses the change in temperature of the material in combination with its heat capacity to store heat.

$$Q_s = \int_{T_i}^{T_f} mc_p \, dt \tag{2.1}$$

The initial and the final temperature are given by T_i and T_f in °C. The m is the mass in kg. The specific heat is c_p in J/(kg K) and Q_s is the heat stored in Joules. The most used material for SHS is water because it has low costs and high specific heat. However, it can only be used until 100 °C in a liquid state. For higher temperatures oils, molten salts, and liquid metals are used. For SHS solid state thermal storage materials can also be used. These materials have high working temperatures, good thermal conductivity, and low cost. However, they have low specific heat and high thermal conductivity. Low specific heat results in larger storage volumes and high thermal conductivity can lead to good heat transfer and higher losses. Table 2.4 gives an overview of the most used materials for SHS.

Table 2.4: *Parameters of sensible heat storage materials[57]*

Medium	Temperature Range (°C)	Density (kg/m3)	Specific Heat (J/kg K)
Water	0-100	1000	4190
Sand-rock minerals	200-300	1700	1.3
Concrete	200-400	2200	0.85
Cast iron	200-400	7200	0.56
Cast steel	200-700	7800	0.6

Underground Thermal Energy Storage

Underground thermal energy storage (UTES) is a storage method where the material in the ground, which can be soil, sand, water, rocks, and clay stores the heat or the cold. The removal and addition of the energy are done through a heat transfer fluid (HTF) that flows through pipes in the ground. The pipes can be placed vertically and be called boreholes or the pipes are placed horizontally. The spacing of the pipes is important because placing the pipes too close together or too far apart will negatively influence the performance of the system. The rates of energy removal or addition from the ground to the system are determined by the arrays of the pipes and the heat transfer rates of the ground. Mass transfer can play a role in UTES systems when the ground is porous. Then evaporation and condensation will also play a role in these systems. UTES systems do not have insulation usually but the ground properties provide the insulation. Often the system is combined with heat pumps to upgrade the temperature provided by the ground. [57]

The most used UTES system is tank thermal energy storage (TTES). The insulated tanks are usually filled with water since water has a high specific heat, volumetric thermal capacity, and low cost. They can be placed above ground and underground. The temperature range, which plays an important role in the amount of heat that can be stored in the tank, is

determined by the process and the vapor pressure of the liquid. Furthermore, the insulation of the tank is important for high performance. An energy balance for the water tank is:

$$mc_p \frac{dt_s}{dt} = Q_u - Q_L - U_S A_S (T_i - T_a) \tag{2.2}$$

Where Q_u is the added heat, Q_L is the removal of heat, U_S is the heat loss coefficient of the storage tank and A_S is the storage surface area. Furthermore, T_a is the ambient temperature of the tank and t is the time. Integrating the energy balance using Euler gives the following equation that can be used to calculate the temperature of the tank at a certain moment in time. The temperature of the tank is relevant to calculate other quantities such as the stored heat.

$$T_s = T_i + \frac{\delta t}{mc_p}(Q_u - Q_L - U_S A_S (T_i - T_a)) \tag{2.3}$$

Water tanks that are used for district hot water storage have a volume of up to 500 L. These size water tanks are also used for short-term storage of solar energy in combination with DHNs. Large water tanks of up to thousands of m^3 are used for seasonal storage of solar energy in combination with DH. The larger the tank, the more efficient the heat storage because losses are related to an area that increases less quickly than the volume when scaling up. Heat pumps are often used in combination with these systems to upgrade the temperature. The efficiency of TTES goes up to 90%. However, the cost of the system is higher than that of other UTES systems, namely 139€/GJ[54].

Aquifer thermal energy storage (ATES) store cold and warm water in wells under the ground. Only water can be used as a storage medium in order not to pollute the ground. In winter the warm well is used to pump water to a heat exchanger and provide heat to the DHN before being pumped back to the cold well. In summer the opposite process happens. It is important that the heat extracted in winter is provided in summer to keep the system in balance. Layers such as clay provide insulation in the ground and stop the water from spreading to other layers. The thermal losses become less during the lifetime of the system because the ground heats up, therefore the efficiency of the system increases. Furthermore, the heat losses get smaller as the volume of the storage medium increases since the heat losses are dependent on the area, not the volume. The heat capacity of aquifers is around 30 to 40 kWh/m^3 and 1 m^3 of water takes up 2 to 3 m^3 of ground to store the energy. The advantage of aquifer storage compared to borehole heat exchangers is the higher power rates because of higher possible pumping rates. However, the areas where aquifer storage is possible are scarce because specific ground conditions are required. [48] In the Netherlands legislation prohibits high-temperature storage in aquifers. The maximal temperature of ATES in the Netherlands is 25 °C. Efficiencies can go up to 80 % and the costs are 14 €/GJ [54].

Borehole Thermal Energy Storage (BTES) works similarly to ATES but it does not make use of aquifers. BTES uses loops in the ground with an HTF to capture the heat stored in the ground. BTES only uses conduction while ATES uses conduction and convection. Therefore BTES needs bigger installations compared to ATES in order to achieve similar heat capacities. BTES systems reach efficiencies up to 90 % and cost 97 €/GJ. [54]

The last type of UTES is the cavern and the pit storage. These techniques make use of deep caverns to create water reservoirs in order to store energy. The technique works almost the same as water tanks with the difference that the heat loss mechanisms are different. The system works efficiently but has high investment costs and is only possible in certain locations because of the required specifications of the location.

Packed-Bed Storage

Packed-Bed energy storage uses particles to store energy that is added and removed with a fluid. The particles which are solid are usually rocks or pebbles and the fluid that is used is usually air. The fluid streams in one direction to remove heat and in the other direction to add heat. In this way, the bed heats up layer per layer and will only reach a uniform temperature when the system is fully charged. This system can't supply and receive heat at the same time. Calculations for this type of storage include numerical techniques which make them more complex.

2.2.6 Latent Heat Storage

LHS is the storage of thermal energy in the phase changes of materials. LHS has a higher energy density compared to SHS and the materials used for LHS are known as phase change materials (PCM). The thermophysical properties of specific heat and specific latent heat should be optimized in order to optimize the energy density and decrease the volume of the system. Another important aspect to be able to use a small storage volume is the change of volume during the phase variation. This volume change should be as small as possible to keep a stable and small system. Furthermore, a high thermal conductivity and high conductivity of the phase change material are necessary to optimize the storage system. Apart from thermo-physical properties, there are also kinetic and chemical properties to take into account. Chemical stability, no toxicity, (almost) no super cooling, no fire hazard, no toxicity, and compatibility with materials of construction are requirements for an LHS medium[57]. The last important aspect when selecting a PCM is the availability and the cost of the medium used in order to make the system economically feasible and economically advantageous.
An advantage of LHS is the temperature stability of the system during the phase change. Furthermore, LHS has fewer heat losses than SHS. LHS can also be easily decentralized. A disadvantage of LHS is that the system is more complex than an SHS system.

LHS is a combination of sensible heat storage in the material and heat storage in the phase change of the material. During the phase change, the temperature of the material stabilizes while heat is stored. After the phase change, the temperature of the material will rise again when heat is added and sensible heat is stored. The storage capacity of the LHS system is given by the following equation which partly corresponds to the equation of storage capacity of SHS[57]:

$$Q_s = \int_{T_i}^{T_m} mc_p \, dt + mf\Delta q + \int_{T_m}^{T_f} mc_p \, dt \tag{2.4}$$

$$Q_s = m(c_{ps}(T_m - T_i) + f\Delta q + c_{pl}(T_f - T_m)) \tag{2.5}$$

T_m is the melting temperature in °C, m is the mass of the PCM medium in kg, c_ps is the specific heat of the PCM between T_i and T_m in kJ/(Kg K), c_pl is the specific heat of the PCM between Tm and Tf in kJ/(Kg K), f is the melt fraction and Δq is the latent heat of fusion in J/kg[57].

LHS can have different types of phase changes. The phase change can be solid to solid, liquid to gas, or solid to liquid, and vice versa. The highest latent heat is in liquid-to-gas phase changes but the volume change is also very large making the storage of the PCM difficult. The most used phase change is solid to liquid. The latent heat of this process is still high and the volume change is very low. The energy densities of LHS can be four times higher than the energy densities of SHS. LHS can be used for long-term and short-term storage.

LHS materials can be classified on their type of phase change, type of material, and heat absorbing and desorbing capabilities[57]. Figure 2.3 gives an overview of the classification of PCMs. First, the classification between organic, inorganic, and eutectic is made. The advantage of organic material compared to inorganic material is that organic materials are not corrosive, have almost no undercooling, and are chemically and thermally stable. The advantage of inorganic material compared to organic material is their higher phase change enthalpy, higher thermal conductivity and they are not inflammable.

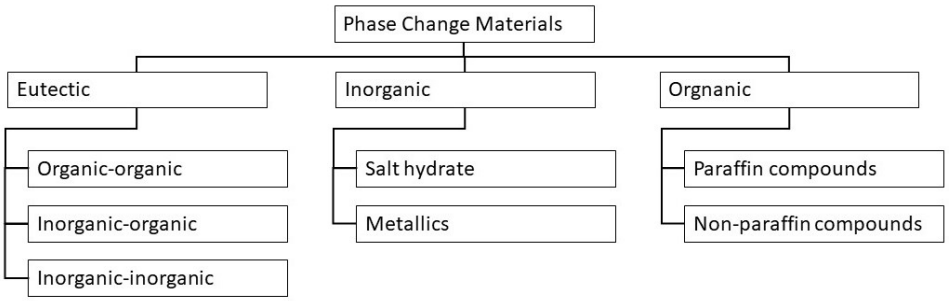

Figure 2.3: *Classification of phase change materials[57]*

The most used PCMs are paraffin, hydrated salts, fatty acids, and water. Table 2.5 gives an overview of these materials and their properties.

Table 2.5: *Parameters of phase change materials[57]*

PCM	Melting Temperatrue (°C)	Density (kg/m3)	Melting Enthalpy (kJ/kg)
Ice	0	920	333
Sodium acetate trihydrate	58	1300	250
Paraffin	-5-120	770	150-240
Erytritol	118	1300	340

Organic Phase Change Materials

Organic PCMs can be divided into paraffin waxes and non-paraffin compounds. Paraffin waxes are built up of straight chaines n-alkynes and the crystallization of the (CH_3) group releases heat[57]. The chain length of the (CH_3) groups determines the melting point and the latent heat of fusion. Usually, technical grade paraffin is used as PCM because of costs. Technical grade means that the material has the lowest quality and purity level. The advantages of paraffin are that they are safe reliable, predictable, cheap, non-corrosive and they have a large temperature range[60]. Non-paraffin compounds exist in many forms such as fatty acids, alcohols, glycols, and esters. The advantages of non-paraffins are the high heat of fusion and the inflammability. The disadvantages of non-paraffins are low thermal conductivity, low flash point, and instability at high temperatures[57].

Inorganic Phase Change Materials

Inorganic PCMs are mostly used for high-temperature applications in combination with solar thermal energy. Inorganic PCMs are more difficult to control than organic PCMs because they are less stable at high temperatures and at low temperatures they freeze. The advantage of inorganic PCMs is that their melting enthalpy does not change over time and they don't super-cool. The two main types of inorganic PCMs are salt hydrates and metallics. Salt hydrates can then be classified into congruent, incongruent, and semi-congruent melting methods. The hydrates consist of alloys of inorganic salts and water. The solid-liquid phase change of these materials is the hydration or dehydration of the salt.

$$AB * nH_2O = AB * mH_2O + (n - m)H_2O \tag{2.6}$$

AB are the alloys of inorganic salts and H_2O is water. Most of the salt hydrates have incongruent melting. This means that when the water is released the solid new compound does not dissolve but settles down at the bottom. The advantages of salt hydrates are the high latent heat of fusion, high density, high thermal conductivity, low corrosiveness, and compatibility with plastics [57]. Disadvantages are incongruent melting and supercooling.

Metallics are not as widely used because of their low melting enthalpy per weight. The advantages of metallics are their high melting enthalpy, high heat of fusion per volume, and high thermal conductivity.

Eutectics

Eutectic materials are a combination of two materials with the same melting and freezing point. Eutectics are not as widely used but have a lot of potential. Eutectics have high thermal conductivity, high density and they do not segregate. Furthermore, the ideal melting or freezing point can be obtained by changing the mixture of materials.

Phase Change Material Containment

PCMs need to be protected from interaction with surroundings in order to prevent changes in chemical composition. Therefore containment of the PCM in the liquid and solid phases is necessary. Other advantages are the increased compatibility with other materials in the storage system, increased hardiness, and a suitable surface for heat transfer[57]. Since the heat density of PCMs is usually higher than the heat density of other materials, the storage tanks need to handle higher heat transfer. Examples of PCM storage systems are bulk storage tanks, macro-encapsulation, and micro-encapsulation.
Encapsulation is often used in combination with a building cooling system. These systems can be based on chemical encapsulation, physic-mechanical encapsulation, or physic-chemical encapsulation.

2.2.7 Thermo-chemical Energy Storage

TCES is the least developed technology for TES. There are two main categories of TCES; TCES with sorption or TCES without sorption. Sorption is the capturing of a liquid or a gas into a material. Absorption is the capturing of a substance by a liquid and adsorption by a solid. Adsoption can happen with van der Waals forces of valency forces; respectively called physical adsorption or chemical adsorption.[39] The capturing and releasing of heat that happens in a reversible reaction is called thermochemical energy storage. When heat is supplied and thus captured by the chemicals, bonds are broken or formed depending on the reaction, and heat is stored. The reactive components from the reaction can then be stored separately and at a later time be put together in order to release the heat in the exothermic reaction. The materials used in these reactions are called thermo-chemical materials (TCM). The reversible reaction for energy storage is shown below.

$$A \rightarrow B + C + \Delta H_a \tag{2.7}$$

$$B + C + \Delta H_a \rightarrow A \tag{2.8}$$

Thermo-chemical Energy Storage Principles and Materials

The energy necessary for the adsorption or absorption reaction of a TCM consists of two parts. The energy that is necessary for the bonding of the working fluid and the sorbent and the energy necessary for the phase change of the working fluid. When this energy is added and the bonding energy barrier of the components is overcome, the working fluid is released in gas form. When the reactive components or working fluids are put together again, a discharge of entropy occurs which results in the release of heat. The energy balance for an adsorption or absorption reaction can be described in the following:

$$\Delta H_a = \Delta H_v + \Delta H_b \tag{2.9}$$

ΔH_a is the energy absorbed or released during the reaction, ΔH_v is the energy necessary for the phase change of the working fluid and ΔH_b is the bonding energy of the working fluid and the sorbent[39].

Four types of TCM exist with their own properties, advantages, and disadvantages. The four types are[39]:

- Adsorption materials
- Absorption materials
- Pure thermo-chemical materials
- Composite thermo-chemical materials

The most important parameters for the selection of a TCM are[39]:

- Rate of reaction
- Volatility sorbate higher than sorbent
- Thermal conductivity
- Heat transfer rate
- Temperature desorption
- Corrosiveness
- Thermal stability
- Molecular stability
- Eco-friendly

The rate of reaction is influenced by the affinity of the sorbent and the sorbate. When the affinity is high, the reaction kinetics will be positively influenced resulting in a high rate of reaction. A high rate of reaction is important for the amount of heat that can be absorbed or released in time. The volatility of the sorbate must be better than the sorbent's volatility to make the phase change more quickly and be taken up or released by the sorbent. The thermal conductivity and the heat transfer rate to the heat transfer medium must be as high as possible to efficiently take up and deliver the heat for the reaction. The temperature of the desorption must be as low as possible. Furthermore, the materials must be noncorrosive in order not to affect the materials necessary for the storage or the heat transfer medium. Thermal and molecular stability is necessary during operating temperature and pressure. Lastly, eco-friendliness is important. The materials used must not be toxic or have a high carbon footprint. Figure 2.4 gives an overview of TCMs sorted per type of TCES:

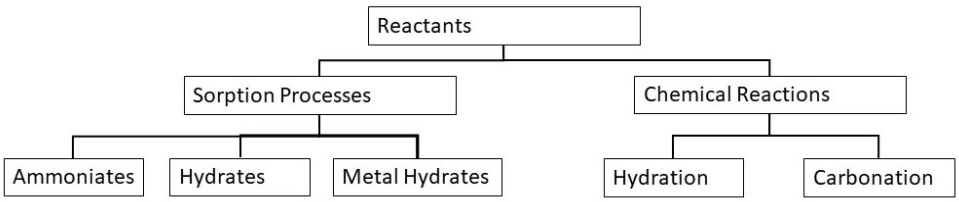

Figure 2.4: *Thermo-chemical energy storage materials classification[39]*

Thermo-chemical Energy Storage Systems

TCES storage can be divided into three types of systems. First, the division between open and closed systems is made, then the division between adsorption and absorption systems is made. The difference between an open and a closed system is that in an open system, the sorbate is released in the gaseous state to the environment while in a closed system, the sorbate is not directly released but the entropy that is released can be taken up through a heat exchanger. Figure 2.5 gives an overview of the types of TCES systems.

Open systems can be applied in buildings where the desorption reaction converts hot dry air into saturated warm air acquiring energy through the high temperature of the hot dry air. The adsorption reaction, which would take place during winter, has cold wet air as input that will be turned into dry warm air. The cold wet air can be taken from outside for example. The high-temperature heat source can be collected from a solar collector[39]. Open systems can also be used in combination with DH as a short-term buffer[39].

Closed adsorption systems use heat from example solar collectors for the desorption of water vapor. The water vapor can be cooled in a condenser and stored. Then at a later time, the condensed water can be heated up with a heat source to evaporate it and combine it with the sorbent to be adsorbed and energy is released. When silica gel is used for closed-system adsorption the water content must be between 3-13 % and the storage system is 30 % less efficient than a water storage system. [39]

Closed absorption is more suitable to be used for long storage. Closed absorption works almost the same as closed adsorption. An example used for closed absorption is NaOH in combination with water as the working fluid. Solar heat is used in combination with a heat exchanger to separate water from NaOH. The water and the concentrated NaOH are stored separately. The water is first cooled and condenses before it is stored in a tank. Excess heat can be collected and reused in the heat exchanger. For the discharge cycle, a heat pump is necessary to use the heat from the ground to evaporate the water. When the water is evaporated it can be added to the concentrated mixture where the energy is released. Research shows that the storage system to facilitate one family house would take up 7m^3 [68].

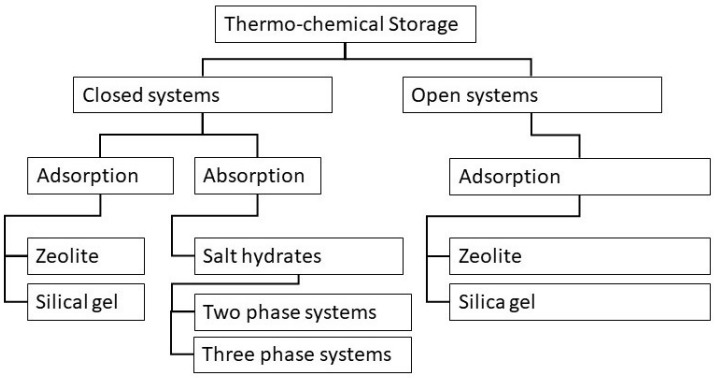

Figure 2.5: *Classification of thermo-chemical energy storage systems[39]*

The IEA has researched long-term storage in combination with solar power for low-energy building applications. The results found are presented in Table 2.6. The working pairs

of materials including silica gel/water, magnesium sulfate/water, lithium bromide/water, lithium chloride/water, and NaOH/water have been considered to have the most potential to be incorporated into TCES energy storage system because of their high heat storage capacity[39].

Table 2.6: *Parameters of thermo-chemical storage materials[49]*

Medium	Type of TCES	Energy Density (kWh/m^3)	Cost of Material ($€/m^3$)
LiCl	Adsorption	250	3600
NaOH	Adsorption	253	250
Silica gel	Adsorption	50	4300
Zeolite 13X	Adsorption	180	2-3000
Zeolite 4A	Adsorption	160	2500-3500
$MgSO_4 7H_2O$	Thermo-chemical	420	4870
K_2CO_3	Absorption	360	2000

Advantages and Disadvantages of Thermo-chemical Energy Storage

An advantage of TCES is the high energy density meaning the storage of the same amount of energy requires less volume. Furthermore, TCES has no self-discharge or thermal heating losses because the reactants of the chemical reaction can be stored separately at ambient temperatures and pressures. This makes TCES suitable for long-term storage. TCES also requires less operational and maintenance costs because it requires smaller pipes without insulation and less pumping capacity because of the higher energy density. Furthermore, TCES has more applications than the storage of heat because it can also be used to control humidity in areas. TCES can also be used in combination with low-quality residual heat. Lastly, TCES is suitable for long-distance storage because of the combination of the high energy density and the lack of self-discharge of the storage medium it can be transported more easily.

Advantages of TCES compared to SHS and LHS[39][32]:

- No self-discharge
- High energy density
- Less maintenance and Operational costs
- More applications
- Possibility to use low quality residual heat
- Suitable for long distances

The disadvantages of TCES are the low technology readiness level and the costs. For long-term storage large amounts of the medium will be necessary to store heat and the costs related to the usage makes many materials unsuitable for this application.

2.3 Conclusions on STES

STES can be divided into three main different categories that all have a lot of subcategories. Three main types of STES are found; SHS, LHS, and TCES heat storage, displayed with parameters in Table 2.7. SHS is the storage of energy in a material by increasing or decreasing the temperature of the material. LHS is the storage of heat captured or released during the phase change of a material. Lastly, chemical heat storage is the storage of energy in chemical bonds that are formed in reversible reactions. To decide what technology types of STES are possible to combine with a small-sized DHN the main parameters of the three categories of STES are shown in Table 2.7. From this overview can be determined that chemical-thermal energy storage has the highest storage capacities and efficiencies but the systems can be costly and have a low technology readiness level. This means the systems are not widely commercially available and research into reliability, phase segregation, and subcooling is still necessary. SHS is already applied in DHNs and has low costs. The disadvantages of SHS are low energy density and geological limitations. LHS has a higher energy density than SHS and lower costs than TCES.

Table 2.7: *Seasonable thermal energy storage categories and parameters*

	Sensible Heat Storage	**Latent Heat Storage**	**Thermo-chemical Heat Storage**
Efficiency (%)	75-90	75-90	75-100
Energy Density (kWh/m^3)	15-50	40-250	150-600
Costs (€)	30-500	50-500	10-5000
Temperature Range (°C)	50-400	20-80	20-200
Technical Readiness Level	High	Medium	Low

2.4 Key Performance Indicators Thermal Energy Storage in District Heating Networks

In this section, the KPIs of the implementation of STES into DHNs are evaluated. The selection of KPIs is important in order to narrow the selection of suitable STES technologies in Section 3.2.1, Section 3.2.2 and Section 3.2.3. Furthermore, to determine what parameters affect the design of the STES in the models in Section 3.3.3, Section 3.3.2, and Section 3.3.4. Lastly to determine what parameters are important to evaluate the potential of STES in DHNs in Chapter 4.

The following performance parameters can be used to evaluate TES[27] [35] [19]:

- Volume [m^3]: the amount of space occupied by the system
- Power capacity [W]: the total amount of power available in the system
- Power density [W/m^3]: the ratio between power capacity and capacity
- Energy storage capacity [kWh]: the total amount of energy available in the system after charging with nominal conditions
- Energy density [kWh/m^3]: the ratio between energy storage capacity and volume of the system
- Storage period [h, or months] duration of storage time
- Cycle life [n]: the amount of charge-discharge cycles the system has under nominal conditions
- Discharge rate [W]: time to fully discharge the storage capacity
- Storage heat losses [kWh]: the amount of energy lost in a specified amount of time during the time of non-use
- Round-trip efficiency (RTE) [%]: the ratio between the energy released during discharge and the energy absorbed during charge

$$\eta = \frac{Q_{disch}}{Q_{ch}} * 100\%$$

- Total efficiency [%]: the ratio between the usable energy in DHN and the energy used to charge the system

$$\psi = \frac{E_{x_{DHN}}}{E_{x_{ch}}} * 100\%$$

- OPEX [€/a]: the operating cost of the system per year
- CAPEX [€] the investment costs
- Total costs [€/kWh]: the investment cost of the system combined with the operating cost per storage capacity in time

$$Totalcosts = CAPEX + OPEX * t$$

- Stratification number [n]: the number of thermal stratification layers in thermal tanks

3 Methodology

From the literature is found that STES has the potential to supply heat to DHNs in the built environment. As Dincer states: "TES is presently identified as the most economical storage technology for building heating, cooling, and air-conditioning applications."[25] However, from the literature it is not possible to define one STES system most suitable in combination with DHNs to deliver peak load. The selection of the most suitable STES system depends on the desired power capacity, desired volume, location, temperature in the DHN, and heat source. Furthermore, high charge and discharge rates, necessary to supply the peak load, are important. In literature, most research is done on the combination of TES and DHNs in order to supply the base load [54][35] [57] [48] [40] [71] [19] [27]. A literature gap exists on the subject of TES in combination with DHNs to supply peak load.

In this chapter, the methodology of the research will be presented in the sequence presented in Figure 3.1. First, the boundary conditions for the TES technology will be calculated with the data provided by Equans on future trends in DHNs in Section 3.1. An analysis of the TES technology with the most potential from each category will be made in Section 3.2. The categories include SHS, LHS, and TCES. Then a methodology for the development of the model per technology will be given in Section 3.3. A model will be made for the technology with the most potential of each of these categories. The STES systems vary in working principles but will be modeled with the same base in order to be able to compare the results. This base consists of a tank that can function as a storage tank or a plug-flow reactor. The goal of these models is to find the losses per technology resulting in the volume and the operational costs per technology. Then a validation per model will be given by comparing the model to the results in Section 3.4. An analysis of the models will be made by comparing the effect of the number of nodes and the value of the time step on the Temperature profile and the total heat loss throughout the year. Lastly, the scenarios that will be used for the simulations in Chapter 4 are described in Section 3.5.

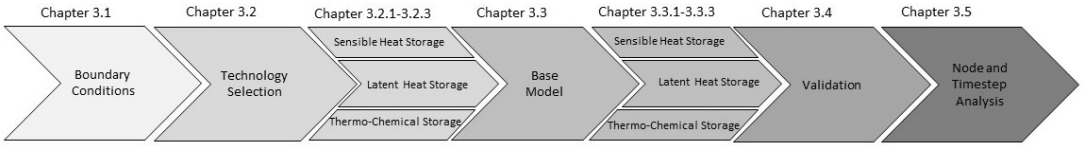

Figure 3.1: *An overview of the methodology used in this research to develop a model to determine the technically and economically optimal heat storage system for peak load of a small-scale DHN*

3.1 Boundary Conditions

The goal of the research is to determine what type of TES has the most potential to supply the peak demand in DHNs. In order to determine the boundary conditions of the TES an

analysis of the most occurring DHNs in the future is made by Equans. Equans expects the most development of DHNs in the built environment with connections to 200 to 1000 households. In literature is found that seasonal TES is more efficient and economically viable for community use than for single use[65][21][25]. Smaller thermal losses, more efficient distribution of heat over a spread-out demand, and lower specific construction costs are important reasons for this. Therefore, the desired TES is centralized storage with a volume as small as possible and low costs. The demand profile is provided by Equans and shown in Figure 3.2. The yellow line represents the total load which equates to 1.9 GWh per year. The base load is shown in orange and has a power of 400 kW providing 1.6 GWh per year. Lastly, the peak load in blue equates to 0.3 GWh per year. The base load is delivered with an ATES system and the heat provided to the TES and the ATES system is a geothermal source. The power of the geothermal source used to deliver heat to this DH is constant and is 217 kW, which is sufficient to supply the full load. The highest load is shown on the 21 of January and equals 1500 Kwh. The base load covers 400 kWh, leaving a peak load of 1100 kWh. The peak load covers one hour meaning the maximum power necessary to be delivered by the TES is 1100 kW. The total capacity of the TES system is the total peak load which equals 284 MWh. Furthermore, the temperature the TES technology needs to provide to the DH is 70 °C.

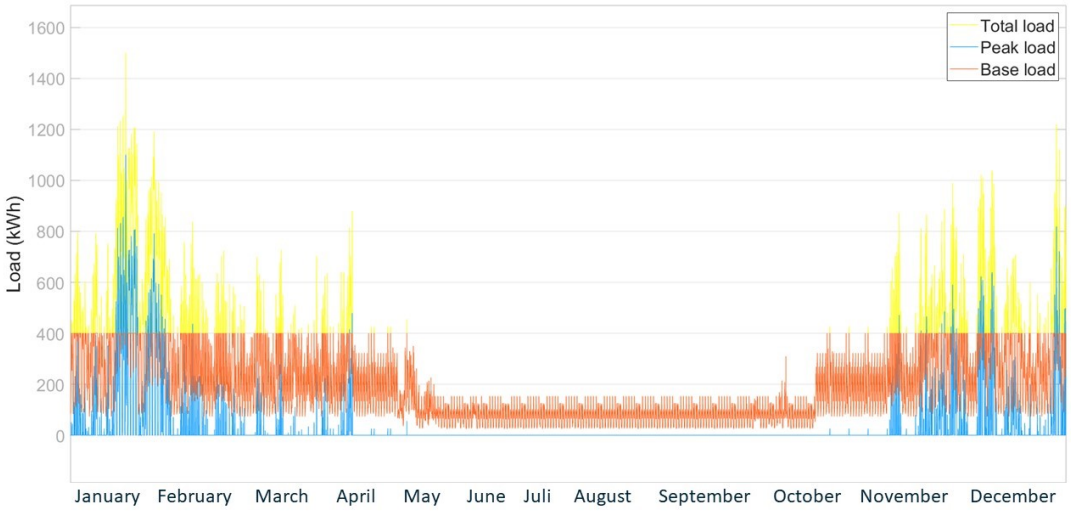

Figure 3.2: *Demand of a district heating network consisting of 200 houses with little insulation in the Netherlands.*

3.2 TES Technologies

In this section, a selection of the technology with the most potential to be integrated into a small-size DHN in the existing built environment from each TES category (SHS, LHS, and TCES) will be computed. The selection will consist of the design of the storage technology and the selection of the storage medium and HTF. The technologies with the most potential per category are used to compare the TES categories in Chapter 4.

3.2.1 Sensible Heat Storage

As elaborated on in Section 2.2.5 SHS is the most developed TES and has the lowest costs [57]. SHS using water as the storage medium is used the most because of the material properties. Water has high specific heat, density, thermal conductivity and is not toxic or costly. The disadvantage of using water is the low-temperature range since it can be used until 100 °C in a liquid state. This results in a lower energy density in comparison to high-temperature SHS and therefore a bigger volume. However, in order to supply the DHN which has a minimum temperature of 70 °C and a maximum temperature of 100 °C the temperature range of water is suitable. Furthermore, an advantage of medium-temperature SHS is lower heat losses. Lastly, the HTF of the DHN is water resulting in a simplified system overall when using water as the storage medium in TES. To conclude the literature study in Section 2.2.5, water is most suitable as a storage medium for SHS in combination with a DHN with a medium temperature demand. Table 3.1 shows the material properties of water.

Table 3.1: *The material properties of water*

Medium	Temperature range (°C)	Density (kg/m3)	Specific heat (J/kg K)	Thermal Conductivity (W/m K)
Water	0-100	250	3600	0.69

Optimal Design for Sensible and Latent Heat Storage

Apart from the storage medium and HTF, multiple configurations for SHS are possible. For large capacities, ATES is used the most because of it is low cost, low losses, and relatively high power rates compared to other forms of UTES such as BTES[48]. Disadvantages of ATES are geographical constraints and the low-temperature ranges because of regulation and therefore the large volumes. For the supply of the peak loads in DHNs, one of the design requirements is a solution with a relatively small volume and high discharging power. The SHS technology with storage medium water and the highest energy density is hot water tank storage (HWTS) as stated in Section 2.2.5. Furthermore, HWTS can handle temperature differences up to 30 K combined with high flow rates; resulting in high discharging power[19]. To conclude, the high energy density in combination with high discharge power and the possibility of application on any location make HWTS the best technology within SHS for the supply of peak loads in combination with a DHN.

The optimal design of an HWTS will first be determined. HWTS systems can be open or closed. Open systems have higher energy density and efficiencies [52]. The design choice for an open system has therefore been made.

The tanks can be used as large-scale single storage or multiple tanks can be used placed in parallel or in series. When the tanks are placed in series, thermal stratification happens sequentially in this configuration. Stratification is improved in the series configuration and therefore the performance of the system is enhanced. However, the external losses are higher. The design choice for one buried tank has therefore been made.
Furthermore, the tanks will have thermal stratification because of thermal buoyancy. Thermal stratification is the effect of different densities caused by temperature differences in the storage medium. Cold water has a higher density and will therefore sink to the bottom of the tank. A TES system without stratification is called a fully mixed TES and is proven to have lower performance because of higher losses[37]. Thermoclines are natural barriers between the layers in the tank with different temperatures. Keeping the thermocline as small as possible means less mixing of layers and therefore fewer losses [19]. Thermal stratification can deteriorate because of the insulation of the tank[46]. An increase in insulation can increase thermal degradation because of vertical conduction through the insulation layer. Increasing the length of the storage tank while decreasing the thickness of the insulation and choosing a material with low conductivity can decrease this effect and improve thermal stratification. Insulation plays an important role in decreasing external losses. Typical insulants are polyurethane, glass wool, expanded polystyrene, foam glass, and extruded polystyrene. Insulation can be placed inside or outside the construction material, which is often concrete or steel [19]. Water tightness is increased with liners. The boundary conditions of the specific site such as soil temperature, and the presence of groundwater or groundwater flow determine the types of insulation in the end. Costs can be decreased by applying less insulation.
Furthermore, the inlet and outlet port should be designed not to create turbulent mixing but to produce a uniform circulation of water. To conclude, the HWTS will consist of a very thin insulation layer on the sides to prevent the water from leaking into the ground and to minimize costs and the degradation of thermal stratification because of vertical conduction through the insulation layer. The lid of the HWTS will consist of a layer of air and a thicker layer of insulation material to minimize losses. The inlet and outlet are placed on the top and the bottom of the tank.

The optimal geometry for HWTS is a vertical cylinder[19]. The design must have a maximum volume compared to a minimum surface area to minimize external thermal losses. The aspect ratio concerning the height and the diameter must be optimized to minimize the internal thermal losses caused by mixing which decays stratification. Heat losses can be minimized when the height is equal to the radius [26].

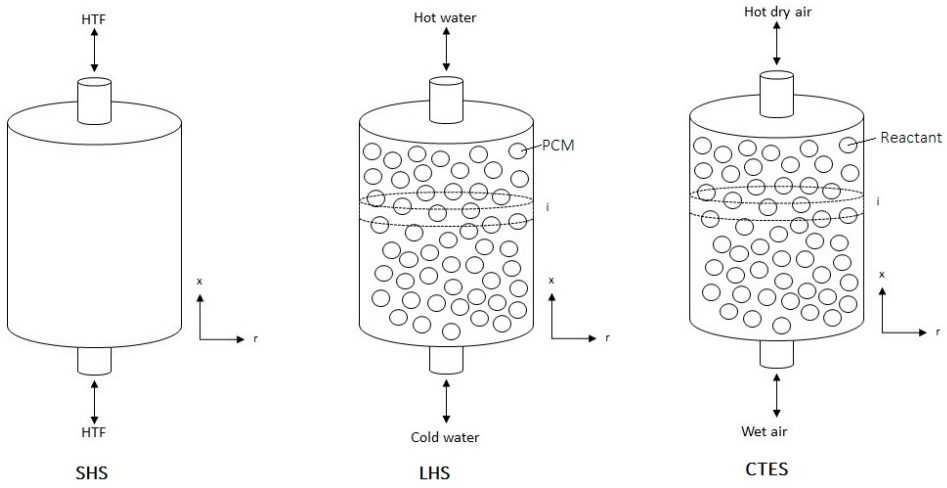

Figure 3.3: *Design of the sensible heat storage tank, latent heat storage tank, and the thermochemical reactor.*

To conclude, the design for HWTS will be a cylinder buried in the ground as can be seen in Figure 3.3 with a radius equal to the height. The insulation on the bottom and sides of the tank will be 0.0025 m and the insulation on the top of the tank will be 0.24 m thick. The HWTS will be an open system with an inlet and outlet on the bottom and top of the tank. The storage medium and thus the HTF will be water.

3.2.2 Latent Heat Storage

The base model for LHS will be the same as for SHS and consist of one large-scale cylinder single-storage tank buried in the ground with a radius equal to its height. The difference between the LHS and the SHS is the storage medium. For LHS the HTF will be water and the storage medium will be paraffin. Paraffin is chosen because they are safe, reliable, predictable, cheap, non-corrosive and they have a temperature range between 60 °C and 100 °C which is suitable for DHNs in the built environment[60] as described in Section 2.2.6. The properties of Paraffin are depicted in Table 3.7.

Table 3.2: *The properties of the phase change material Paraffin*

Melting Temperature (K)	Latent Heat of Fusion (kJ/kg)	Density (kg/m3)		Specific Heat (J/kg K)		Thermal Conductivity (W/m K)	
		Solid	Liquid	Solid	Liquid	Solid	Liquid
334.15	174.7	1038.15	915.75	1722	2147	0.4	0.4

3.2.3 Thermochemical Thermal Energy Storage

The thermochemical storage can be based on sorption or on a chemical reaction. As described in Section 2.2.7 thermochemical energy storage based on a chemical reaction has the advantage that there is a wide range of materials to choose from with a wide range of operating temperatures[23]. Furthermore, solid adsorption materials have lower energy density but better heat mass transfer rates. Therefore, reaction-based thermochemical energy storage has been chosen to model.
Potassium carbonate (K_2CO_3) will be researched because of the low cost of the material (+/- 0.50 € /kg [30]) and its availability. Furthermore, it has a high capacity for water uptake and energy storage density. It is also more chemically stable than other salt hydrates, it has low corrosiveness and it is not toxic. The operating temperatures are between 65 °C and 100 °C, making it safe to use in the built environment.

The Potassium carbonate hydration and dehydration reaction are the following:

$$K_2CO_3 1.5H_2O + \Delta H_R \leftrightarrow K_2CO_3 + 1.5H_2O \tag{3.1}$$

Optimal Design Thermochemical Reactor

The base of the design for TCES will be the same as for SHS and LHS. The base of the design is a cylinder. From the literature review presented in Section 2.2.7 the rest of the design for a thermochemical reactor has been made. The first design choice is an open or closed reactor. Open reactors have a higher overall efficiency[8] and need a lower heat input[23]. Lastly, an open reactor has lower costs than a closed reactor[23]. The design will therefore consist of an open reactor.
The thermochemical energy storage will consist of a fixed-bed reactor. A cross-flow reactor releases a higher thermal energy density in the transport medium and has a constant thermal power output which the fixed bed reactor does not have. However, the cross-flow reactor has other disadvantages compared to a fixed-bed reactor. The reaction control has higher demands and a uniform mass flow with low bulk velocities has to be realized in the reactor which is technically very difficult [44]. Therefore, the design choice for a fixed-bed reactor has been made.

The design for a large thermochemical reactor can best be achieved with a modular setup in order for the reactants to react instantaneously instead of sequentially [11]. When the Chemical TES reactor is designed to consist of a number of separate reactors, the reaction kinetics and the heat transfer are optimized and the temperature in the reactor can be controlled as has been proven by Angerer et al.[11]. Furthermore, when the reactor is made in a modular setup the inlet temperature and the height have a limited influence on the overall reactor performance[11]. The design will be optimized in order for the temperature in the reactor not to achieve higher temperatures than 617.85 K in Section 3.2.3, because this corresponds to the melting temperature of potassium carbonate. Furthermore, the reactors will have a maximum height of 0.5 m and a maximum diameter of 0.15m. This is the maximum volume of the reactor where the volume has a limited effect on the reactor performance so that the reaction rate is not slowed down [11]. The mass flow used is 0.05 kg/s.

The reactor is simultaneously the storage tank since the material performing the chemical reaction is kept in the tank and for dehydration, humid air is blown through the tank while for hydration the tank is heated up with warm air. This system will need extra equipment compared to the LHS and SHS which only need a water pump. The TCES system will need an air pump to supply the reactor with air, a humidifier to humidify the air for dehydration and an air-to-water heat exchanger. The volume of an air pump that has a suction rate of 62.7 l/min[AG and KG] is 1 *10^{-6} m^3. The volume of a humidifier is 0.05 m^3, which can handle 250 l/min[6]. A heat exchanger that can handle 200 m^3/min has a volume of 0.077 m^3 [GmbH].

3.3 Model

In this section, the built-up of the models for SHS, LHS, and TCES will be explained and validation for the models per category will be given. First, the base model from which all three models are built will be outlined, then a model and validation per category will be given. Lastly, a validation for the number of nodes and the timestep that is used will be given.

The model will be constructed in the sequence presented in Figure 3.4. First, a pre-design will be made based on the literature review and the boundary conditions provided by Equans. After this, the design will be modeled in Matlab reaching a more detailed design. The model will be validated with experiments and the results will be evaluated. Then the model will be used to optimize the design for the given scenarios by Equans.

Figure 3.4: *Model design steps*

The predesign is especially important to determine parameters such as the thermal capacity, thermal losses, thermal stratification, and geometry of the HWT. The thermal capacity can be determined using the storage volume and specific heat capacity. Thermal losses are determined by the area versus volume (A/V) ratio, insulation thickness, and position of the in and outlets. Furthermore, thermal stratification is determined by the height versus diameter (h/d) ratio. Parameters determined by the location of the storage tank also have an influence on heat losses. However, in this research, the tank will be modeled in a general setting where influences determined by the location of placement will not be taken into account for the design.

In the detailed design, the thermal behavior of the storage tank is modeled. A numerical model consisting of computational fluid dynamics can be used where component geometry is modeled using a discretization method[19]. Computational fluid dynamics (CFD) models give detailed results however large-scale TES systems require too much computational effort and will therefore not be available in the near future[51]. When assumptions are made to simplify the model in geometry, material properties, and boundary conditions the model is called a coarse model. By reducing the accuracy of the calculation of the thermal-hydraulic behavior and therefore losses, computational efforts are reduced.

The coarse model can consist of a three-dimensional model or a one-dimensional model. For analysis of specific problems within the TES systems three-dimensional models deliver a more accurate calculation. However, one-dimensional models are found to be accurate enough in describing the temperature profile in the tank and therefore the thermal behavior and losses, especially when analyzing complete TES systems instead of components[14].

The tank will be modeled using thermal stratification. This method describes the tank consisting of layers of the storage medium with different temperatures. The mixing between layers can be neglected as its presence is minimal and therefore has minimal effect on the temperature profile in the tank[52].

The thermal behavior, of the TES tank, will be modeled using multidimensional partial differential equations describing energy, momentum, and mass balance[52]. Furthermore, equations describing the geometry and heat transfer are used. A one-dimensional model describing the tank with 20 to 30 layers with limited thickness is determined to be accurate enough to replace more time-consuming three-dimensional methods [52].

3.3.1 Base Model

The base model will consist of a storage tank in which all three categories will be modeled. The base model can be used as a simple storage tank or as a plug-flow reactor. The design of the base model must therefore meet the following requirements: suitable for thermal stratification, minimization of internal losses, minimization of external losses, continuous mass flow possible, and a constant area over the height. Thermal stratification is important to minimize external losses and optimize the performance of the SHS and LHS[52]. Constant mass flow possible and a constant area over the height of the tank are requirements of the plug flow reactor[44]. In order to make optimal use of the thermal stratification in the tank the in and outlets must be placed as far from each other as possible. A cylindrical shape with in- and outlets at the top and bottom is therefore chosen for the base design. The base model consists of a layer of 2.5 mm polyurethane to stop the water from leaking. The ground functions as an insulation layer. The top of the storage is a 0.24 polyurethane cover with 0.5 m air between the cover and the water which also functions as an insulation layer. Figure 3.5 shows the base design. The dimensions will be determined per category in the more detailed design.

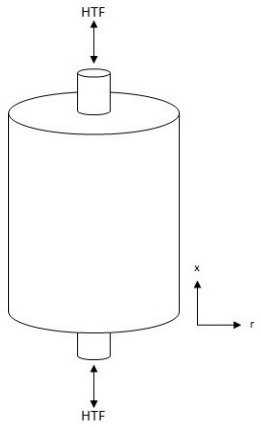

Figure 3.5: *Base Model*

The tank consists of a wall and insulation layer as is shown in Figure 3.6.

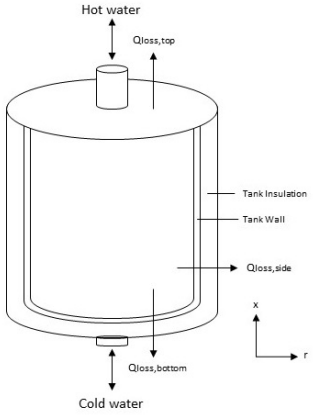

Figure 3.6: *Design of the storage tank with insulation*

The resistance network of the conduction to the ground is shown in Figure 3.7. The network only consists of resistance for the insulation and the ground because the wall temperature is assumed equal to the water temperature in the tank. The ground has been modeled as a resistance with a length. The length that will be used in the calculation is determined by calculating the temperature gradient and setting the length at the distance where the temperature gradient is close to zero.

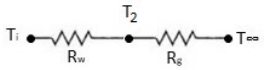

Figure 3.7: *Conduction to the ground resistance network*

The resistances are formulated as follows:

$$R_{w,side} = \frac{d_w}{k_{ins} A_{i,w}} \tag{3.2}$$

$$R_{g,side} = \frac{r^*}{k_g A_{i,w}} \tag{3.3}$$

The bottom has the same insulation as the side of the tank and therefore has the same losses but the area through which the heat is conducted is different. The resistances for the bottom is formulated as follows:

$$R_{w,bottom} = \frac{d_w}{k_{ins} A_c} \tag{3.4}$$

$$R_{g,bottom} = \frac{r^*}{k_g A_c} \tag{3.5}$$

The top of the tank is not buried in the ground but is covered with a lid that is placed 0.5 m above the top of the water level. The insulation is therefore consisting of a layer of 0.5 m air and 0.24 polyethylene lid. The resistances for the top are as follows:

$$R_{w,top} = \frac{d_{lid}}{k_{ins} A_c} \tag{3.6}$$

$$R_{g,top} = \frac{d_{air}}{k_{air} A_c} \tag{3.7}$$

The thermal conductivity of the insulation is k_{ins}, k_g is the thermal conductivity of the ground, $A_{i,w}$ is the area of the wall of part i of the tank, A_c is the area of the top or bottom of the tank, d_w is the thickness of the wall and r^* is the distance the heat travels through the ground before the temperature gradient becomes close to zero. To determine the total heat resistance, resistances in series are added and resistances in parallel are divided by one before they are added. The resistance for the side, top, and bottom of the tank are the following:

$$R_{side} = R_{g,side} + R_{w,side} \tag{3.8}$$

$$R_{bottom,1} = R_{g,bottom} + R_{w,bottom} \tag{3.9}$$

$$R_{top,1} = R_{g,top} + R_{w,top} \tag{3.10}$$

The top and bottom nodes consist of a side and a top or bottom area where the resistances are parallel. The total resistance for the top and bottom node are the following:

$$R_{bottom} = 1/(\frac{1}{R_{bottom,1}} + \frac{1}{R_{side}}) \tag{3.11}$$

$$R_{top} = 1/(\frac{1}{R_{top,1}} + \frac{1}{R_{side}}) \tag{3.12}$$

To determine the radius in the ground that is affected by the heat transfer from the tank the solution by Carslaw and Jaeger is used[16]:

$$T(z,t) = Tg + (Ttank - Tg)erfc(\frac{2}{D\sqrt{D*t}}) \tag{3.13}$$

To determine the distance, z, where the temperature gradient is close to zero a Matlab script is executed to show the temperature profile in the ground. The time is set to 15768000 s, equal to half a year. This is the storage time for seasonal storage. T_{tank} is the temperature of the outside of the tank and is calculated with the following equation:

$$q_{cond_{total}} = q_{cond,ins} + q_{cond,ground} = (\frac{k_{ins}A_{i,w}}{d_w})(T_i - T_{tank}) + \frac{k_g A_{i,w}}{r^*})(T_{tank} - T_g) \tag{3.14}$$

T_{tank} is then determined the following:

$$T_{tank} = \frac{((\frac{k_{ins}A_{i,w}}{d_w})T_i) + (\frac{k_g A_{i,w}}{r^*})T_g)}{\frac{k_{ins}A_{i,w}}{d_w} + \frac{k_g A_{i,w}}{r^*}} \tag{3.15}$$

The temperature profile in the ground is calculated with the average temperature in the tank throughout the year. Assuming the tank is charged with the same total amount of energy as being discharged, T_i is assumed to be the average of the charge and discharge temperature which is 318.15 K. The time is set to 365 days. Equation 3.3.1 and Equation 3.3.1 are then combined to find r^* and T_{tank}. The temperature pattern in the ground is shown in Figure 3.8.

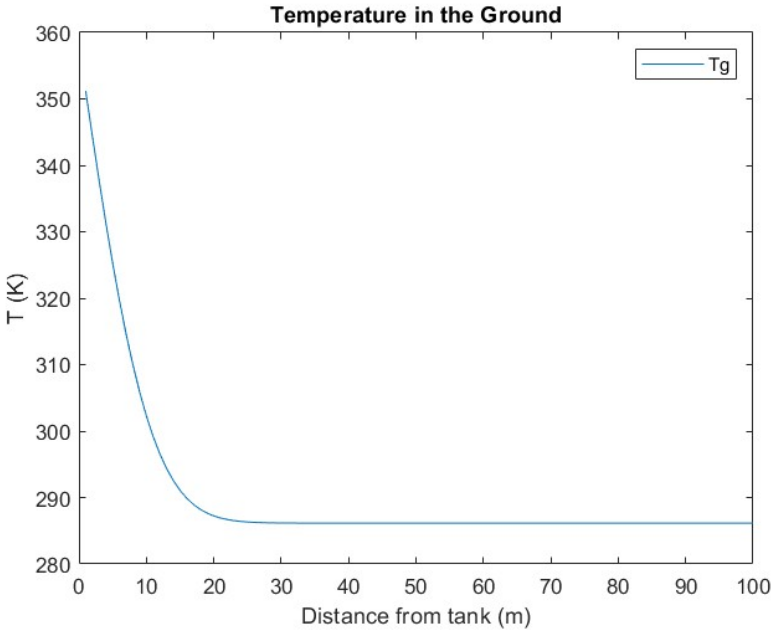

Figure 3.8: *The temperature in the ground around a thermal energy storage tank*

The temperature change is smaller than 0.01 K/m for a thermal radius of 25 m. T_{tank} with an insulation layer of 0.0025 m is found to be 317.7 K. An analysis is made to estimate the influences of errors in the assumptions in Section 3.4.

3.3.2 Model Sensible Thermal Energy Storage

First, the optimal design for an SHS tank will be described with the information provided in Chapter 3 applied to the base design for all three categories of TES. The HTF is water as is has a high specific heat, it is readily available, not costly and it operates in the suitable temperature range Section 2.2.5. The optimal design for an HWTS is a cylinder with a height equal to the radius to minimize losses Chapter 3.

Then the numerical model is set up to analyze the temperature gradient in the tank int the time. The assumption has been made that the temperature in the radial direction is constant and there is no inlet mixing. To model the stratification in the tank the tank has been divided into i number of vertical parts as is depicted in Figure 3.9.

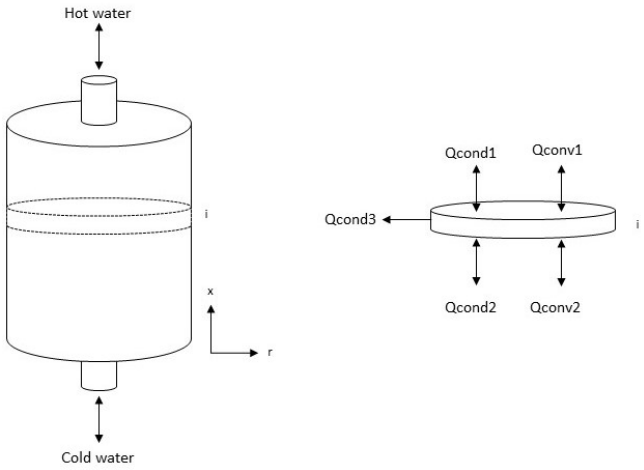

Figure 3.9: *The heat transfer in a sensible energy storage tank*

The model consists of convection of the fluid in the axial direction, caused by the pumping in and out of the fluid. Furthermore, conduction in the axial direction is split up into two parts: conduction through the fluid itself and conduction through the wall of the tank. Lastly, conduction through the tank wall is called conduction$_3$.

The total heat flux can with this information be calculated as follows:

$$q_{cond_3} = (\frac{k_{ins}A_{i,w}}{d_w} + \frac{k_g A_{i,w}}{r^*})(T_i(t) - T_g) \tag{3.16}$$

T_i and T_{i+1} are the temperature in part i of the tank and part i+1. The resistance for the conduction through the tank wall can be conducted using the model developed by Newton [47], where the assumption that the wall temperature is equal to the temperature of the water still holds. The total heat flux through conduction can be written as follows:

$$q_{cond_{1,2}} = (\frac{k + \Delta k)A_c}{\Delta x}(T_{i+1}(t) - T_i(t) \tag{3.17}$$

k is the thermal conductivity of the water and Δk is the conductivity of the tank wall.

$$\Delta k = \frac{k_{wall}A_{c,wall}}{A_c} \tag{3.18}$$

Convection is determined by the pumping of the fluid.

$$q_{conv_2} = \dot{m}c_{p,w}(T_{i-1}(t) - (T_i(t)) \tag{3.19}$$

$$q_{conv_1} = \dot{m} c_{p,w}((T_i(t) - T_{i+1}(t)) \tag{3.20}$$

$C_{p,w}$ is the specific heat capacity of water and $\dot{m}$ is the transported fluid in the tank. The transported fluid is equal to the mass flow rate of the injected and extracted water.

For charging $\dot{m}$ is $\dot{m_{down}}$ and for discharging $\dot{m}$ is equal to $\dot{m_{up}}$. During storage $\dot{m}$ is equal to zero because no water is pumped in and out of the tank and mixing between layers is neglected. The total power balance during charge is equal to:

$$\begin{aligned}\frac{dT_i}{dt} m_i c_{p,i} =& - \dot{m}_{down} c_{p,w}((T_{i-1}(t) - T_i(t)) + -\dot{m}_{down} c_{p,w}((T_i(t) - T_{i+1}(t)) \\ &+ \frac{(k + \Delta k) A_c}{\Delta x}((T_{i+1(t)} - T_i(t)) - (T_i(t) - T_{i-1}(t))) \\ &- \frac{1}{R_{side}}(T_i(t) - T_g)\end{aligned} \tag{3.21}$$

The total power balance during discharge is equal to:

$$\begin{aligned}\frac{dT_i}{dt} m_i c_{p,i} =& \dot{m}_{up} c_{p,w}((T_{i-1}(t) - T_i(t)) + \dot{m}_{up} c_{p,w}((T_i(t) - T_{i+1}(t)) \\ &+ \frac{(k + \Delta k) A_c}{\Delta x}((T_{i+1(t)} - T_i(t)) - (T_i(t) - T_{i-1}(t))) \\ &- \frac{1}{R_{side}}(T_i(t) - T_\infty)\end{aligned} \tag{3.22}$$

During storgae the $\dot{m}$ is zero and the power balance will be:

$$\begin{aligned}\frac{dT_i}{dt} m_i c_{p,i} =& \frac{(k + \Delta k) A_c}{\Delta x}((T_{i+1(t)} - T_i(t)) - (T_i(t) - T_{i-1}(t))) \\ &- \frac{1}{R_{side}}(T_i(t) - T_\infty)\end{aligned} \tag{3.23}$$

The equations can be discritizatised to create a numerical model for Matlab.

$$\frac{dT_i}{dt} = A_i T_{i-1} + B_i T_i + C_i T_{i+1} + D_i \tag{3.24}$$

$$A_i = (\dot{m}_{up} c_{p,w} + (\frac{k + \Delta k) A_c}{\Delta x})) / (\dot{m}_i c_{p,i}) \tag{3.25}$$

$$B_i = (-2\frac{(k + \Delta k) A_c}{\Delta x} - \frac{1}{R_{side}} / (\dot{m}_i c_{p,i}) \tag{3.26}$$

$$C_i = (-\dot{m}_{up} c_{p,w} + (\frac{k + \Delta k) A_c}{\Delta x})) / (\dot{m}_i c_{p,i}) \tag{3.27}$$

$$D_i = (T_g (\frac{k_{ins} A_{i,w}}{d_{ins}} + \frac{k_g A_{i,w}}{r^*}) / (\dot{m}_i c_{p,i}) \tag{3.28}$$

To numerically solve the equation with a finite difference method the Crank-Nicolson method can be applied to this problem [66]. The Crank-Nicolson method is implicit and is also unconditionally stable[53]. The Crank-Nicolson method is defined as follows:

$$\frac{T_i^{t+1} - T_i^{t+1}}{\Delta t} = \frac{1}{2}(F_i^{t+1} + F_i^t) \tag{3.29}$$

For the discretized power balance the equation becomes the following:

$$\frac{T_i^{t+1} - T_i^{t+1}}{\Delta t} = \frac{1}{2}(A_i (T_{i-1}^{t+1} + T_{i-1}^t) + B_i (T_i^{t+1} + T_i^t) + C_i (T_{i+1}^{t+1} + T_{i+1}^t) + 2D_i) \tag{3.30}$$

This can be rewritten the following:

$$-\frac{\Delta t}{2} A_i T_{i-1}^{t+1} + (-\frac{\Delta t}{2} + 1) B_i T_i^{t+1} - \frac{\Delta t}{2} C_i T_{i+1}^{t+1} = \tag{3.31}$$

$$\frac{\Delta t}{2} A_i T_{i-1}^t + (\frac{\Delta t}{2} + 1) B_i T_i^t + \frac{\Delta t}{2} C_i T_{i+1}^t + D_i \Delta t) \tag{3.32}$$

This can be simplified to the following matrix equation:

$$E * T_i^{t+1} \frac{\Delta t}{2} = F * T_i^t \frac{\Delta t}{2} + Di \Delta t + G \tag{3.33}$$

To solve this equation Gaussain elimination is used. The boundary conditions determine the vector G and the top left corner and bottom right corner of the matrices E and F. The top left corners of matrices E and F are called eleft and the bottom right corners are called eright.

$$eleft = \frac{(-\dot{m}_{up} c_{p,w} - \frac{(k+\Delta k) A_c}{\Delta x} - R_{bottom}) - \frac{\Delta t}{2} + 1}{(\dot{m}_i c_{p,i})} \tag{3.34}$$

$$eright = \frac{(\dot{m}_{up} c_{p,w} - \frac{(k+\Delta k) A_c}{\Delta x} - R_{top}) - \frac{\Delta t}{2} + 1}{(\dot{m}_i c_{p,i})} \tag{3.35}$$

$$G(1) = \frac{((2\dot{m}_{up} c_{p,w} T_{in}) - (R_{side} T_g) + (R_{bottom} T_g)) \Delta t}{(\dot{m}_i c_{p,i})} \tag{3.36}$$

$$G(n) = \frac{((-2\dot{m}_{up}c_{p,w}T_{out}) - (R_{side}T_g) + (R_{top}T_g))\Delta t}{(\dot{m}_i c_{p,i})} \tag{3.37}$$

From the model, the power output and the energy loss can be calculated. With these, the total energy put in the tank and the total energy extracted from the tank can be calculated. The total energy extracted will be set equal to the total capacity necessary for the energy storage and the power output will be equal to the peak demand. The $\dot{m}$ can be calculated necessary to produce the power and the total capacity leading to the calculation of the total volume of the tank. With this information, a calculation of the size of the tank and the costs can be made to evaluate the potential of tank storage for peak demand in district heating networks.

$$P_{out}(t) = \dot{m}_{out}c_{p_{out}}(T_{out}(t) - T_{in}(t) \tag{3.38}$$

$$E_{out} = \int_{t_1}^{t_2} \dot{m}_{out}c_{p_{out}}(T_{out}(t) - T_{\infty}(t)\,dt \tag{3.39}$$

$$Q_{loss} = \sum_{i=1}^{i=n} \int_{t_1}^{t_2} \frac{(T_i(t) - T_{\infty}(t)}{(R_w + R_g)}\,dt \tag{3.40}$$

$$E_{in} = \int_{t_1}^{t_2} \dot{m}_{out}c_{p_{out}}(T_{in}(t) - T_{\infty}(t)\,dt \tag{3.41}$$

$$\eta = \frac{E_{out}}{E_{in} + \dot{W}_{pump}} \tag{3.42}$$

3.3.3 Model Latent Thermal Energy Storage

The LHS tank is the same as the SHS tank with spherical particles of the PCM material added. The numerical model for LHS has been constructed with the same method as the SHS tank model to analyze the temperature gradient in the tank in time. The assumptions that the temperature in the radial direction is constant and there is no inlet mixing are still valid. Furthermore to model the stratification in the tank the tank has again been divided into i number of vertical parts as is depicted in Figure 3.10.

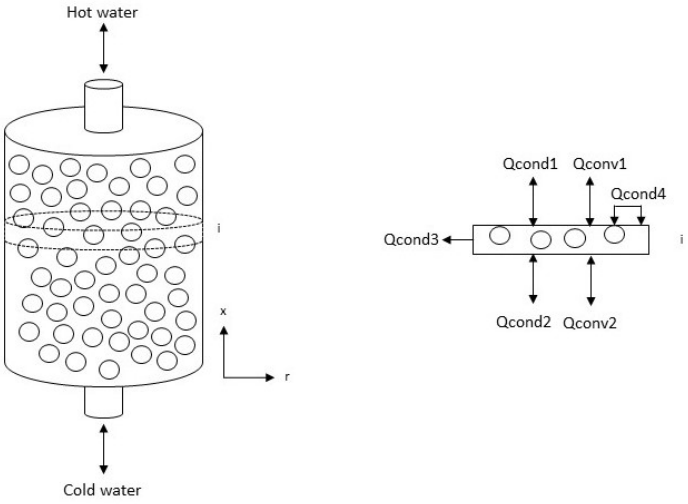

Figure 3.10: *The heat transfer in a latent energy storage tank*

The model consists of the same heat fluxes apart from Q_{cond_4}. Q_{cond_4} is the conduction from the HTF, in this case water, to the PCM material depicted in the black blocks. The conduction between the water and the PCM material is the following:

$$q_{cond_4} = (UA_i(T_w(t) - T_{pcm}(t)) \tag{3.43}$$

U is the overall heat transfer coefficient. U depends on PCM geometry, the Reynolds number, Prandl number and the PCM liquid fraction. U * A_i can be replaced by U_v which is the volumetric heat transfer in porous regions[7].

$$U_v = \frac{6U_0(1-\epsilon)}{D_c} \tag{3.44}$$

ϵ is the porosity of the bed, D_c is the diameter of the PCM material and U_0 is the heat transfer coefficient.

$$U_0 = \frac{1}{A_p}\frac{1}{R_{p,out} + R_{p,cond} + R_{p,in}} \tag{3.45}$$

A_p is the area of one PCM particle, $R_{[}p, out]$ is the heat transfer resistance generated by heat convection between the outer surface of the PCM capsules, $R_{[}p, cond]$ is the heat conduction resistance by the PCM surface, $R_{[}p, in]$ is the heat transfer resistance generated by the phase change[63].

$$R_{p,out} = \frac{1}{4_{ext} r_0^2} \tag{3.46}$$

$$R_{p,cond} = \frac{1}{4\pi k_{htf}(\frac{1}{r_i} - \frac{1}{r_0})} \tag{3.47}$$

$$R_{p,in} = \frac{1 - \delta^{\frac{1}{3}}}{4_{eff} r_0 \delta^{\frac{1}{3}}} \tag{3.48}$$

h_{ext} is the convective heat transfer coefficient between the outer surface of the capsule and the HTF. k_{eff} is the effective thermal conductivity of phase change heat transfer.

$$h_{ext} = \frac{Nuk}{D_c} \tag{3.49}$$

$$k_{eff} = 0.18 k_{pcm} Ra^{0.25} \tag{3.50}$$

Nu is the Nusselt number and k is the fluid conductivity. Ra is the Rayleigh number and can be calculated with the Grashof and Prandtl numbers. The Grashof number represents the influence of natural convection flow intensity on the heat convection intensity, and Prandtl number reflects the influence of the physical properties of the fluid on the process of heat convection. δ is the ratio of PCM change and can be a number between 0 and 1.

$$Nu = 2.0 + 1.1(6(1-\epsilon))^{0.6} Re_{D-c}^{0.6} PR_f^{1/3} \tag{3.51}$$

$$Re_{D-c} = \frac{\rho_f \overline{u} D_c}{\mu_f} \tag{3.52}$$

$$Ra = GrPr = \frac{g\beta d_9^3 \Delta T}{v^2} \frac{\mu_{pcm} c_{pcm}}{k_{htf}} \tag{3.53}$$

PR_f is the fluid Prandl number, ρ_f is the density of the fluid, μ_f is the viscosity of the fluid and $\overline{u}$ is the superficial velocity in the bed.

$$\overline{u} = \frac{4\dot{m}_f}{\rho_f \pi D_c^2} \tag{3.54}$$

The total power balance for the water during charge is equal to:

$$\begin{aligned}\frac{dT_w,i}{dt}\dot{m}_{w,i}c_{p,w,i} =& -\dot{m}_{w,down}c_{p,w}((T_{w,i-1}(t)-T_{w,i}(t))+\dot{m}_{w,down}c_{p,w}((T_{w,i+1}(t)-T_{w,i}(t))\\ &+(\frac{k+\Delta k)A_c}{\Delta x}((T_{w,i+1(t)}-T_{w,i}(t))-(T_{w,i}(t)-T_{w,i-1}(t)))\\ &-(U_v(T_{w,i}(t)-T_{pcm,i}(t))-\frac{1}{R_{side}}(T_{w,i}(t)-T_)\end{aligned} \tag{3.55}$$

The power balance during the charge for the PCM:

$$\frac{dT_{pcm,i}}{dt}\dot{m}_{pcm,i}c_{p,pcm,i} = (U_v(T_{w,i}(t)-T_{pcm,i}(t)) \tag{3.56}$$

The total power balance for the water during discharge is equal to:

$$\begin{aligned}\frac{dT_w,i}{dt}\dot{m}_{w,i}c_{p,w,i} =& \dot{m}_{w,up}c_{p,w}((T_{w,i-1}(t)-T_{w,i}(t))-\dot{m}_{w,up}c_{p,w}((T_{w,i+1}(t)-T_{w,i}(t))\\ &+(\frac{k+\Delta k)A_c}{\Delta x}((T_{w,i+1(t)}-T_{w,i}(t))-(T_{w,i}(t)-T_{w,i-1}(t)))\\ &+(U_v(T_{w,i}(t)-T_{pcm,i}(t))-\frac{1}{R_{side}}(T_{w,i}(t)-T_)\end{aligned} \tag{3.57}$$

The power balance during charge and during storage for the PCM stays the same. Furthermore, the power balance during storage for the water is:

$$\begin{aligned}\frac{dT_w,i}{dt}\dot{m}_{w,i}c_{p,w,i} =& (\frac{k+\Delta k)A_c}{\Delta x}((T_{w,i+1(t)}-T_{w,i}(t))-(T_{w,i}(t)-T_{w,i-1}(t)))\\ &+(U_v(T_{w,i}(t)-T_{pcm,i}(t))-\frac{1}{R_{side}}(T_{w,i}(t)-T_)\end{aligned} \tag{3.58}$$

The discritizatisation for the LHS model is as follows:

$$\frac{dT_i}{dt} = A_iT_{i-1}+B_iT_i+C_iT_{i+1}+D_i \tag{3.59}$$

$$A_i = (\dot{m}_{up}c_{p,w}+(\frac{k+\Delta k)A_c}{\Delta x}))/(\dot{m}_ic_{p,i}) \tag{3.60}$$

$$B_i = (-2\frac{(k+\Delta k)A_c}{\Delta x}-\frac{1}{R_{side}}-U_vV_{pcm,i})/(\dot{m}_ic_{p,i}) \tag{3.61}$$

$$C_i = (-\dot{m}_{up} c_{p,w} + (\frac{k + \Delta k) A_c}{\Delta x})) / (\dot{m}_i c_{p,i}) \tag{3.62}$$

$$D_i = (T_g R_{side}) / (\dot{m}_i c_{p,i}) \tag{3.63}$$

E_{left}, E_{right} and the vector G are determined the following:

$$E_{left} = \frac{(-\dot{m}_{up} c_{p,w} - \frac{(k+\Delta k) A_c}{\Delta x} - R_{bottom} - U_v V_{pcm,i}) - \frac{\Delta t}{2} + 1}{(\dot{m}_i c_{p,i})} \tag{3.64}$$

$$E_{right} = \frac{(\dot{m}_{up} c_{p,w} - \frac{(k+\Delta k) A_c}{\Delta x} - R_{top} - U_v V_{pcm,i}) - \frac{\Delta t}{2} + 1}{(\dot{m}_i c_{p,i})} \tag{3.65}$$

$$G(i) = \frac{U_v V_{pcm,i} T_{pcm,i} \Delta t}{\dot{m}_i c_{p,i}} \tag{3.66}$$

$$G(1) = \frac{U_v V_{pcm,i} T_{pcm,i} \Delta t}{\dot{m}_i c_{p,i}} + \frac{((2\dot{m}_{up} c_{p,w} T_{in}) - (R_{side} T_g) + (R_{bottom} T_g)) \Delta t}{(\dot{m}_i c_{p,i})} \tag{3.67}$$

$$G(n) = \frac{U_v V_{pcm,i} T_{pcm,i} \Delta t}{\dot{m}_i c_{p,i}} + \frac{((-2\dot{m}_{up} c_{p,w} T_{out}) - (R_{side} T_g) + (R_{top} T_g)) \Delta t}{(\dot{m}_i c_{p,i})} \tag{3.68}$$

The temperature increase or decrease of the PCM material does not follow a constant linear pattern. The pattern can be divided into three linear parts as visualized in Figure 3.11. The ideal situation is depicted by the dotted lines where there would be one melting temperature. In reality, the melting temperature has a lower and a higher point and does not stay constant during the latent heat absorption or extraction.

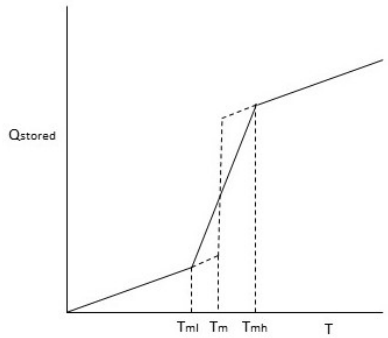

Figure 3.11: *The temperature versus the stored heat in a phase change material with the ideal situation depicted with a dotted line and the realistic situation depicted with a straight line.*

The liquid fraction can be determined as follows;

$$\epsilon_b(T) = \frac{T_{pcm,i} - T_{ml}}{T_{mh} - T_{ml}} \tag{3.69}$$

The specific enthalpy of the bed, h_b, is determined as follows:

$$h_b = c_{p,s}\Delta T_b, T_b < T_{ml} \tag{3.70}$$

$$h_b = \Delta h_s \epsilon_b, Tml < Tb < T_{mh} \tag{3.71}$$

$$h_b = c_{p,l}\Delta T_b, T_b > T_{mh} \tag{3.72}$$

$c_{p,s}$ and $c_{p,l}$ are the specific heats for the solid and liquid phases of the PCM material.

The total energy stored in the PCM can be calculated in the following:

$$Q_{stored,pcm} = \sum_{i=1}^{i=n} m_{pcm,i}\left(\int_{T_{pcm,0}}^{T_{pcm,ml}} c_{pcm,s}\, dT + \int_{T_{pcm,ml}}^{T_{pcm,mh}} c_{pcm,s}\epsilon_b(T)\Delta h_b\, dT + \int_{T_{pcm,mh}}^{T_{pcm,f}} c_{pcm,l}\, dT\right. \tag{3.73}$$

The power output, total energy put in the storage system, extracted from the storage system, and lost in the storage system can be calculated the same as for the SHS:

$$P_{out}(t) = \dot{m}_{out} c_{p_{out}}(T_{w,out}(t) - T_{w,in}(t) \tag{3.74}$$

$$E_{out} = \int_{t_1}^{t_2} \dot{m}_{out} c_{p_{out}}(T_{w,out}(t) - T_g(t)\, dt \tag{3.75}$$

$$Q_{loss} = \sum_{i=1}^{i=n} \int_{t_1}^{t_2} \frac{(T_{w,i}(t) - T_g(t)}{(R_w + R_g)}\, dt \tag{3.76}$$

$$E_{in} = \int_{t_1}^{t_2} \dot{m}_{out} c_{p_{out}}(T_{w,in}(t) - T_g(t)\, dt \tag{3.77}$$

$$\eta = \frac{E_{out}}{E_{in} + \dot{W}_{pump}} \tag{3.78}$$

3.3.4 Model Thermochemical Energy Storage

Figure 3.12 gives a visual representation of the fixed bed reactor and the energy transport within the layers that are modeled. The solid and the air in the reactor at height x are assumed to be equal. The equations that can be used in the model are the following for sorption and reaction-based energy storage:

$$A_{(s)} + H_2OA_{(g)} \leftrightarrow B_{(s)} + \Delta H_R \tag{3.79}$$

$$A_{(s)} + \Delta H_R \leftrightarrow B_{(s)} + C_{(s)} \tag{3.80}$$

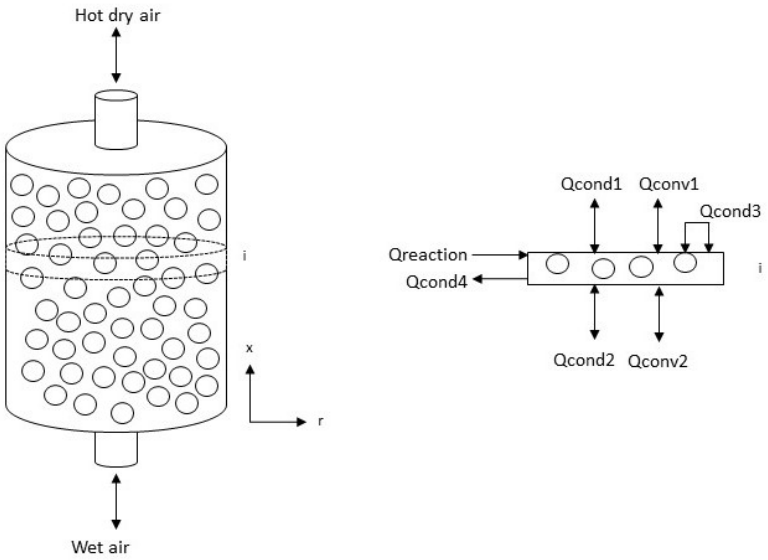

Figure 3.12: *The heat transfer in a thermo-chemical energy storage tank*

The Energy balance is used to create an equation to determine the temperature at layer i and time t.

$$\begin{aligned}\frac{dT_i}{dt} V_i(\epsilon c_{p,htf}\rho_f + (1-\epsilon)c_{p,pc}\rho_s) = &- \Delta T_{i-1}\dot{m}c_{p,htf} - \Delta T_{i-1}U_{eff}A_i \\ &+ \Delta T_{i+1}\dot{m}c_{p,htf} + \Delta T_{i+1}U_{eff}A_i + \Delta H_R R_s N_s (1-\epsilon)V_i\end{aligned} \tag{3.81}$$

ϵ is the porosity of the bed. $c_{p,htf}$ $c_{p,pc}$ are the specific heat capacity of the HTF and the Potassium Carbonate. The effective thermal conductivity is U_{eff} and the area of the top

and bottom of the layer of the tank is A_i. The volume of the layer is called V_i and the concentration of the zeolite is given by N_s. Lastly, the reaction enthalpy is depicted by ΔH_R.

The power balance during the charge for the Potassium Carbonate:

$$\frac{dT_{pc,i}}{dt}\dot{m}_{pc,i}c_{p,pc,i} = (U_v(T_{htf,i}(t) - T_{pc,i}(t)) + \Delta H_R R_s N_s V_i \tag{3.82}$$

The discritizatisation for the LHS model is as follows:

$$\frac{dT_i}{dt} = A_i T_{i-1} + B_i T_i + C_i T_{i+1} + D_i \tag{3.83}$$

$$A_i = (\dot{m}_{up}c_{p,w} + (\frac{k+\Delta k)A_c}{\Delta x}))/(\dot{m}_i c_{p,i}) \tag{3.84}$$

$$B_i = (-2\frac{(k+\Delta k)A_c}{\Delta x} - \frac{1}{R_{side}} - V_{chem,i}U_{eff})/(\dot{m}_i c_{p,i}) \tag{3.85}$$

$$C_i = (-\dot{m}_{up}c_{p,w} + (\frac{k+\Delta k)A_c}{\Delta x}))/(\dot{m}_i c_{p,i}) \tag{3.86}$$

$$D_i = (T_g R_{side})/(\dot{m}_i c_{p,i}) \tag{3.87}$$

E_{left}, E_{right} and the vector G are determined the following:

$$E_{left} = \frac{-\frac{\Delta t}{2}(-\dot{m}_{up}c_{p,w} - \frac{(k+\Delta k)A_c}{\Delta x} - R_{bottom} - U_{eff}V_{chem,i}) + 1}{\dot{m}_i c_{p,i}} \tag{3.88}$$

$$E_{right} = \frac{-\frac{\Delta t}{2}(\dot{m}_{up}c_{p,w} - \frac{(k+\Delta k)A_c}{\Delta x} - R_{top} - U_{eff}V_{chem,i}) + 1}{\dot{m}_i c_{p,i}} \tag{3.89}$$

$$G(i) = \frac{U_{eff}V_{chem,i}T_{chem,i}\Delta t}{\dot{m}_i c_{p,i}} \tag{3.90}$$

$$G(1) = \frac{U_{eff}V_{chem,i}T_{chem,i}\Delta t}{\dot{m}_i c_{p,i}} + \frac{((2\dot{m}_{up}c_{p,w}T_{in}) - (R_{side}T_g) + (R_{bottom}T_g))\Delta t}{(\dot{m}_i c_{p,i})} \tag{3.91}$$

$$G(n) = \frac{U_{eff} V_{chem,i} T_{chem,i} \Delta t}{\dot{m}_i c_{p,i}} + \frac{((-2\dot{m}_{up} c_{p,w} T_{out}) - (R_{side} T_g) + (R_{top} T_g))\Delta t}{(\dot{m}_i c_{p,i})} \tag{3.92}$$

The reaction rate for reaction-based thermochemical storage can be calculated using the following equation[30]:

$$R_s = A e^{\frac{-E_a}{RT}} (1 - y_f)^n \frac{P_w}{P_{eq}} \tag{3.93}$$

A is the pre-exponential factor, y_f is the conversion, E_a is the activation energy, R is the gas constant and n is the reaction order. P_w is the vapor pressure and P_eq is the equilibrium water vapor pressure. The vapor pressure can be measured and the equilibrium water vapor pressure can be calculated the following:

$$P_{eq} = 4.228 * 1012 e^{\frac{-7337}{T}} \tag{3.94}$$

Gaeini et al found the activation energy and the pre-exponential factor for potassium carbonate, shown in Table 3.3, experimentally.

Table 3.3: *The material properties of Potassium Carbonate*

Potassium Carbonate				
	$E_a(J/mol)$	A(min^{-1})	$H_r(J/kg)$	Pw/Peq
Hydration	46220	1083800	710000	16.25
Dehydration	78305.63	88980*10^6	710000	0.45

From the model the following outputs can be used;

$$Q_{th} = \int_{t1}^{t2} \dot{m}_f c_{pf} (T_{out} - Tin)\, dt \tag{3.95}$$

$$P_{th} = \dot{m}_f c_{pf} (T_{out} - Tin) \tag{3.96}$$

3.4 Validation

In this section, the validation for the models will be given. First, the models will be compared to experiments. The parameters are set to the parameters of the experiments and the results are plotted versus the data of the experiment. The root mean square error (RMSE) is then calculated in absolute values and in percentages.
The SHS model will be validated in charging mode with two different mass flows to validate the temperature profile and the thermal stratification in the tank. The SHS will also be validated in storage mode to validate the losses of the HWTS. The temperature profile will be validated with an experiment of 75 minutes and the yearly losses will be validated with the yearly losses of existing PIT storage.
The LHS will be validated in charging and discharging mode with two different experiments to validate the temperature profile in the tank and the heat exchange between the HTF and the PCM.
Lastly, the reaction rate and conversion for hydration and dehydration are validated. Furthermore, the heat extraction during hydration is validated.
Then, an analysis will be made for the number of nodes and the timestep that is used in the model. To make this analysis the model is used to simulate the supply by the heat storage technologies with the yearly demand of 200 households connected to a DHN. The temperature profile in the tank throughout one year and the heat losses are used to compare the results.
The last step is an analysis of the thermal radius calculated to determine the losses in the ground for SHS and LHS. The temperature in the tank and the time are varied to find the length of the thermal radius.

Sensible Heat Thermal Energy Storage Experiment Validation

The model is validated by comparing the results of a simulated situation to the results of an experiment with the same circumstances. The experiment was executed by Chu. [17]. The experiment consisted of a water tank with a height of 1/575 m, a volume of 0.454 m^3, and a tank loss coefficient of 1.224 $\frac{kJ}{hm^2K}$. The water inlet is placed at the top and the water outlet is placed at the bottom of the tank. Furthermore, the inlet temperature was set to 335.15 K and the uniform starting temperature of the water tank was set to 295.15 K. The charging of the tank was executed with an inlet mass flow of 2 $\frac{L}{s}$ and a duration of 2.5 hours. The temperature profile in the tank was measured with a probe with nine thermocouples. The thermocouples are placed approximately 15 cm apart and start at the top of the tank. The temperature at the bottom of the tank is therefore not measured. The results of the experiment and the model are depicted in Figure 3.13. The experiment was also executed with a mass flow of 3 $\frac{L}{s}$ which is depicted in Figure 3.14.

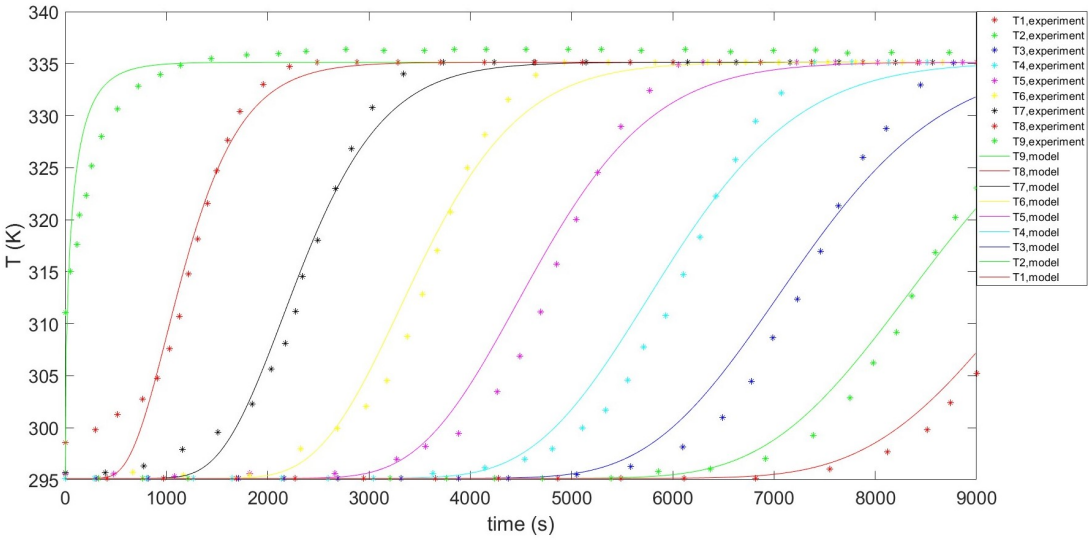

Figure 3.13: *SHS model validation with the experiment by Chu et al[17], with a massflow of 2L/s. The colors represent different locations in the tank with the first green line as the top of the tank. The lines are the model and the dots are the experimental values.*

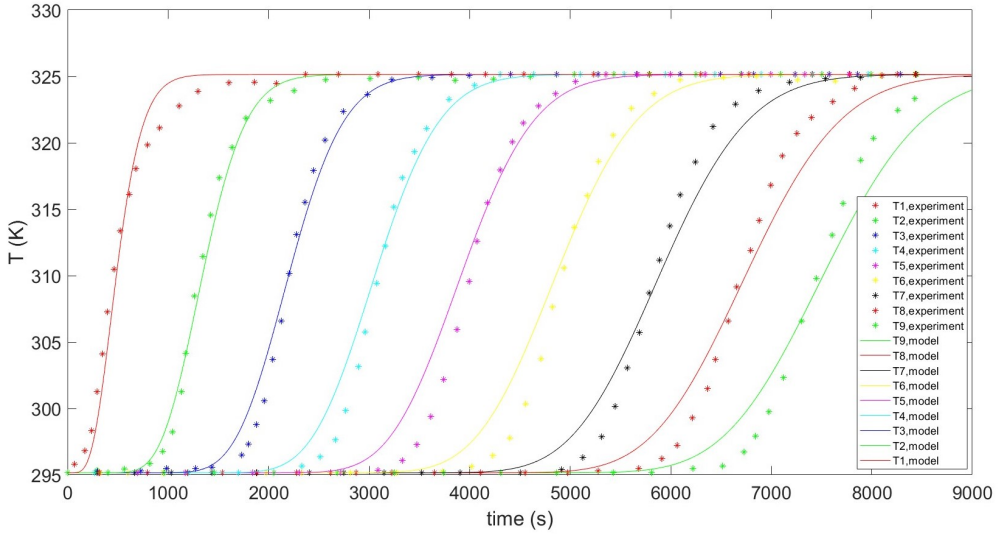

Figure 3.14: *SHS model validation with the experiment by Chu et al[17], with a massflow of 3L/s. The colors represent different locations in the tank with the first green line as the top of the tank. The lines are the model and the dots are the experimental values.*

In order to quantify the modeling error the root mean square error (RMSE) in percentage can be calculated[28].

$$RMSE = \sqrt{\frac{\sum_{i=1}^{n}((T_{experiment,i} - T_{model,i})/T_{experiment,i})^2}{n}} \tag{3.97}$$

The RMSE of the experiment with a mass flow of 2 $\frac{L}{s}$ is shown per layer in Table 3.4 and for 3 $\frac{L}{s}$ in Table 3.5.

Table 3.4: *Root mean square error of the model and the experiment by Chu et al. [17] with a mass flow of 2L/min in charging mode*

T(K)	**Top**	**Layer 8**	**Layer 7**	**Layer 6**	**Layer 5**	**Layer 4**	**Layer 3**	**Layer 2**	**Bottom**
RMSE	1.98	1.83	1.46	1.69	2.00	2.10	2.33	1.17	0.76
RMSE (%)	0.62	0.59	0.46	0.52	0.63	0.66	0.72	0.38	0.25

Table 3.5: *Root mean square error of the model and the experiment by Chu et al. [17] with a mass flow of 3L/min in charging mode*

T(K)	**Top**	**Layer 8**	**Layer 7**	**Layer 6**	**Layer 5**	**Layer 4**	**Layer 3**	**Layer 2**	**Bottom**
RMSE	1.63	0.88	1.05	1.27	1.61	1.52	1.54	1.66	1.75
RMSE (%)	0.52	0.28	0.35	0.42	0.54	0.50	0.50	0.53	0.56

The biggest difference between the model and the experimental data is the rounding shape at the beginning and the end of the heating up of a layer. A possible explanation of this difference is the mixing between layers. In the model, this has not been taken into account however it is a phenomenon that occurs in tanks with thermal stratification. In the bottom of the tank the data of the experiments match the data provided by the model better and this might be explained by the fact that mixing between layers has less effect in the bottom of the tank because other forms of heat conduction and convection have had more time to progress and therefor creating a slower heating up of the bottom of the tank creating more round shapes of the temperature lines.

The storage losses of the model are also important to validate because the storage losses determine the size and therefore energy capacity of the tank necessary to supply the load after half a year of storage. As stated by Xu et all. it is difficult to validate the storage losses of PTES systems: "Since only a few large-scale PTES are running, it is difficult to validate and modify existing models due to limited experimental data."
No data of HWTS without charging and discharging for long timeframes exist. In order to validate the model without long-term data, the experiments by Bai et al. [12] are used. The experiments provide losses over a timeframe of 75 minutes. Pit storage with a height of 5 m, a volume of 3000 m^3, and a concrete wall of 0.3 m are modeled in storage mode. The lid consists of a 0.2 m polystyrene board covered by 1 m soil. The tank is discharged with a mass flow of 0.6 $\frac{kg}{s}$. Figure 3.15 shows the model compared to the experiment and Table 3.6 shows the root mean square error.

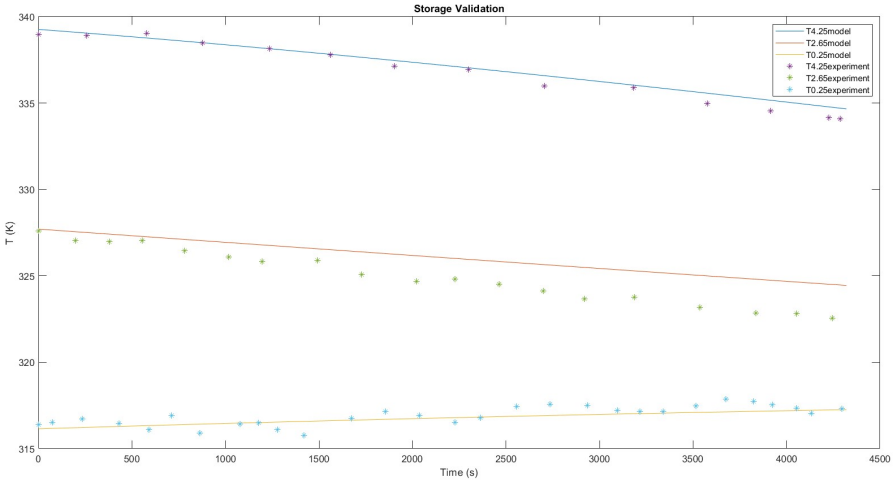

Figure 3.15: *Validation of the model with the experiments by Bai et al. [12] in storage mode*

The RMSE in percentage is shown in Table 3.6.

Table 3.6: *Root mean square error of the model with the experiments by Bai et al. [12] in storage mode*

T(K)	**Top**	**Middle**	**Bottom**
RMSE	0.40	1.77	0.97
RMSE (%)	0.12	0.55	0.29

The data provided by the models made by Dahash et al. is validated with experiments of tank TES and pit TES [Dahash et al.]. These models are used to provide calculations of the annual energy loss of the tanks underground. A tank underground is simulated with a diameter of 50.5 meters and a height of 50 meters. The tank is covered with a lid. The total heat transfer coefficient of the top is 0.1 $\frac{W}{mK}$ and of the wall and bottom are 0.3 $\frac{W}{mK}$. The results of the simulation are presented in Figure 4.22b.

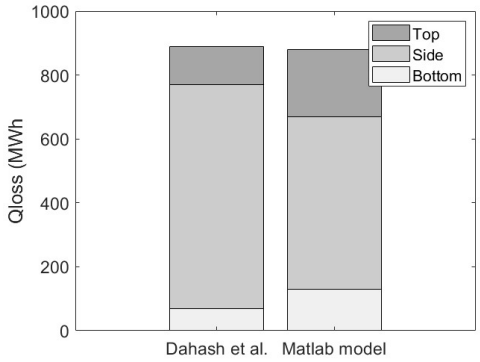

Figure 3.16: *The losses calculated with the model by Dahash et al. [Dahash et al.] and the losses from the Matlab model per area of the tank.*

The Pit TES in Dronningland is a state-of-the-art system[61] and data from this Pit storage is used to validate the Matlab model. The Pit consists of a lid of 91 by 91 meters and the bottom is 26 by 26 meters. The height of the storage is 16 meters. Furthermore, the volume is 62000 m^3. In summer the temperature in the storage tank varies between 50 °C and 85 °C and in winter it varies between 12 °C and 50 °C. The annual heat loss estimated by Sifnaios is 2260 MWh per annum. The model estimates 1986 MWh. This is a difference of 12 %. The difference can be explained by the estimation of the water temperatures in the tank. In the model, average temperatures are used while in the real-time data, the exact temperatures vary.

Latent Heat Thermal Energy Storage Experiment Validation

The experiment conducted by Nallusamy et al. was used to validate the model[45].

The tank in this experiment has a height of 460 mm and a diameter of 360 mm. The PCM is encapsulated and has a diameter of 55 mm. The tank is filled with 264 capsules with PCM material having a volume of 0.023 m^3. This is equal to the volume of the HTF, water, which leads to a ϵ of 0.5. The mass flow rate of the HTF is 2 $\frac{L}{min}$ and has a temperature of 243.15 K. The temperature of the water in the tank and the PCM material at the beginning of the experiment is 305.15 K. The properties of the PCM used are depicted in Table 3.7.

Table 3.7: *Material properties of the phase change material Paraffin used in the experiment by Nallusamy et al. [45]*

Melting Temperature (K)	Latent Heat of Fusion (kJ/kg)	Density (kg/m3)		Specific Heat (J/kg K)		Thermal Conductivity (W/m K)	
		Solid	Liquid	Solid	Liquid	Solid	Liquid
333.15	213	861	778	1850	2384	0.4	0.15

The model is run with the inputs from the experiment. Figure 3.17 shows the results of the experiment and the model for the charging process and Figure 3.18 for the discharging

process.

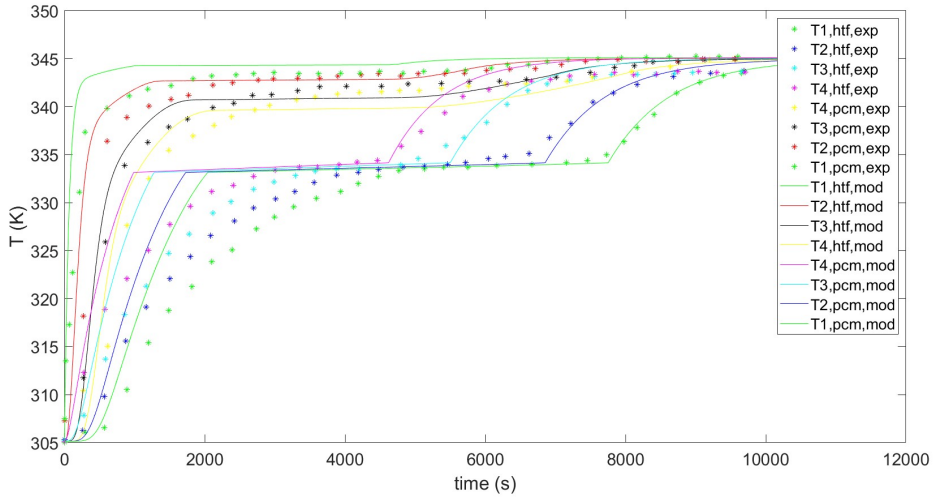

Figure 3.17: *LHS model validation for charging with experiment by Nallusamy et al.[45]. The colors represent different locations in the tank with the first green line as the top of the tank. The lines are the model and the dots are the experimental values.*

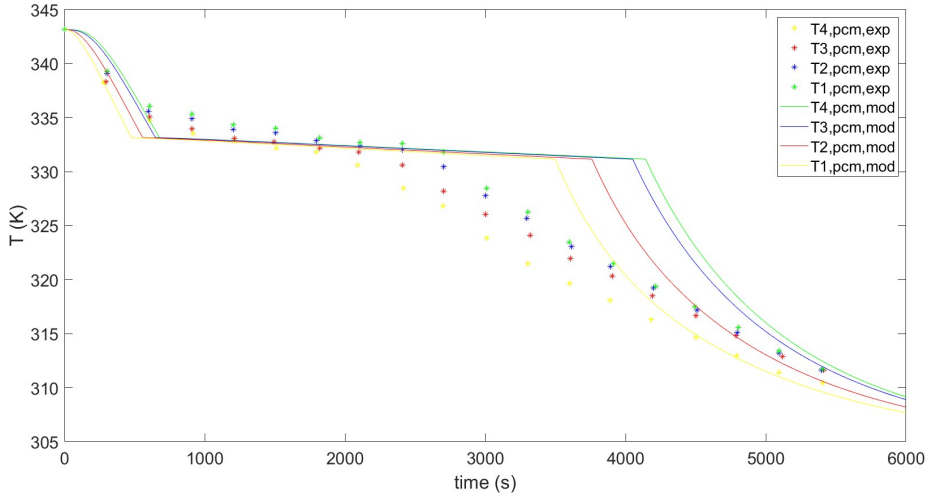

Figure 3.18: *LHS model validation for discharging with experiment by Nallusamy et al.[45]. The colors represent different locations in the tank with the first green line as the top of the tank. The lines are the model and the dots are the experimental values.*

The RMSE for charge is shown in Table 3.8 and for discharge in Table 3.9.

Table 3.8: *Root mean square error for the model validation for charging with experiment by Nallusamy et al.[45]*

Material	**HTF**				**PCM**			
T(K)	**Top**	**Layer 3**	**Layer 2**	**Bottom**	**Top**	**Layer 3**	**Layer 2**	**Bottom**
RMSE	13.9	10.3	5.6	4.7	5.1	8.2	13.6	17.4
RMSE (%)	4.1	3.0	1.6	1.4	1.5	2.5	4.2	5.5

Table 3.9: *Root mean square error for the model validation for discharging with experiment by Nallusamy et al.[45]*

T(K)	**Top**	**Layer 3**	**Layer 2**	**Bottom**
RMSE	6.8	4.9	3.1	2.5
RMSE (%)	2.1	1.5	1.0	0.8

The experiment conducted by Sun et al. is also used to validate the model[63]. The tank in this experiment has a height of 260 mm and a diameter of 170 mm. The PCM is encapsulated and has a diameter of 50 mm. The tank is filled with 40 capsules with PCM material having a volume of 0.0026 m^3. This is equal to the volume of the HTF, water, which leads to a ϵ of 0.5. The mass flow rate of the HTF is 0.0331 $\frac{kg}{s}$ and has a temperature of 353.15 K. The temperature of the water in the tank and the PCM material at the beginning of the experiment is 308.15 K. The properties of the PCM used are depicted in Table 3.10.

Table 3.10: *Material properties of the phase change material Paraffin in the experiment by Sun et al. [63]*

Melting Temperature (K)	**Latent Heat of Fusion (kJ/kg)**	**Density (kg/m3)**		**Specific Heat (J/kg K)**		**Thermal Conductivity (W/m K)**	
		Solid	**Liquid**	**Solid**	**Liquid**	**Solid**	**Liquid**
334.15	174.7	1038.15	915.75	1722	2147	0.4	0.4

The model is run with the inputs from the experiment. Figure 3.19 shows the results of the experiment and the model.

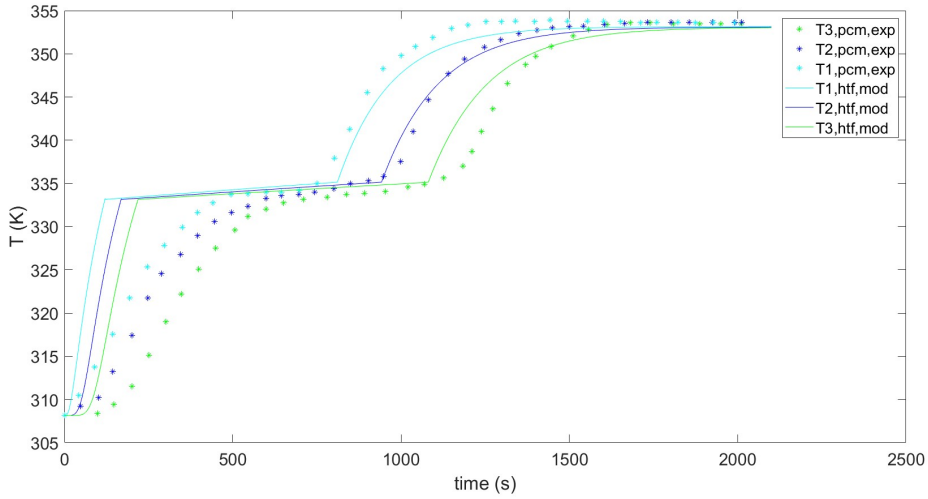

Figure 3.19: *LHS model validation for discharging with experiment by Sun et al.[63]. The colors represent different locations in the tank with the first green line as the top of the tank. The lines are the model and the dots are the experimental values.*

The RMSE in percentage is shown in Table 3.11.

Table 3.11: *Root mean square error for the model validation for charging with experiment by Sun et al.[63]*

T(K)	**Top**	**Middle**	**Bottom**
RMSE	18.0	16.0	15.5
RMSE (%)	5.6	5	4.8

Both Figure 3.17 and Figure 3.19 show that the PCM material temperature, calculated in the model, follows the temperature trend of the experiment. The biggest differences between the model and the experiment are found in the region where the pcm material stores sensible heat before reaching the melting temperature. Furthermore, in both experiments, the PCM temperature has a more fluid temperature change around the melting temperature than in the model as is visible in Figure 3.17 and Figure 3.18. The combination of these differences between the experiments and the model can possibly be explained by varying δ which is affected by the ratio of the PCM material that has gone through the phase change and that therefore affects the internal heat resistance of the PCM material. The model depicts the ideal situation where the PCM material will not enter the phase change before the melting temperature is reached. However during the experiment part of the PCM material can already reach the phase change region before the center of the PCM material has reached the melting temperature, increasing the internal heat resistance. When the internal heat resistance has increased the temperature of the PCM material will increase less rapidly which can be the explanation for the slower increase in PCM temperature before the phase change region in the experiments.

For the charging process, the model follows the experimental results when the melting temperature is reached. For the discharging process, shown in Figure 3.18, the process happens

the other way around and the model follows the experimental results until the melting temperature is reached after which a difference occurs until the temperature of the PCM material reaches 303.15 K.

The difference between the model and the experiments can possibly have an effect on the energy storage calculations. The energy storage calculations consist of sensible heat storage and latent heat storage. In the model, the PCM material has completely stored all the sensible heat storage before reaching the melting phase and storing latent heat. However, in practice, these heat storage mechanisms can happen simultaneously in the same PCM capsule. Resulting in a different temperature profile the time. This does not have an effect on the amount of heat that is stored in the material in total. The amount of heat stored in the PCM material is determined by the heat transferred to the material from the HTF. Whether this heat is then stored as sensible heat or as latent heat does not affect the amount of heat that is stored. As Figure 3.17 and Figure 3.18 show the process is completely reversible and the amount of heat transferred to or from the material therefore too. Since the heat resistance of the material is assumed constant throughout the process the heat transfer is determined by the temperature difference between the HTF and the PCM material. This temperature difference has a maximum of 10 K at 4000 s during the discharging process. The maximum temperature difference between the model and the experimental results is thus 3 % difference of the PCM temperature, leading to a maximum error of 3 % in the energy storage calculations for the PCM material between the melting temperature and the discharge temperature. In practice, this difference will be smaller with each step the time frame is made longer and when the whole cycle is chosen to compare the error is 0 %.

Thermochemical Energy Storage Experiment Validation

First, the model for the reaction kinetics of Potassium Carbonate will be validated. The experiments conducted by Gaieni et al. will be used. The experiments are conducted with a flow rate of 500 $\frac{ml}{min}$. The sample is dehydrated in dry air with a heating rate of 10 $\frac{K}{min}$ from ambient temperature to 100 °C. Then the temperature is cooled down back to ambient temperature. The hydration is then executed by adding humid air to the sample. In order to validate the reaction rate the experiment with a hydration temperature of 26 °C and a $\frac{P_w}{P_{eq}}$ of 16.25 is used. The results are depicted in Figure 3.20.

The RMSE is shown in Table 3.12.

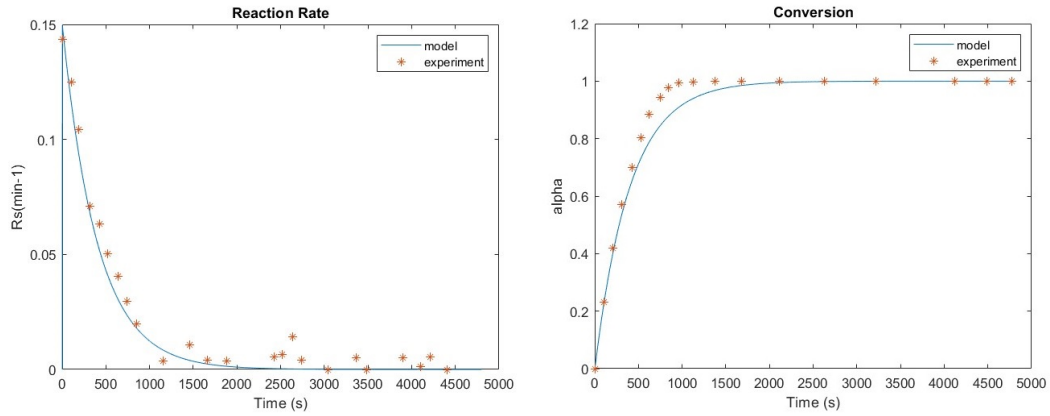

Figure 3.20: *Thermo-chemical energy storage model validation for hydration reaction rate and conversion with the experiment by Gaeini et al.[30]*

The RMSE is shown in Table 3.12. The absolute RMSE is very small, but the RMSE for the reaction rate in percentage is relatively high. The reason for this high RMSE is the reaction rates from the experiment after 2000 seconds that are not zero. These affect the RMSE a lot more than the absolute RMSE. The reason for these differences between the model and the experiment can be measurement errors.

Table 3.12: *Root mean square error for the model validation for hydration reaction rate and conversion with the experiment by Gaeini et al.[30]*

	Rs	**Alpha**
RMSE	0.007	0.053
RMSE (%)	68.1	6.1

The heat produced during the reaction can be calculated with the reaction enthalpy and the reaction rate and is plotted in Figure 3.21. This is the heat produced per gram of material. The weight of the material is taken as constant in the model. However in reality the weight changes during hydration and dehydration. The trend in the experimental data is more linear than in the model and the addition of the weight of the material can be the reason for this. During hydration, water molecules are adsorbed onto the Potassium Carbonate leading to a higher weight as the conversion increases. When weight increases the heat extraction per g decreases. This phenomenon could lead to a steeper decrease in heat produced per gram than calculated in the model where this increase in weight is neglected.

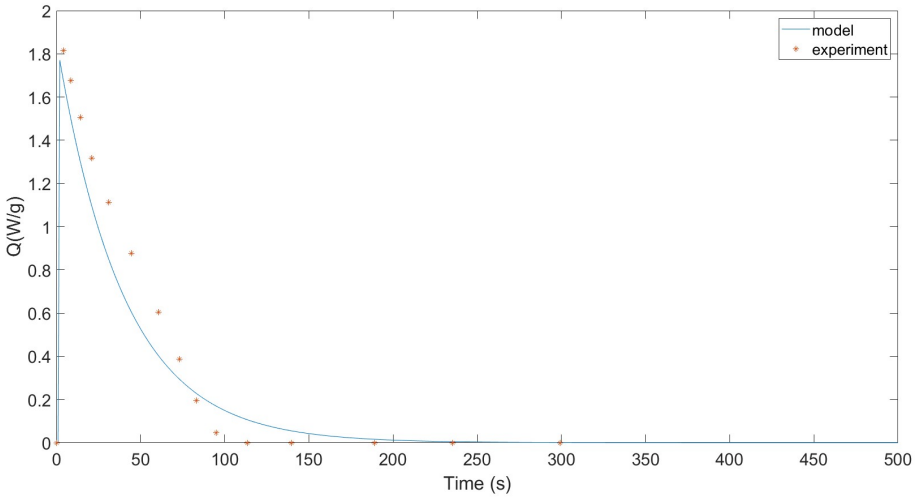

Figure 3.21: *Thermo-chemical energy storage model validation for heat extraction with the experiment by Gaeini et al.[30]*

The RMSE is shown in Table 3.13.

Table 3.13: *RMSE Heat Extraction*

	Q
RMSE (W/g)	0.154
RMSE (%)	16.7

The reaction kinetics and the conversion for the dehydration are plotted in Figure 3.22.

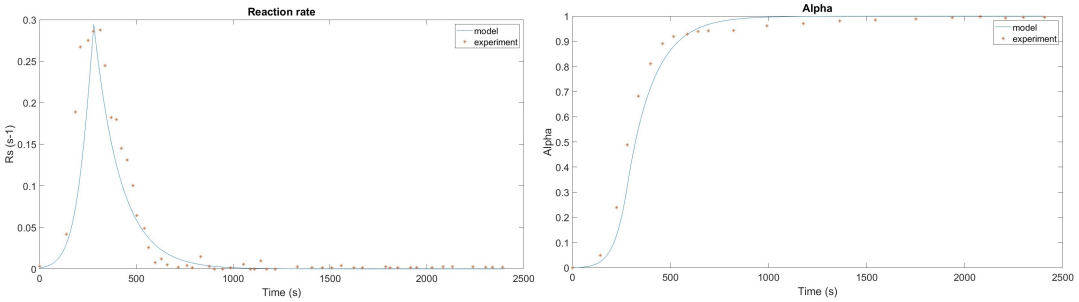

Figure 3.22: *Thermo-chemical energy storage model validation for dehydration reaction rate and conversion with the experiment by Gaeini et al.[30]*

The RMSE is shown in Table 3.14.

Table 3.14: *Root mean square error of the thermo-chemical energy storage model validation for dehydration reaction rate and conversion with the experiment by Gaeini et al.[30]*

	Alpha	**Rs**
RMSE	0.062	0.034
RMSE (%)	15.9	37.7

The energy released in the experiment is 4.796 J [30]. The energy released by the reaction in the experiment called $Q_{reaction}$, is calculated to be 5.3570 J. The outcome has an error of approximately 10 % compared to the outcome of the experiment because the calculated energy that is released depends on the reaction rate which is not exactly the same as the reaction rate in the experiment as is shown in Figure 3.21. The energy transported by the air, called $Q_{reactor}$, is 5.3164 J. The energy necessary for dehydration is calculated to be 5.6800 J. This results in an efficiency of 94 %.

$$Q_{reaction} = H_r R_s m_{zeo} \tag{3.98}$$

$$Q_{reactor} = (T_{out} - T_{in}) c_{p,air} \dot{m}_{air} \tag{3.99}$$

3.4.1 Sensible Heat Thermal Energy Storage Node and Timestep Analysis

The analysis for the number of nodes will be performed with a timestep of one hour for the demand profile of a whole year with the SHS model. Figure 3.23 gives an overview of the simulations with a different number of nodes. The more nodes are used, the more the temperature of the layers fluctuates and is influenced by the demand. This was expected because the more nodes, the smaller the water layers and the more influence and extraction or addition of hot or cold water have on each layer. When the nodes are increased above ten, a temperature rise can be seen for the bottom layer. This is not expected because the tank is only discharged in this scenario and no warm water is added. The temperature rise can be explained by the decrease in layer thickness again. When the layers are smaller the addition of cold water has a more local and greater effect on some layers. When after the addition of cold water at the bottom during discharge the tank is not being discharged the water has a chance to distribute its heat. The temperature rise happens after this discharge when the tank is distributing the heat more equally.

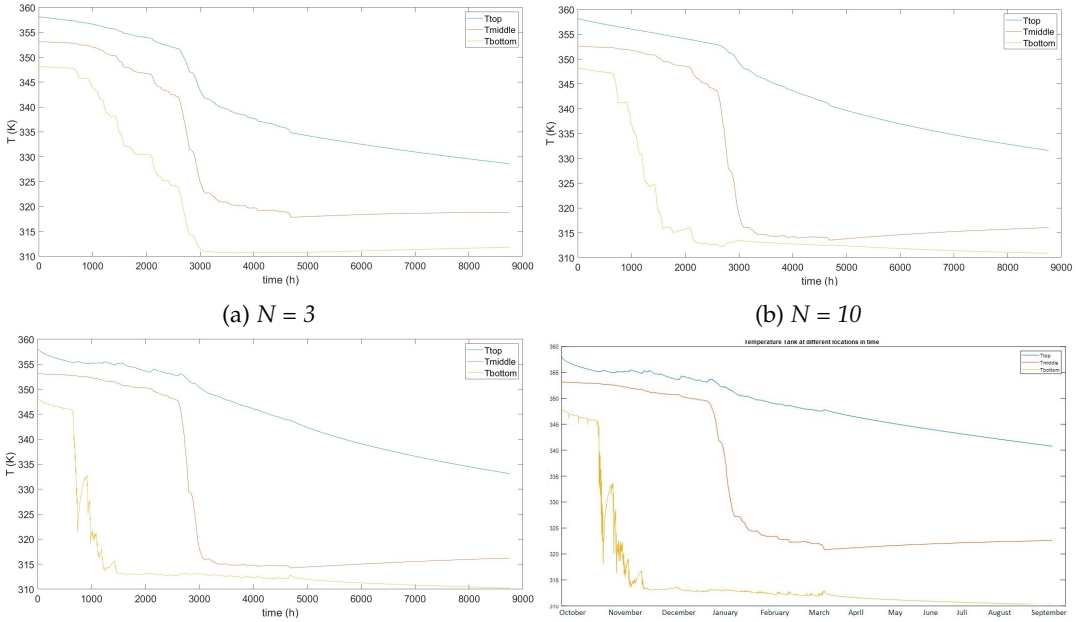

(a) $N = 3$ (b) $N = 10$

(c) $N = 100$ (d) $N = 1000$

Figure 3.23: *Analysis of the temperature profile for the number of nodes for sensible energy storage*

Table 3.15: *Analysis of the heat loss for the number of nodes for sensible energy storage*

n	3	10	100	1000
Qloss (kWh)	48.90	48.40	47.93	47.85

Then the analysis for the time step will be made with the number of nodes set to 10 and is displayed in Figure 3.24.

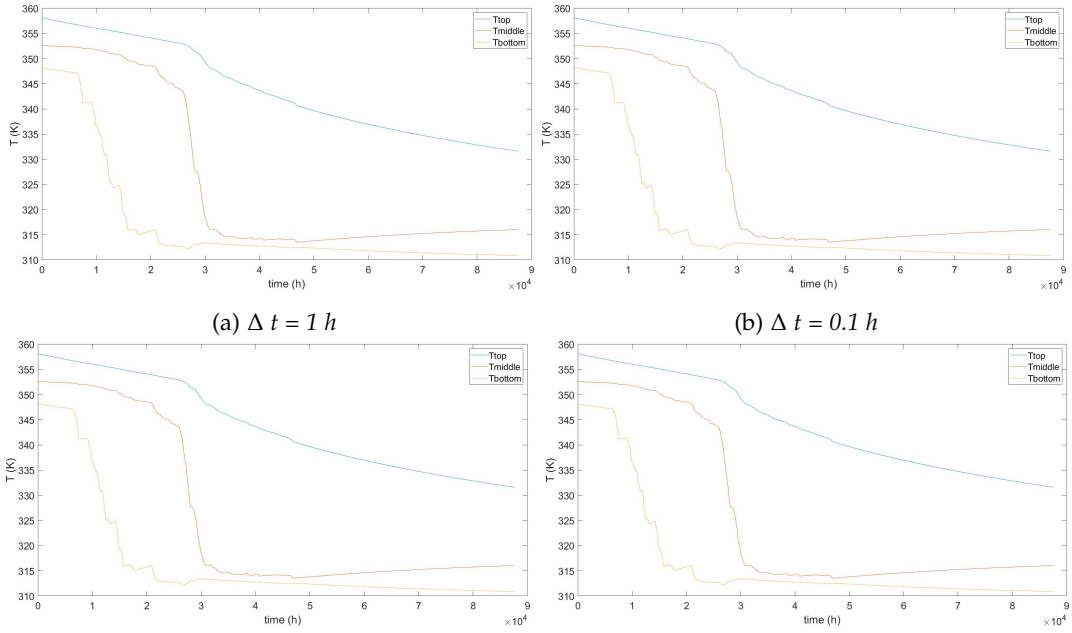

(a) Δ t = 1 h (b) Δ t = 0.1 h

(c) Δ t = 0.01 h (d) Δ t = 0.001 h

Figure 3.24: *Analysis of the temperature profile for the timestep for sensible energy storage*

Table 3.16: *Analysis of the heat loss for the timestep for sensible energy storage*

Δ t	1	0.1	0.01	0.001
Qloss (kWh)	48.40	48.40	48.40	48.40

The time step analysis shows that the temperature profile becomes more accurate when the time step is set to 0.1 hours and will not become more accurate when the time step is set to smaller.

The increase in the number of nodes shows a more accurate result for every increase. This was expected because the number of thermal stratification layers increases. The amount of heat loss changes with each increase in the number of nodes while it stays the same for the decrease in time step as is shown in Table 3.16. This is not expected because the temperature profile is different for different time steps. The heat loss for a time step of 1 h in joule is 1.74227e+11 j and for a time step of 0.1 h, the heat loss is equal to 1.74232e+11 j. The difference is visible here but is too small to be expressed in kWh. The model with 1000 nodes and a time step of one hour had a running time of 14 hours. Therefore the results of this research for the SHS model will be computed with 100 nodes and a time step of 0.1 hours.

3.4.2 Latent Heat Thermal Energy Storage Node and Timestep Analysis

The analysis for the LHS model will also include an analysis of the influence of the number of nodes and the time step. The increase in complexity of the model increases the compu-

tational time. Therefore the analysis is made with time steps ranging from 0.01 hours to 1 hour and the number of nodes varies from 3 to 100. First, an analysis of the time step will be made. Figure 3.25 and Table 3.17 show the temperature profile and the total annual heat loss for different time steps. The temperature profile becomes more accurate when the time step is decreased. The biggest difference is visible between a time step of 1 hour and 0.1 hours. In order to minimize the computational time, but still find an accurate enough result the choice for a time step of 0.1 hours has been made.

Figure 3.25: *Analysis of the temperature profile for the timestep for latent energy storage*

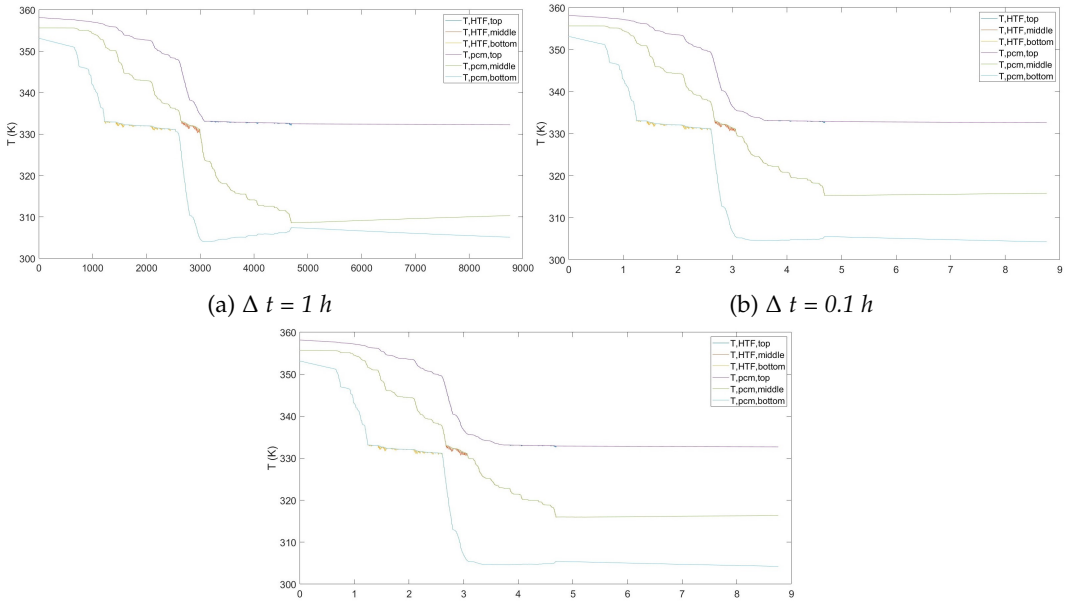

(a) $\Delta\ t = 1\ h$

(b) $\Delta\ t = 0.1\ h$

(c) $\Delta\ t = 0.01\ h$

Table 3.17: *Analysis of the heat loss for the timestep for latent energy storage*

delta t	1	0.1	0.01
Qloss (kWh)	31.84	22.98	22.05

The analysis for the number of nodes will then be made with a time step of 0.1 hours which is displayed in Figure 3.26.

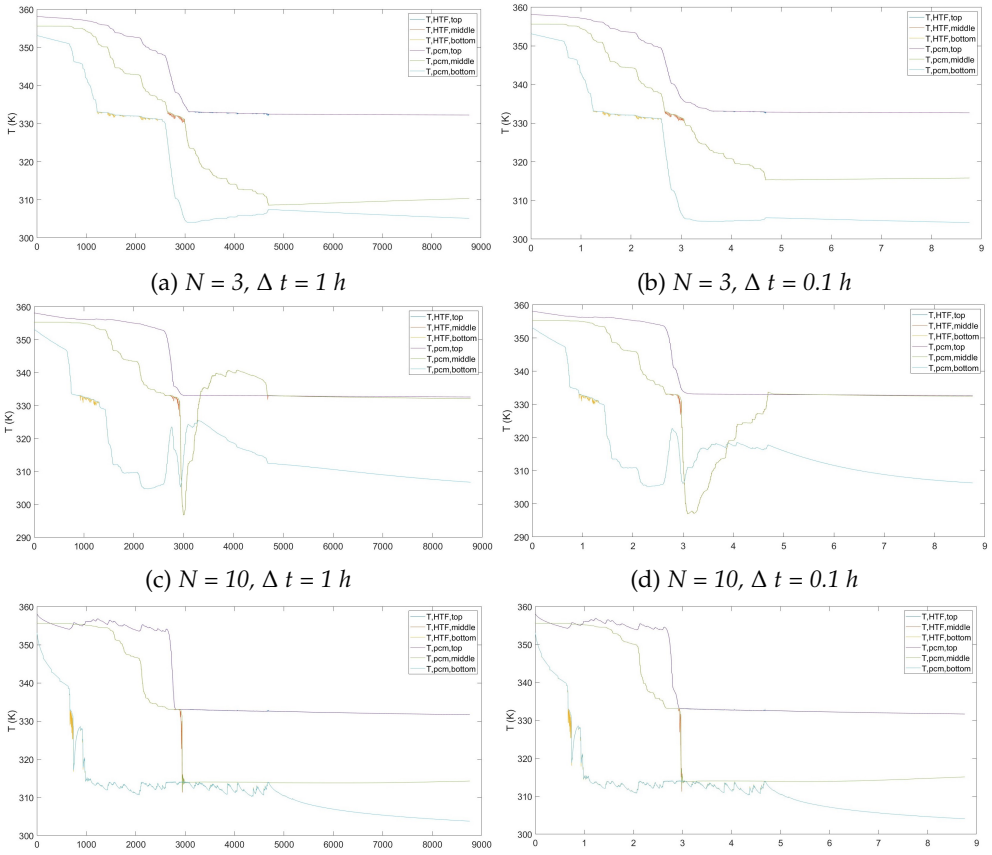

(a) $N = 3$, $\Delta\, t = 1\ h$ (b) $N = 3$, $\Delta\, t = 0.1\ h$

(c) $N = 10$, $\Delta\, t = 1\ h$ (d) $N = 10$, $\Delta\, t = 0.1\ h$

(e) $N = 100$,$\Delta\, t = 1\ h$ (f) $N = 100$, $\Delta\, t = 0.1\ h$

Figure 3.26: *Analysis of the temperature profile for the number of nodes for latent energy storage*

Table 3.18: *Analysis of the heat loss for the number of nodes for latent energy storage*

n	3	10	100	1000
Qloss (kWh)	31.84	-15.27	50.08	-

Figure 3.26 displays the temperature profile within the tank and Table 3.18 shows the heat loss for different numbers of nodes. The simulations with three nodes follow the trend that is expected. The simulations with ten nodes give a result that is not expected and not correct. The temperature of layers positioned above is lower than the temperature of layers positioned below. This is a result of too high mass flows for the size of the thermal stratification layers.
In the built-up of the base model, the assumption has been made that there is no internal mixing which was found in the literature to be applicable to hot water storage tanks. In this model, the PCM material was added.
When high mass flows occur this might cause internal mixing of layers because of turbulent flow. This internal mixing is not taken into account between layers., Within layers, the temperature is assumed uniform and internal mixing is therefore taken into account.

Section 3.4 displays the validation of the model with ten nodes and with forty nodes. For these validations, the number of nodes that could be used was higher because the mass flow in the experiments was lower and the size of the PCM materials was equal. Therefore the turbulent flow is less than in the simulations for the analysis with the size and mass flows of the tank for a winter peak demand of 200 households. With a lower turbulent mass flow, less internal mixing occurs leading to a valid model.
Sub-figure e and f in Section 3.4 show the simulations with 100 nodes. Here the model shows similar results to the simulations with three nodes. The lacking of internal mixing between layers in the model is not as relevant anymore with 100 layers because the convection between layers plays a more relevant factor when the height of the layer is decreased while the surface area of the layer stays equal.
The simulations with 1000 nodes show unstable results that are caused by too high mass flows compared to the volume of the nodes. This makes the model unstable.
The conclusion from the analysis and the validation of the LHS model is that the model is valid for any number of nodes when low mass flows are used and for a limited number of nodes when high mass flows are used because of internal mixing. For the simulations run in this research the mass flows are high because of the peak loads and therefore the results will be computed with 3 nodes and a time step of 0.1 hours.

3.4.3 Thermochemical Energy Storage Node and Timestep Analysis

First, an analysis of the time step is made for the hydration of the TCES model. The temperature profile for different time step sizes and number of nodes is shown in Figure 3.27 and the heat extraction is shown in Table 3.19. When the time step is larger than 0.001 hours the model does not give a temperature profile. This was expected because the reactor is smaller than the tanks in the other models and the mass flow is larger thus a smaller time step necessary was expected. The analysis will therefore only include a time step of 0.001. The number of nodes will vary between 3 and 100.

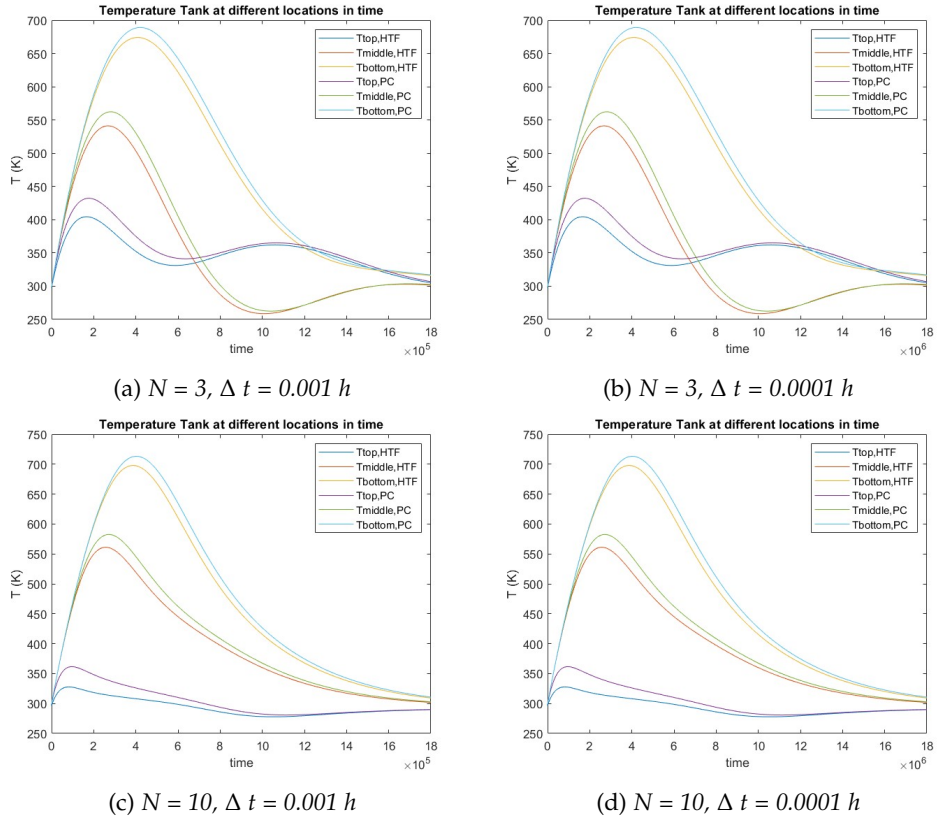

(a) $N = 3$, $\Delta\, t = 0.001\ h$

(b) $N = 3$, $\Delta\, t = 0.0001\ h$

(c) $N = 10$, $\Delta\, t = 0.001\ h$

(d) $N = 10$, $\Delta\, t = 0.0001\ h$

Figure 3.27: *Analysis of the temperature profile for the number of nodes and timestep for thermo-chemical energy storage*

From this analysis can be concluded that a smaller time step than 0.001 hours does not improve the performance of the model. The increase in nodes improves the performance of the model. In Section 3.4 the model for the reactor with 10 nodes and a time step of 0.001 hours was validated and an increase in nodes of more than 10 does not show improved performance. Therefore, the analysis of TCES concludes that the model will be used with 10 nodes and a time step of 0.001 hours.

Table 3.19: *Analysis of the heat extraction per reactor for the number of nodes and timestep for thermo-chemical energy storage*

Nodes	3		10	
Timestep (h)	0.001	0.0001	0.001	0.0001
Qout (kWh)	1.1552	1.1552	1.1923	1.1923

3.4.4 Thermal Radius

The analysis of the thermal radius will first consist by varying the temperature at the outside of the tank. Figure 3.28 shows the analysis for the thermal radius in the ground. The

temperature of the tank will be set to the maximum temperature which is 358.15 K. The thermal radius is still found to be 25 K. Then the time is set to five years and the thermal radius is calculated to be 49 m. The thermal radii calculated in the analysis are equal to or higher than in the original scenario. The heat loss will therefore not be more than calculated for a thermal radius of 25 meters. When the time is set shorter than one year the thermal radius is smaller which means a smaller part of the ground functions as an insulation layer. This could lead to more heat losses and lower performance of the tank. The model is therefore appropriate for calculations on tanks that have been in usage for at least one year.

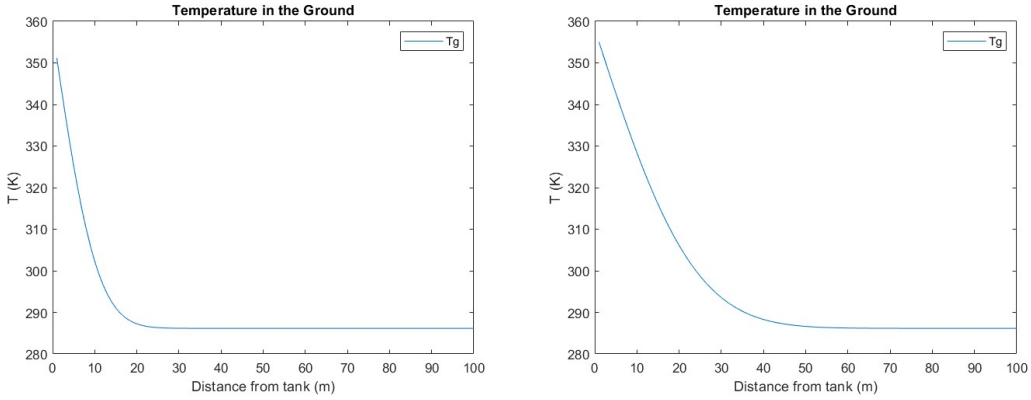

(a) *T = 358.15* (b) *Time is 5 years*

Figure 3.28: *Thermal radius of a thermal energy storage tank with insulation in the ground*

3.5 Scenarios

This section will describe the scenarios. The scenarios will consist of a base scenario in which the demand will be supplied by a gas boiler and a standard scenario where the demand will be supplied with TES. Other scenarios are created by adjusting parameters in the base scenario as is visualized in Table 3.20.
In the standard scenario, the highest and thus the charging temperature in the SHS and LHS will be 85 °C, and the lowest and thus the temperature of the water used to fill the tank during discharging will be 40 °C. A temperature of 85 °C is common in Pit storage [61]. The charging temperature is 40 °C because that is the return temperature of a DHN with houses with little insulation. Furthermore, in order to supply heat to the existing built environment, the demand temperature is at least 70 ° because the houses are not as well insulated as newly built houses. In order to make the best comparison, the starting temperature profile of the LHS is the same. For the TCES reactor, the starting temperature is room temperature.
The demand is the top 20 % of the heating demand of a DHN with 200 houses with little insulation for one year in the standard scenario. Figure 3.2 is a visualization of the demand throughout the year.
The height is equal to the radius in the standard scenario and the insulation on the side and the bottom consists of 0.0025 m polyethylene. The top insulation consists of 0.5 m air and 0.24 m polyethylene.
Lastly, in the standard scenario, the charging of the tank is only possible in summer. Furthermore, a heat pump is available to make the temperature of the water higher.

Table 3.20: *Scenarios to run simulations for sensible, latent and thermo-chemical energy storage*

Scenario	Demand	Height	In Between Charging	Maximum Temperature	Insulation	Heat Pump
1	Standard	Standard	no	Standard	Standard	yes
2	***1.5**	Standard	no	Standard	Standard	yes
3	**/4**	Standard	no	Standard	Standard	yes
4	Standard	**Low**	no	Standard	Standard	yes
5	Standard	**High**	no	Standard	Standard	yes
6	Standard	Standard	**yes**	Standard	Standard	yes
7	Standard	Standard	no	**Low**	Standard	yes
8	Standard	Standard	no	**High**	Standard	yes
9	Standard	Standard	no	Standard	**Low**	yes
10	Standard	Standard	no	Standard	**High**	yes
11	Standard	Standard	no	Standard	Standard	**no**

3.5.1 Relevance of Scenarios

In this section, the societal relevance of the scenarios will be given.
Global warming has more extreme weather events as a result[59]. While the overall temperature will increase extreme cold winter days will occur more often. The base heat supply in the DH systems will not cover these extremely cold days but the STES will. Therefore the second scenario will be an increase in load with a factor of 1.5.

Scenario 3 will analyze the volume of STES for a DHN of 50 houses instead of 200. In rural areas, fewer houses can be connected to a DHN because of lower population densities and

limitations on the lengths of DHNs because of losses. The demand from scenario one is divided by four.

In the fourth scenario, a limitation on the height of the tank will be set. This is a relevant scenario because in a lot of areas in the Netherlands, groundwater plays a role from not too deep heights in the ground making heat loss a greater factor than calculated in the model. As described in Section 3.2.1 the optimal geometry for HWTS is a vertical cylinder[19], with the height equal to the radius [26] in order to minimize losses. Xiang et all. confirm that maximizing height improves thermal stratification and reduces heat loss but also states that groundwater can enormously increase heat loss from lower parts of the thermal energy storage [70]. Therefore it is relevant to research what influence a different height diameter ratio has on the design and the losses of the thermal energy storage. The height will be half of the ratio in this scenario.

In scenario 5 the height of the storage tanks will be maximized. An increase in height will increase thermal stratification. Therefore it is relevant to research what an increase in height has as an effect on the total volume of the STES.

Heat can be delivered by geothermal or solar thermal sources which are most abundant or residual in summer leading to seasonal storage. Or heat can be delivered by factories in the form of waste heat. Waste heat is available throughout the whole year and charging the TES system could therefore also happen in between loads. In the sixth scenario, charging in between will be possible.

The seventh scenario will consist of a maximum temperature in the storage tank of 75 °. Heat losses will decrease, but the storage density will also decrease. In order to determine which parameter has the greatest effect on the volume the maximum storage temperature is decreased in scenario 7 and increased in scenario 8. In scenario 8 the maximum storage temperature is 95 °.

The thickness of insulation layers influences the amount of heat loss. When the insulation layer is made thicker, fewer losses are expected, which would lead to a decrease in the volume necessary for the storage tanks. The increase in insulation material would be more costly. In the first scenarios, the insulation layer on the sides and the bottom consist of 0.0025 m polyethylene. The top consists of a layer of 0.5 m air and 0.24 m polyethylene. in Scenario 10 the insulation layer will be made ten times thicker resulting in a layer of 0.025 m on the side and bottom and 2.4 m on the top.

The losses in the tank are partly determined by the losses through the lid. Decreasing the thickness of the lid would decrease costs and CO_2 emissions because of the production of the material. In the 10th scenario, the insulation of the lid will be half as thick and a layer of air between the water and the lid of 0.5 m will be removed.

In order to make optimal use of the energy stored in the tanks, the supply temperature to the DHN has not been taken as a minimum for the output temperature of the storage facilities. A heat pump would be necessary to reach the correct temperature of the water to deliver to the DHN. This would require electricity. However, because of the energy transition, net congestion is becoming a problem in the Netherlands. It is therefore relevant to research a scenario in which heat pumps are not available because of net congestion. In scenario 11 a calculation of the size of the storage facilities is made when the output temperature of the storage must be at least 343.15 K, which is the temperature necessary to supply heat to not well-insulated houses in the existing built environment.

3.5.2 Calculation of Results

The thermo-energetic analysis will consist of an evaluation of eleven scenarios where the models described in Chapter 3 will be used to calculate the KPI's per scenario per TES category. Table 3.21 gives an overview of the built-up of the KPIs used to evaluate the TES technologies.

The volume of the SHS and LHS will be determined by calculating the usable power with the temperature of the outlet of the tank versus the temperature of the water pumped in the tanks and the mass flow. The temperature at the outlet varies throughout the year depending on the amount of energy left in the tank and the losses. The mass flow is adjusted to deliver the power demand. This information combined with the boundary condition that the temperature of the top, middle and bottom layers are not allowed to mix, is used to determine the minimum volume of the storage facility. For TCES the energy output of the reactor is used to calculate how many reactors are needed to supply the demand. This information combined with the volume of the reactors is used to calculate the total volume necessary.

The total efficiency is calculated with the usable energy output and the total energy input. The energy output is for all TES and the gas boiler the energy demand of the DHN. The energy input for the gas boiler is the energy value of the amount of gas necessary to supply the energy demand.
The energy input for SHS and LHS consists of the energy demand, the heat losses, and the energy needed for the heat pump and the water pump.
For TCES the energy input consists of the energy necessary for dehydration, the humidifier and the air pump.

The storage losses for SHS and LHS are the conduction losses through the insulation to the ground and through the lid to the atmosphere.

The economic performance is analyzed by calculating the operational expenditure (OPEX) which are the recurring costs and the capital expenditure (CAPEX) which are the investment costs.
The OPEX of the gas boiler is calculated by the total demand multiplied by the current gas price. The CAPEX of the gas boiler is the cost price multiplied by the number of houses connected to the DHN.

For the SHS the OPEX consists of the levelized costs of the energy source for the charging of the heat storage, the operational costs of the water pump, and the operational costs of a heat pump. The levelized costs instead of the operational costs of the heat source are used because the assumption is made that the heat is bought and the heat source is not owned. The levelized costs of geothermal energy necessary to charge the thermal battery are 0.2 €per kWh [10]. The operational costs of a heat pump are dominated by the electricity price which is 0.63 €/kWh. With a COP of 3 the costs will be 0.21 /kWh for the water that has to be heated to 70 ∘C when the heat storage delivers water with a lower temperature. The operational costs of the water pump are determined by the amount of water that is pumped through the DHN, the length the water has to travel and the height difference the water has to travel. The length and the resistance of the DHN network are unknown and negligible compared to the energy necessary for the water pump to pump the water in the vertical direction of the tank. The water pump has an efficiency of 80%.
The CAPEX consists of the construction costs, the insulation, and the site facilities.

For LHS the operational costs consist of the same components as the operational costs for sensible heat storage. The difference in costs is the amount of energy necessary to charge the thermal energy storage and the electricity necessary for the heat pump and the energy necessary for the water pump.
The CAPEX consists of the construction costs, the insulation, site facilities, and the costs of the PCM material.

The operational costs for chemical heat storage consist of the costs of the heat, the electricity costs of the air pump, and the electricity costs of a humidifier.
The CAPEX consists of the material of the reactor, the potassium carbonate in the reactor, and the costs of the humidifier.

Table 3.21: *The built-up of the key performance indicators of seasonable thermal energy storage*

	Gas Boiler	**SHS**	**LHS**	**C_TES**
Volume	Boilers	Storage Tank	Storage Tank	Reactors
Total Efficiency	(Energy demand * η boiler) /Energy demand	(Energy demand + losses + heat pump + water pump) /Energy demand	(Energy demand + losses + heat pump + water pump) /Energy demand	(Heat of reaction + sensible heat + energy humidifier + air pump) /Energy demand
Storage Losses	0.01%	conduction	conduction	0%
OPEX	Gas and CO_2	Waste heat + heat pump + water pump	Waste heat + heat pump + water pump	Waste heat + humidifier + air pump
CAPEX	Boilers	Excavation, wall, bottom, cover of the tank + water pumps + heat pumps	Excavation, wall, bottom, cover of the tank + water pumps + heat pumps + PCM material	Reactor + reactant + humidifiers + air pumps

4 Results

This chapter will discuss the results of the research. The results will be presented in the sequence shown in Figure 4.1. Each section will discuss the thermo-energetic and economic performance of the system used to supply the peak load to a small-scale DHN. First, the base scenario which consists of a gas boiler will be evaluated in Section 4.1. Then the standard scenario with sensible heat storage, latent heat storage, and thermo-chemical heat storage will be evaluated in Section 4.2. Different parameters will be adjusted to create various scenarios in which the effect of differences in demand, storage location, heat source, insulation thickness, and the availability of a heat pump on the volume will be evaluated in Section 4.3. Lastly, an analysis of the costs per scenario will be presented in Section 4.4.

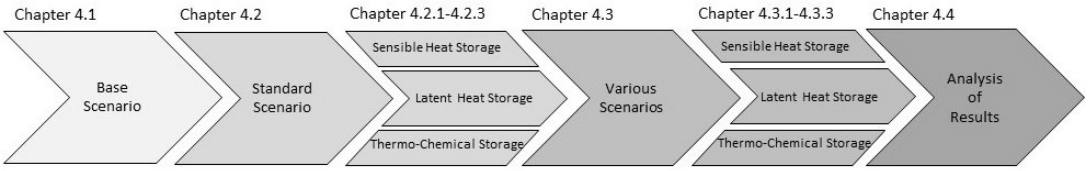

Figure 4.1: *An overview of the step-by-step approach used in this research to determine the technically and economically optimal heat storage system for peak load of a small-scale DHN.*

4.1 Base Scenario

The base scenario evaluates the current situation in which the peak load of a DHN is delivered by a gas boiler. In this situation, each household has a gas boiler in their house. The boilers need a power of at least 5.5 kW, which is the total peak load in a DHN of 1100 kW divided by 200 households. To minimize the volume and maximize the efficiency of the system, the smallest gas boiler that is suitable can be applied in this scenario.
The thermo-energetic and economic performance of the gas boiler used are provided in Table 4.1. For a total demand of 284,576 kWh of 200 households, the total investment is 440,000 €, the operational costs per year for burning gas are 74,437 €and the total volume is 18 m^3. Burning 1 m^3 gas equals an emission of 1.78 kg CO_2. To supply the load in the base scenario the CO_2 emissions are 57,608 kg. With a current CO_2 price of 100 €per tonne the total OPEX results in 80 thousand €.

Table 4.1: *Thermo-energetic and economic performance gas boiler*

	Gas Boiler
Volume (m^3)	0.08
Efficiency (%)	90
CAPEX (€)	2200
OPEX (€/kWh)	0.26

4.2 Standard Scenario

In this section, the results for the standard scenario in which heat storage will be used to supply the winter peak load in a DHN are presented. These are the results applicable for the winter peak demand of an average dutch winter where 200 households with little insulation are connected to a DH network.
A thermo-energetic and economic evaluation of sensible heat storage, latent heat storage, and thermo-chemical heat storage will be provided. The thermo-energetic evaluation will consist of a calculation of the temperature profile of the heat storage throughout the year resulting in the losses, power output, and necessary power input. The results from the thermo-energetic evaluation will result in a calculation of the total volume of the storage technology and the operational costs necessary for the power supply.

4.2.1 Sensible Heat Storage

In this section, the thermo-energetic evaluation of the design described in Section 3.2.1 will be given. The sensible heat storage will be used to supply the peak load described in Section 3.1 with the water pumped out of the top of the tank. The bottom of the tank will simultaneously be filled with the return water of the DHN with a temperature of 40 ° C. Figure 4.2 shows the power demand and the mass flow of the water supplied by the top of the storage facility.

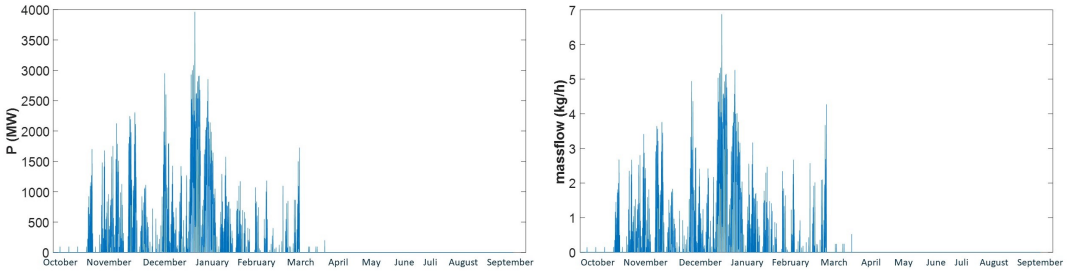

(a) *Power Demand* (b) *Massflow*

Figure 4.2: *The power output and mass flow of the sensible heat storage for peak demand of a DHN with 200 households for one year*

The storage facility is scaled in order to find a temperature profile throughout the tank where the top, bottom and middle layers do not mix in order to keep thermal stratification and

optimize the performance of the tank. Figure 4.3 displays the temperature of the different water layers in the storage tank for one year.
In Figure 4.2 it is visible that the mass flow follows the trend of the power demand but increases through time. This is explained by the decreasing temperature at the top of the tank as can be seen in Figure 4.3. When the temperature at the top of the tank decreases, more water is necessary to supply the same amount of power so the mass flow increases.

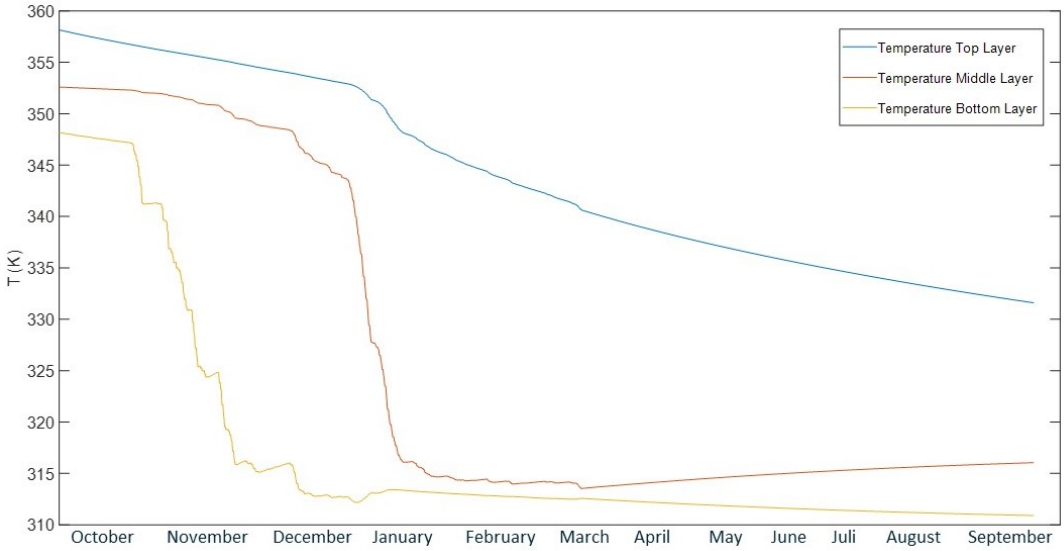

Figure 4.3: *Temperature of the bottom, middle, and top node throughout the year of the sensible heat storage tank with a standard peak load of DHN with 200 households*

In order to supply the demand for the standard scenario, the diameter of the Sensible Heat Storage tank is 28 m. The height of the tank is 14 m. This results in a volume of 8620 m^3.
The Energy stored at the start of the year is plotted next to the energy demand, the losses, and the energy left in Figure 4.4.

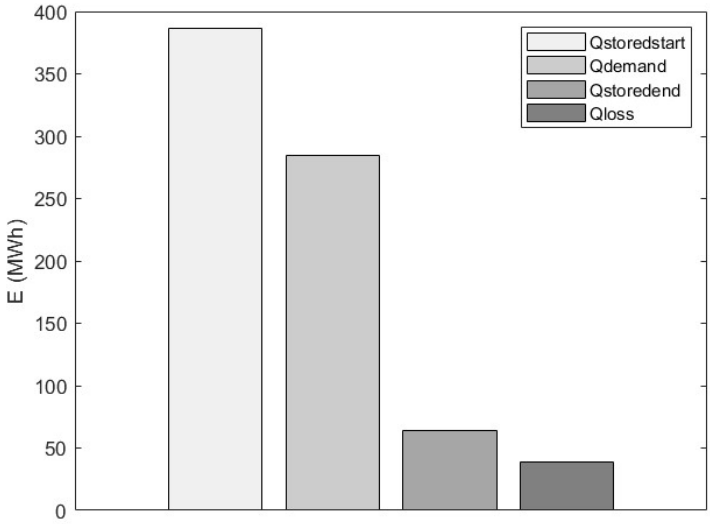

Figure 4.4: *Energy distribution of the sensible heat storage for peak demand of a DHN with 200 households for one year*

The results show that 10 % of the energy in the tank at the start of the year is left at the end of the year. Furthermore, the demand is 80 % of the total energy stored at the start and the losses are about 10 %. The losses are 38.5 kWh and the energy necessary to charge the thermal storage is 323 MWh.
To calculate the operational costs with the electricity price of 0.21 /kWh and a thermal energy price of 0.20 /kWh, the charging energy, water pump energy and energy used by the heat pump are necessary.

The operational costs for sensible heat storage consist of the levelised costs of the energy source for the charging of the heat storage, the operational costs of the water pump and the operational costs of a heat pump. The energy used by the heat pump is calculated with the energy necessary for heating up water that is discharged by the TES with a temperature below 70 °C. The energy needed to heat up the water is 2,443 kWh. To calculate the energy used by the water pump, the total mass flow and height of the tank are used. The total mass flow through the year is $2.4*10^6$ kg. The height of the tank is 14 m. The total energy necessary to pump the water with a water pump with an efficiency of 80% is 112 kWh. The total operational costs are:

OPEX = 2,443 kWh * 0.21 €/kWh + 323 MWh * 0.2 €/kWh + 112 kWh * 0.21 €/kWh
OPEX = $65 * 10^3$ €

The CAPEX consists of the construction costs, the insulation, site facilities, heat pump and water pump. The maximum power of the heat pump is 4.5 kW. This corresponds to a heat pump of 9,000 €. The maximum power needed for the water pump is 1.1 kW. The costs of a 1.5 HP water pump are equal to 500 €. The The CAPEX of the sensible heat storage is roughly 75 €/m^3 [20]. With a volume of 8620 m^3 the total CAPEX is:

CAPEX = 75 €/m^3 * 8620 m^3 +9,000€+ 500 €= 656 * 10^3 €

4.2.2 Latent Heat Storage

In this section, the thermo-energetic evaluation of the design described in Section 3.2.2 will be given for latent heat storage in the standard scenario. Figure 4.5 shows the power demand and the mass flow of the water supplied by the top of the storage facility.

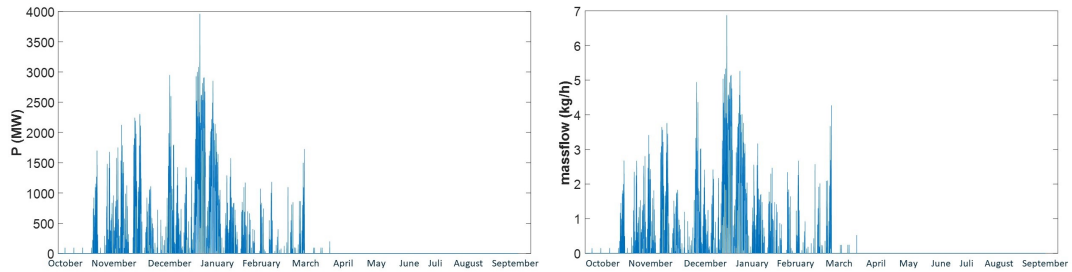

(a) *Power Demand* (b) *Massflow*

Figure 4.5: *The power output and mass flow of the latent heat storage for peak demand of a DHN with 200 households for one year*

Figure 4.6 shows the temperature profile of the HTF and the PCM in the latent storage facility. The temperature of the HTF follows the temperature of the PCM except when the PCM reaches the melting temperature. When the melting temperature is reached the HTF cools down faster than the PCM, but returns to the temperature of the PCM after some time because of the heat transfer between the two substances.

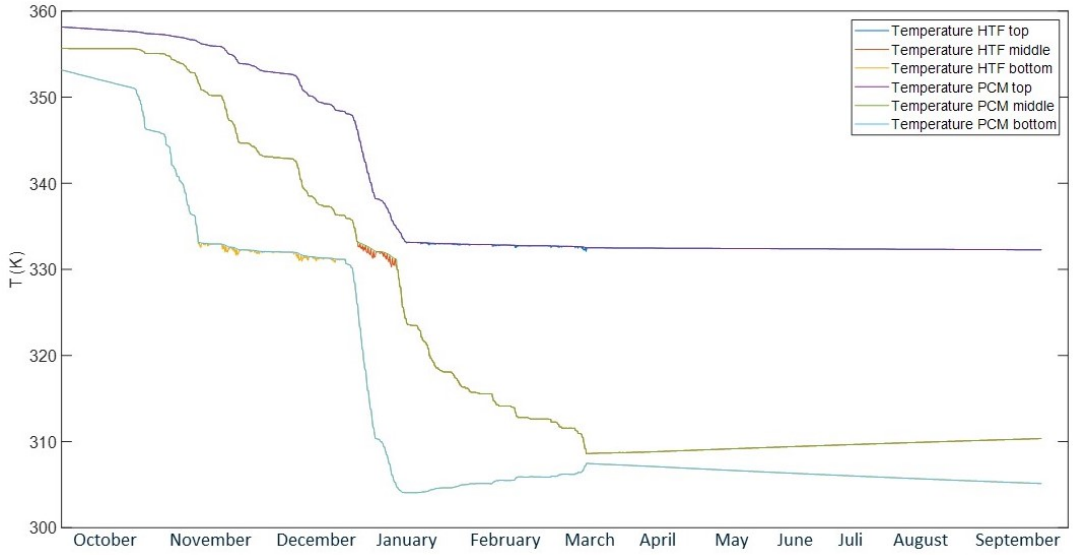

Figure 4.6: *Temperature of the HTF and PCM material of the bottom, middle, and top node throughout the year of the latent heat storage tank with a standard peak load of DHN with 200 households*

In order to supply the demand for the standard scenario without mixing layers the diameter of the Latent Heat Storage tank is 25 m. The height of the tank is 12.5 m. This results in a volume of 6135 m^3.
Figure 4.7 shows the energy distribution of the tank. The results show that 25 % of the energy in the tank at the start of the year is left at the end of the year. Furthermore, the demand is two third of the total energy stored at the start and the losses are about 10 %. The PCM material at the bottom and the middle of the tank have gone through the phase change while the top of the tank still has some latent heat stored.

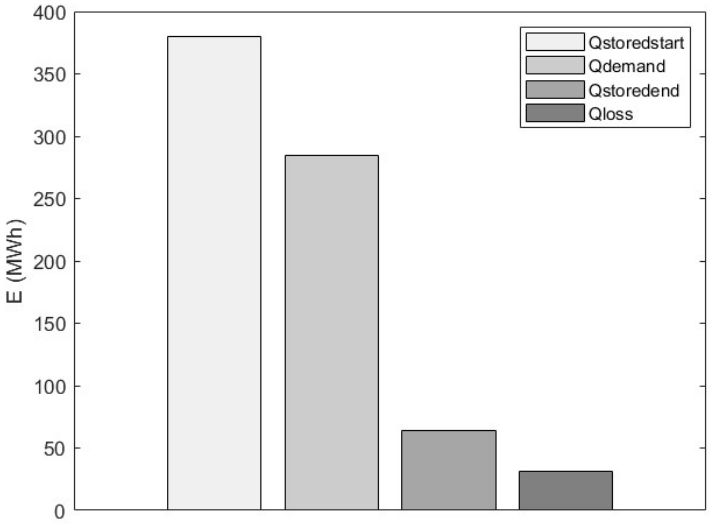

Figure 4.7: *Energy distribution of the latent heat storage for peak demand of a DHN with 200 households for one year*

The amount of energy necessary to charge the heat storage is determined by the demand which stays the same and the losses which have decreased compared to sensible heat storage. The energy necessary to charge the heat storage is 316 MWh. The power needed to heat up the water is 2,687 kWh. The energy used by the water pump is 109 kWh. The total operational costs are:

OPEX = 109 kWh * 0.21 €/kWh + 2,687 kWh * 0.21 €/kWh + 316 MWh * 0.2 €/kWh
OPEX = 63 * 10^3 €

The maximum power of the heat pump is 11.5 kW. This corresponds to three heat pumps of 9,000 €. The maximum power needed for the water pump is 1.1 kW. The costs of a 1.5 HP water pump are equal to 500 €. The CAPEX of the sensible heat storage is roughly 75 €/m^3 [20]. The costs of the paraffin is 1.80 €/kg [15]. With a total storage volume of 6135 m^3 and 3,185,000 kg paraffin used, the total CAPEX is:

CAPEX = 75 €/m^3 * 6135 m^3 + 3,185,000 kg * 1.80 €/kg +3*9,000€+ 500€= 6 * 10^6 €

4.2.3 Thermo-chemical Energy Storage

In this section, the thermo-energetic evaluation of the design described in Section 3.2.3 will be given for thermo-chemical energy storage in the standard scenario. As described in Section 3.2.3 the TTCES reactors are designed in a modular built-up. The reactors are designed to reach a maximum temperature of 617.85 K, because this corresponds to the melting temperature of potassium carbonate. The melting temperature of the glass is higher. Figure 4.8

shows the temperatures that are reached within the reactor.
Each reactor produces 1.192 kWh in half hour and has a peak power of 5.5 kW. As the heated air has to go through an air-to-water heat exchanger which has an efficiency of 90 % the Energy produced will be 1.073 kWh per reactor per half hour.

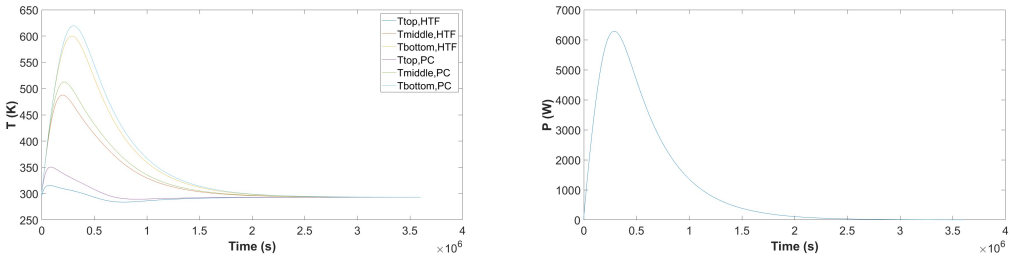

(a) *Temperature Profile HTF and PC material* (b) *Power Reactor*

Figure 4.8: *The temperature profile and the power output per reactor*

Then the number of reactors will be determined by matching the power output per reactor to the power demand which is depicted in Figure 4.9.

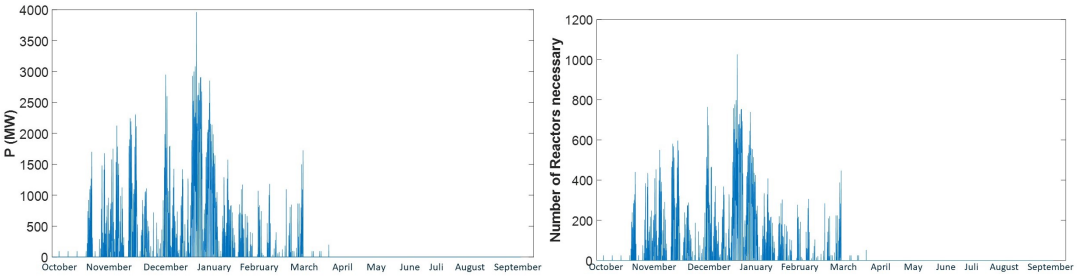

(a) *Power Demand* (b) *Number of Reactors*

Figure 4.9: *The power demand of the district heating network and the number of reactors necessary to supply the demand in the time*

In Figure 4.9 it is visible that the number of reactors necessary to supply the demand follows the power demand. The total amount of reactors necessary is 265864. With a volume of 0.0088 m^3 per reactor, this results in a total volume of 2349 m^3.
The heat supplied to the reactor is calculated with the energy necessary to heat the air to reach a full conversion for dehydration. Figure 4.10 shows the temperature profile of the heated air. The full conversion is reached after 1000 seconds and the mass flow is 0.375 m^3/s.
The total energy provided to the reactor consists of the heat of the reaction and the heating of the material.

$$E_{in} = 710,000 \frac{J}{kg} * 6kg + 6kg * 114.4 \frac{J}{molK} * 70K / 0.138205 \frac{kg}{mol}$$
$$E_{in} = 1.28 \text{ kWh}$$

The energy released by the reaction is 1.19 kWh, resulting in an efficiency of 93% for the reactor without heat exchangers.

A water-to-air heat exchanger has an efficiency of 84 %. Resulting in 1.52 kWh of waste heat necessary per reactor. The total charging energy for all reactors in the base scenario is 405 MWh.

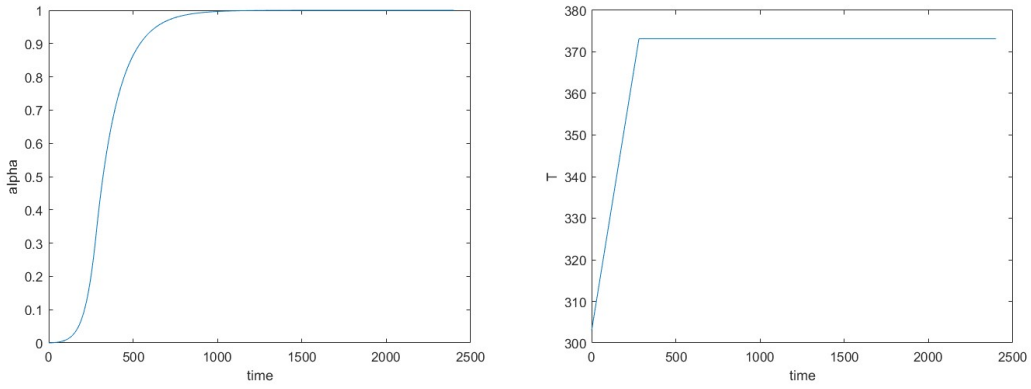

(a) *Conversion Dehydration* (b) *Temperature Air*

Figure 4.10: *The conversion and the temperature in the reactor during dehydration in the reactor*

The operational costs for chemical heat storage consist of the costs of the heat, the electricity costs of the air pump and the electricity costs of a humidifier. Per reactor, the air pump will pump 5055 kg of air through the reactor per cycle. Per reactor, this results in the usage of 0.0002 kWh of electricity. Furthermore, 180 kg of air needs to go through a humidifier. The humidifier has a mass flow of 78 kg of air per hour and a power of 1500 W. The total energy per reactor necessary for the humidifier is 3.46 kWh. Lastly, 1.52 kWh of heat is necessary per reactor for dehydration. The electricity used by the air pump can be neglected compared to the other electricity costs. The total operational costs are:

OPEX = 265864* (3.46 kWh * 0.21 €/kWh + 1.52 kWh * 0.2 €/kWh)= 68 * 10^3 €

The CAPEX consists of the material of the reactor, the potassium carbonate in the reactor and the costs of the humidifier. 2,368 humidifiers are necessary that cost 1000 €. Potassium Carbonate costs 50 €/kg and each reactor uses 6 kg. 58,728 kg of glass is necessary for the reactors. The costs of glass are 0.06 €/kg. The total CAPEX is:

CAPEX = 1000 €* 2,368 + 50 €/kg * 6kg * 65,864 + 58,728 kg * 0.06€/kg = 22 * 10^6 €

The CAPEX is dominated by the costs of the Potassium Carbonate, which corresponds to 66 % of the total investment costs. The OPEX is dominated by electricity costs.

4.2.4 Comparison Standard Scenario and Base Scenario

In this section, the results for the supply of peak demand in a DHN for 200 households with thermal heat storage will be compared to the base scenario, which is a gas boiler. Figure 4.11 shows that the volumes, charging energy, OPEX, CAPEX and heat losses for SHS, LHS and TCES with a built up of the calculations in Table 3.21. The volume, charging energy, and

CAPEX are higher for TES than for a gas boiler. The OPEX calculated with current electricity and gas prices is lower except for TCES.
Within thermal heat storage, SHS has the largest volume and the lowest costs while TCES has the smallest volume and the highest costs.

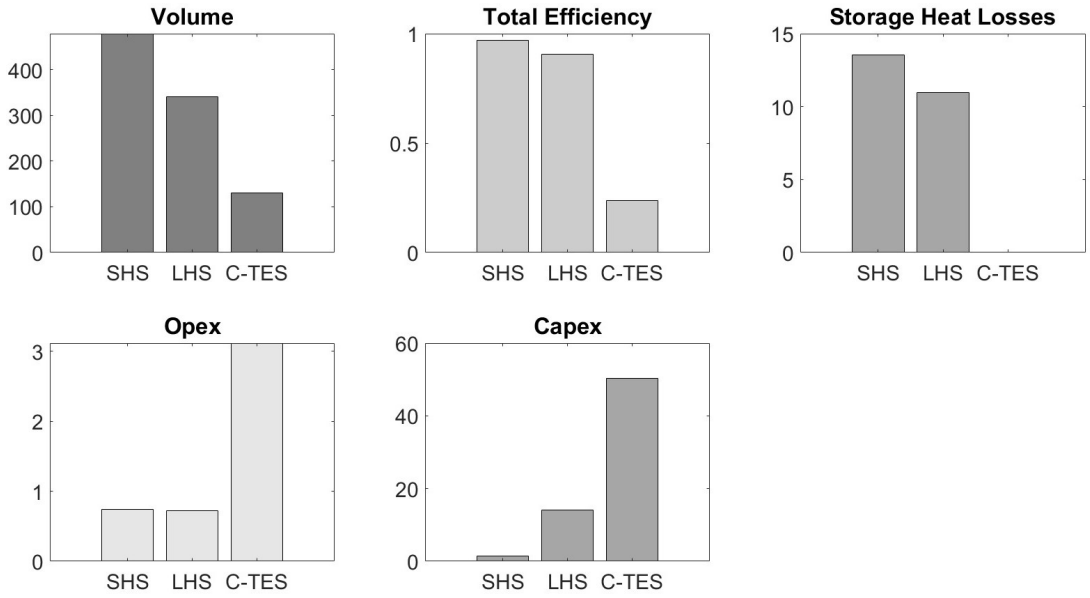

Figure 4.11: *The volume, charging energy, storage losses, OPEX and CAPEX for SHS, LHS and TCES divided by the values for a gas boiler. Lighter colors indicate more favorable ratios.*

Figure 4.12 shows that with current prices SHS will have lower total costs than the gas boiler in 15 years. LHS and TCES are not financially attractive within more than 300 years.

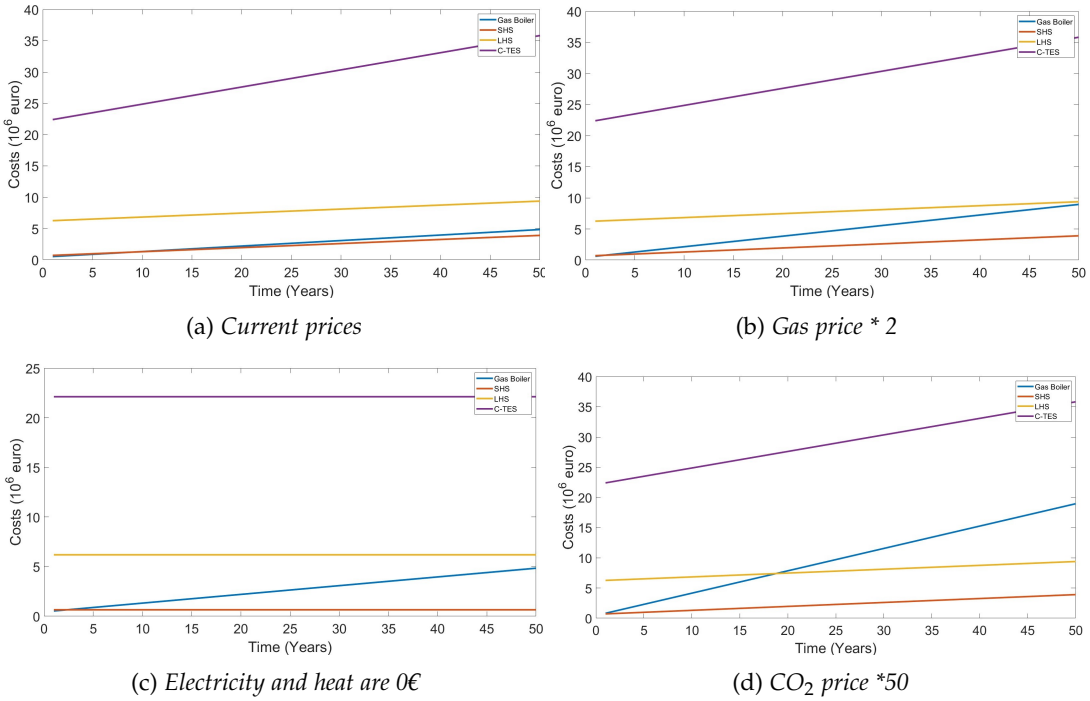

(a) *Current prices*

(b) *Gas price * 2*

(c) *Electricity and heat are 0€*

(d) *CO_2 price *50*

Figure 4.12: *Total cost of the supply of the peak demand in a DHN with 200 households with a gas boiler, SHS, LHS and TCES for a time span of 50 years*

Table 4.2 shows the number of years per TES technology necessary to have lower total costs than a gas boiler. In order for SHS and LHS to be cheaper than a gas boiler within 20 years the price of CO_2 has to be multiplied by 50. If the CO_2 price is multiplied with a factor 110, TCES will have lower total costs than a gas boiler in 50 years. If the gas price is doubled compared to the current situation SHS and LHS will financially be favorable to a gas boiler within 70 years.

Table 4.2: *Number of years necessary for the total costs of TES to be lower than a gas boiler to supply the peak demand in a DHN with 200 households*

	SHS	**LHS**	**TCES**
Current Prices	10	238	-
Gas Price *2	2	55	-
Electricity and Heat 0 €	3	66	247
CO2 price *50	1	19	226

4.3 Volume Comparison of Different Scenarios

In this section the results of the volume calculation of the scenarios described in Table 3.20 are given. First, a general overview of the results is given. Then an elaboration per scenario is given.

As visualized in Figure 4.13, in most scenarios SHS has the largest volume and TCES has the smallest volume. The energy density of the storage material is higher for TCES and the thermal losses are zero because it can be stored at room temperature.
The effect of maximizing insulation on the efficiency of TCES is negligible while the volume increase is high. This is the only scenario where TCES has a higher volume.
Furthermore, the scaling of the demand and storage temperature does not affect the ratios between the volumes of the TES technologies. Increasing storage temperature does decrease the volume of TES compared to the base scenario.
The only scenario with relatively low volumes without decreasing the demand is the scenario where interim charging is possible.

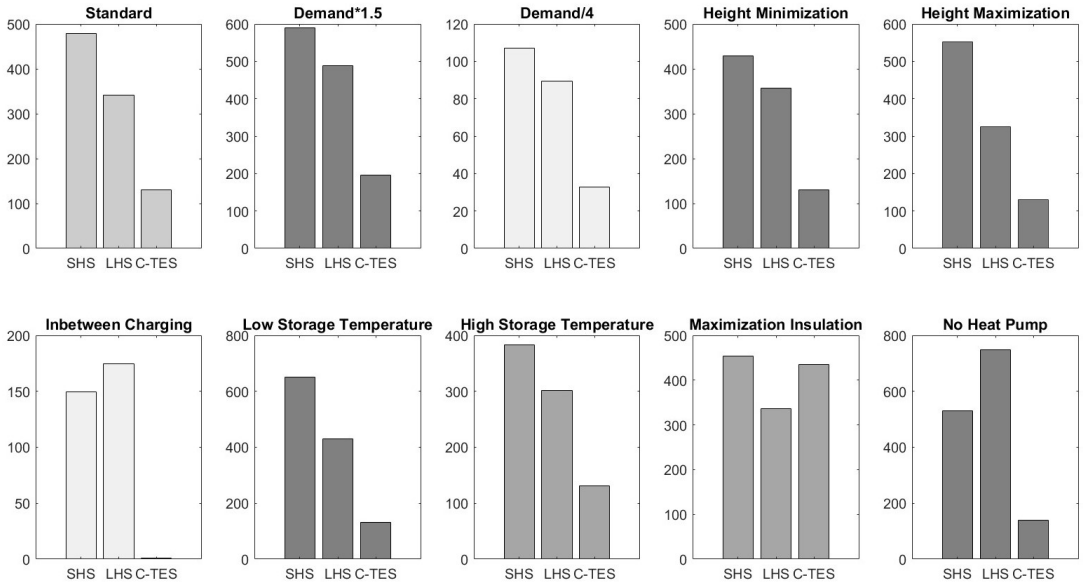

Figure 4.13: *Volume TES in different scenarios compared to the volume of the base scenario. The darker the bar chart, the higher the ratio of the volume of the TES compared to the gas boiler.*

4.3.1 Demand

The volumes of SHS and LHS increase less quickly than the increase in load. The losses for larger storage volumes are relatively smaller than for smaller volumes. For SHS and LHS the losses correspond to 9 % and the demand to 74 % of the total energy stored in the tank when the load is increased with a factor 1.5 as illustrated in Table 4.3.
Furthermore, the decrease in load leads to a relatively larger volume for SHS and LHS as expected because the losses relative to the stored energy increase for smaller volumes.
The volume of TCES scales with the same ratio as the load.

Table 4.3: *The volume increase of TES with an increase and decrease in load.*

Demand	SHS	LHS	TCES
***1.5**	1.23	1.43	1.5
/4	0.27	0.26	0.25

4.3.2 Height

The minimization of height leads to a lower volume compared to the base scenario for SHS and the maximization of height results in a lower volume for LHS compared to the base scenario as visualized in Table 4.4. The volume of TCES stays the same because the TES is built modular and can therefore be scaled to any shape without effect on the total volume.

Table 4.4: *The volume increase of TES with minimization and maximization of height.*

Height	SHS	LHS	TCES
Minimized	0.90	1.05	1
Maximized	1.15	0.95	1

The difference in heat loss determines this difference in volume. Maximizing height means minimizing losses through the lid while increasing losses on the sides of the TES and vice versa for the minimization of height. The losses in the base scenario for SHS are 38.5 MWh and the losses with a minimal height are 36.2 MWh. Figure 4.14 displays the annual heat loss per part of the tank per scenario. The losses on the side of the tank are smaller for TES with a minimized height because the side area is smaller in scenario four. The losses on the top and the bottom of the tank are bigger, but do not weigh up to the decrease in losses on the side. SHS with a maximized height has a relatively larger volume. Even though thermal stratification is increased, the losses have increased more leading to a larger volume necessary to supply the demand.

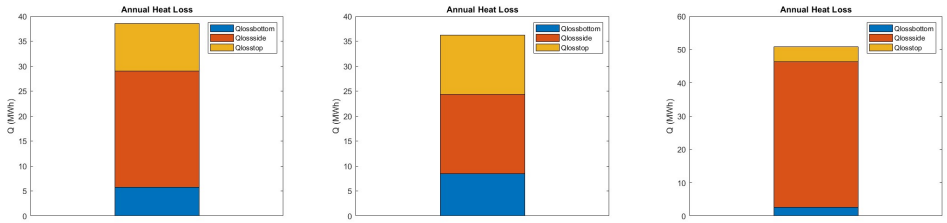

(a) *Base Scenario* (b) *Minimization of Height* (c) *Maximization of Height*

Figure 4.14: *The heat losses for sensible heat storage per area of the tank.*

For LTS the losses on the side of the tank are smaller because the thermal resistance between the PCM material and the surrounding soil is higher than the thermal resistance of the HTF to the soil. The increase in thermal stratification increases the performance of the tank. However, when the height is minimized the volume of the LHS tank is larger. The reason

for the difference in volume is the minimum height an LHS tank needs for the thermal stratification layers not to mix. The layers separately go through the phase change where they store latent heat and keep a constant temperature. The power extracted can cause such high mass flows that the temperature of the middle layer can become the same temperature of the bottom layer if the tank is not high enough. This results in a minimum height necessary for the TES to work more efficiently.

4.3.3 Interim Charging

The volumes decrease compared to the base scenario when interim charging is possible as is visualized in Table 4.5. The volume for TCES decreases most, because charging and discharging of TCES tanks can happen simultaneously because of the modular setup. For the SHS and the L-TES this is not possible because the water flow for charging is in the opposite direction from discharging in order to keep the thermal stratification. The hours that are available for charging in the winter months are scarce as is visulized in Figure 4.15. This makes it impossible for the SHS and L-TEs to make the volume as small as for TCES.

Table 4.5: *The volume decrease of thermal energy storage per category for interim charging*

	SHS	**LHS**	**TCES**
Interim Charging	0.31	0.51	0.0072

As can be seen in Figure 3.22 the dehydration happens faster than the hydration, which makes recharging within the following hour possible. The peak number of reactors necessary is 1026. In the following hour 891 reactors are used. This makes the total amount of reactors necessary 1917 resulting in a total volume of 17 m^3.

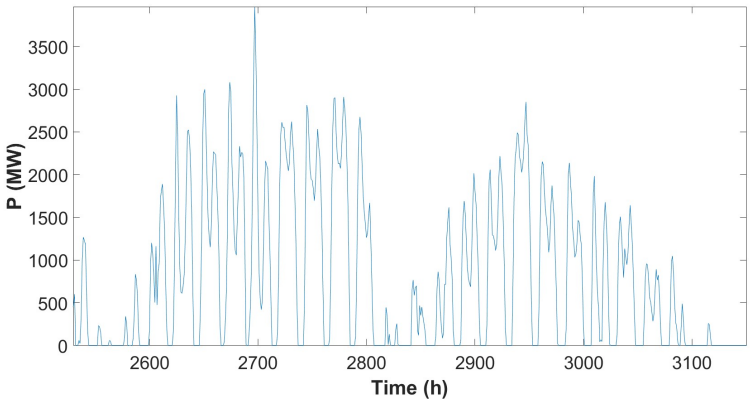

Figure 4.15: *Enlarged part of the yearly peak demand in the winter months.*

The volume of SHS decreases by two third. The temperature profile and the power removed (positive) and added to the tank (negative) are visualized in Figure 4.16.

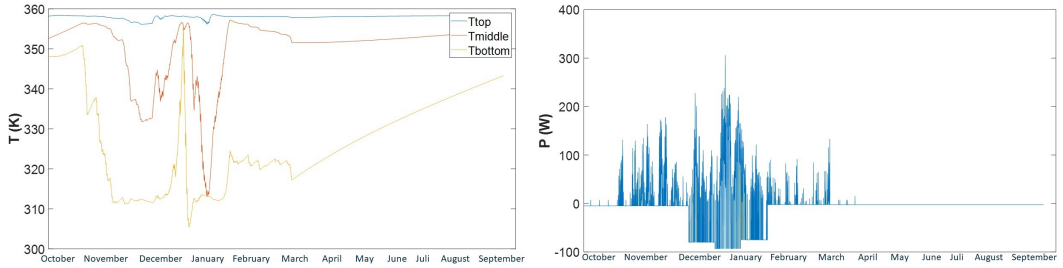

(a) *Temperature Profile* (b) *Power output*

Figure 4.16: *Temperature profile and power output for sensible heat storage with interim charging*

For LHS a smaller decrease in volume compared to SHS can be seen. The temperature profile and the power removed (positive) and added to the tank (negative) are visualized in Figure 4.17 The thermal stratification layers mix more easily in LHS than in SHS because of the PCM material which creates relatively less HTF and increases turbulence in the mass flow of the HTF. Therefore smaller charging rates are possible leading to a larger LHS volume compared to SHS.

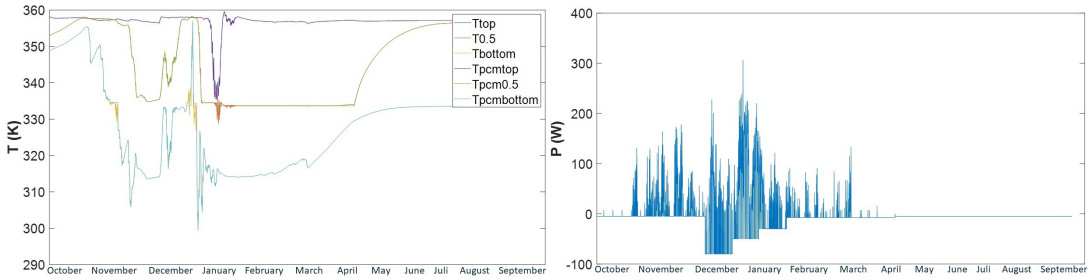

(a) *Temperature Profile* (b) *Power output*

Figure 4.17: *Temperature profile and power output for latent heat storage with interim charging*

4.3.4 Maximum Storage Temperature

Increase in maximum storage temperature increases the energy density and the losses of SHS and LHS. Losses and energy densities of TCES are not affected because the material is stored at ambient temperature. Lower maximum storage temperatures result in higher volumes and higher maximum storage temperatures result in lower volumes compared to the base scenario for SHS and LHS as is shown in Table 4.6. The energy density of the TES increases relatively more quickly than the increases in losses.

Table 4.6: *The volume increase and decrease of thermal energy storage per category with lower and higher maximum storage temperature.*

Maximum Storage Temperature	SHS	LHS	TCES
Low	1.36	1.26	1
High	0.80	0.88	1

4.3.5 Insulation

An increase in insulation thickness results in smaller volumes for SHS and LHS as is shown in Table 4.7. The increase in insulation decreases the losses resulting in a smaller storage volume. Figure 4.20 shows the ratio of the losses per area of the tank for SHS with thicker insulation. The losses for SHS with ten times thicker insulation are 77 % of the losses in the base scenario. For LHS the losses with ten times thicker insulation are 86 % of the losses in the base scenario.

Table 4.7: *The volume increase and decrease of thermal energy storage per category with lower and higher insulation thickness.*

Insualtion	**SHS**	**LHS**	**TCES**
Low	-	-	1
High	0.95	0.99	3.33

Figure 4.18 shows the temperature profile of the SHS storage and Figure 4.19 for LHS when the insulation on the top is decreased. When the height is equal to the radius of the tank, no volume can be determined where the top layer of the tank does not reach a temperature lower than the middle of the tank. This is undesirable because of the mixing of layers leads to lower performance.

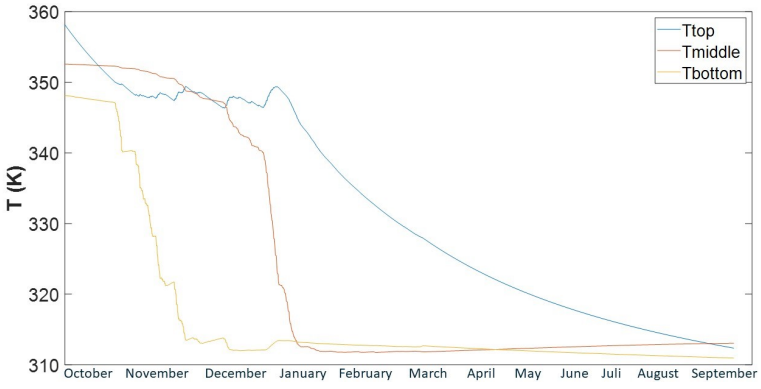

Figure 4.18: *Temperature profile of three layers in a sensible heat storage tank without top insulation*

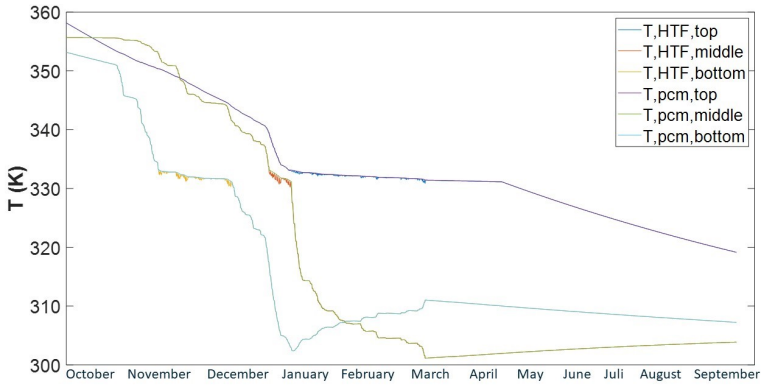

Figure 4.19: *Temperature profile of three layers in a latent heat storage tank without top insulation*

For TTCES the storage of the reactants is possible at room temperature not leading to heat loss. However, during the chemical reaction, the temperature almost reaches 700 °C leading to losses even though the reaction time is relatively short. Minimizing insulation is important for two reasons for TTCES. First, the decrease in costs when insulation material is minimized, and second the minimization of extra volume caused by the insulation layer. This extra volume is more important than the extra volume created by the insulation layers in the other categories because the insulation is necessary per reactor and since many reactors are necessary this extra volume is relatively a lot larger.

In the first scenario, the insulation layer is set to 0.001 m. The losses per reactor for the full chemical reaction are 222 $*10^3$ J. When the insulation layer is increased to 0.01 m, the losses are 22.1 J per reactor for the full chemical reaction. When the insulation is increased to 0.05 m, the losses decrease to 4.4 J per reactor. The ratio of the losses of the top, bottom and side stays the same when the insulation is increased or decreased. Figure 4.20 shows the ratio of the losses of the reactor. The top accounts for 0.01 % of the losses. The bottom accounts for 16.66 % and the side for 83.33 %. The losses at the top are minimal because there the cold air is supplied to transport the heat to the bottom and finally out of the reactor.

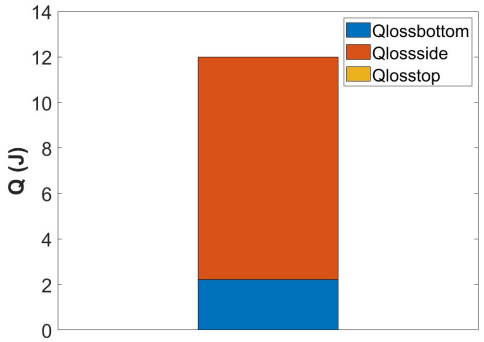

Figure 4.20: *Heat losses in a thermo-chemical reactor during hydration per area of the reactor*

The total energy released for the reactor with 0.001 m insulation is 4292.0 kJ. For the reactor

with 0.05 m insulation, the total usable energy released is 4292.1 kJ. This is a difference of 0.023 % of the total energy released per reactor. When the demand needs to be supplied with the reactors with 50 times thicker insulation layer (insulation is 0.05 m) there are 4 fewer reactors necessary for a total of 265868 reactors. The increase in insulation does not result in much higher efficiencies but the volume of the insulation compared to the volume of the reactor increases enormously. The volume per reactor has changed from 0.0088 m^3 to 0.0295 m^3. The total volume for TTCES with ten times higher insulation will result to be 7830 m^3.

When the insulation is decreased from 0.05 m to 0.01 m, the total usable energy emitted by the tank is 1.17 kWh which is equal to the energy emitted in the base scenario. Therefore the total volume of the system is equal to the volume of the base scenario.

4.3.6 Heat Pump

In this section, a calculation of the size of the storage facilities is made when the output temperature of the storage must be at least 343.15 K, which is the temperature necessary to supply heat to not well-insulated houses in the existing built environment. All TES show larger volumes compared to the base scenario as is visualized in Table 4.8. LHS shows the largest increase in volume.

Table 4.8: *The volume decrease of thermal energy storage for integration in a district heating network without a heat pump*

Heat pump	SHS	LHS	TCES
Yes	1	1	1
No	1.11	2.20	1.07

For SHS and LHS the temperature of the top layer of the tank will have to be above 343.15 K during the whole winter. The temperature profile are shown in Figure 4.21a and Figure 4.21b with the red line showing the minimum temperature necessary for the top layer.

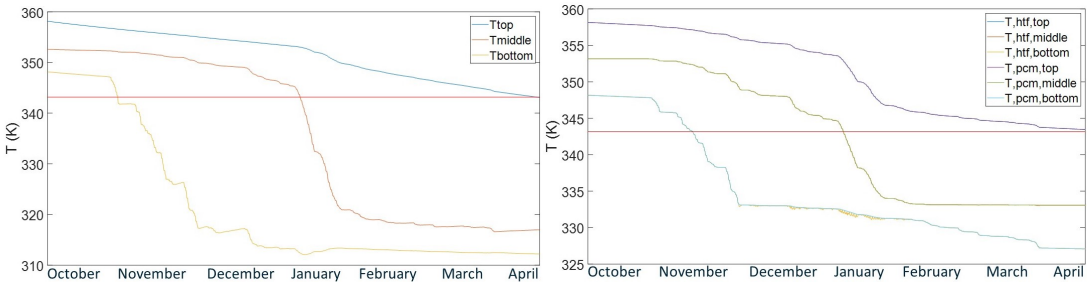

(a) *Sensible Heat Storage* (b) *Latent Heat Storage*

Figure 4.21: *Temperature profile of sensible heat storage and latent heat storage during winter for integration in a district heating network without heat pump and minimum supply temperature of 343.15 K*

The larger increase for LHS than for SHS can be explained by the relatively faster velocity of the HTF. In SHS the HTF also functions as the storage medium and the mass flows move the thermal stratification layers. In LHS only half of the storage medium consists of HTF, and the other half is the PCM material. The HTF, therefore, has a faster absolute velocity and the temperature layers will therefore mix more quickly. Figure 4.22 shows a comparison between the SHS tank and the LHS tank when the LHS tank would have the same dimensions as the SHS tank. The temperature gradient is lower for LHS caused by the higher absolute velocity of the HTF.

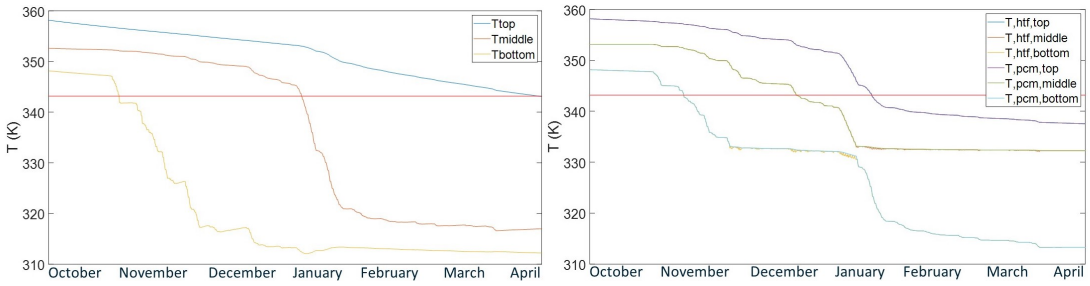

(a) *Sensible Heat Storage* (b) *Latent Heat Storage*

Figure 4.22: *Temperature profile of sensible heat storage and latent heat storage with the same power demand, volume and insulation thickness during winter for integration in a district heating network without heat pump and minimum supply temperature of 343.15 K*

For TTCES first the energy output of the reactor from scenario 1 is calculated where only the thermal energy from HTF with a temperature above 343.15 K is taken into account. This amount of energy equals 4016 kWh. Then this amount of energy is multiplied by 90% in order to account for the losses of the air-to-water heat exchanger. With this amount of energy per reactor the amount of reactors necessary is 283963. The total volume of the storage is 2509 m^3.

4.4 Cost Comparison of Different Scenarios

In this section, the results of the cost calculation of the scenarios described in Table 3.20 are given. First, a general overview of the results is given. Then an elaboration per scenario is given.
The CAPEX of SHS, LHS and TCES scales linearly with the volume. For SHS and LHS the costs per m^3 become lower when the volume increases above 100,000 m^3, which does not happen in one of the scenarios.
The OPEX for TCES depends on the amount of material that reacts which scales linearly with the volume except for the scenario with interim charging. In the scenario with interim charging the reactors and thus the reactant material is used multiple cycles in a year decreasing the volume without decreasing the OPEX.
The OPEX of SHS and LHS depend on the energy needed from the heat source to charge the TES, the electricity of the heat pump and the electricity necessary by the water pump. These factors do not scale linearly with the volume.
In Table 4.9 the OPEX of SHS, LHS and TCES are shown of the TES for all scenarios. The

OPEX for SHS is for most scenarios almost equal to the standard scenario. The biggest difference is visible for a smaller demand and thus a smaller volume. The increase in losses increases the OPEX. The Lowest OPEX can be obtained by maximizing insulation and thus minimizing losses or maximizing demand and thus storage volume which minimizes losses. For LHS the OPEX increases in all scenarios compared to the standard scenario except when the insulation is increased. The highest increase is visible when the TES is scaled down. A smaller volume corresponds to higher losses relative to the total stored energy.

Table 4.9: *The operational costs compared to the operational costs of a gas boiler for SHS, LHS, and TCES in different scenarios.*

	SHS	**LHS**	**TCES**
Standard	0.82	0.80	3.44
Demand*1.5	0.80	0.82	3.44
Demand/4	1.15	1.10	3.44
Height minimization	0.86	0.89	3.44
Height maximization	0.84	0.83	3.44
Interim charging	0.81	0.81	3.44
Low storage temperature	0.86	0.88	3.44
High storage temperature	0.84	0.88	3.44
Maximization of insulation	0.80	0.80	3.44
No heat pump	0.87	1.03	3.44

5 Discussion and Recommendations

This chapter provides an evaluation and discussion of the results. Furthermore, recommendations for further research are made.
This research can be used as a roadmap for what STES can be implemented in a DHN based on location, heat source, and available resources such as money. Furthermore, outcomes of this research indicate aspects of STES that need improvement to make the potential of the implementation of STES higher by improving efficiency or decreasing costs. Lastly, the models developed in the research can be used in specific case studies to determine the necessary volume of the STES, temperature profile throughout the year in the STES, mass flows and temperature of the supply HTF to the DHN, and the total losses of the STES, using the heat demand of the DHN and the heat supply of the source as inputs. First, an evaluation of the developed model and recommendations for future research with the model are given. Then an error discussion will be provided to discuss the accuracy of the model. Furthermore, the quantitative and qualitative effects on society of the outcomes of this research, which can be expressed in the mitigation of global warming, other environmental impacts, continuity of heat supply, safety, costs for society, and implementation will be discussed in the following sections. Lastly, outcomes of this research regarding efficiency, volume, the effect of the heat source, net congestion, and climate change on the design of STES will be discussed.

Model

The models developed in the research can be used in specific case studies to determine what STES is most suitable in that situation. The models can determine the necessary volume of the STES, temperature profile throughout the year in the STES, mass flows and temperature of the supply HTF to the DHN, and the total losses of the STES, using the heat demand of the DHN and the heat supply of the source as inputs as is depicted in Table 5.1.

Table 5.1: *The inputs and outputs of the developed model to simulate seasonable thermal energy storage integration in small-size heating networks.*

Input	**Output**
Demand profile of the DHN (including power in time and minimum supply temperature)	Volume of the seasonable thermal energy storage
Supply profile of the heat source (including power and temperature in time)	Temperature profile in the seasonable energy storage throughout the year
Shape of the storage tank	Mass flows and temperature of the supply heat transfer fluid to the district heating network
Insulation thickness and material properties	Total losses of the seasonable thermal energy storage
Heat transfer fluid	
Phase change material (for LHS)	
Reactant (for TCES)	

With the outputs of the developed models, the costs can be calculated with the method presented in Chapter 3. The maximum volume and costs of the case study can then be used to select the optimal STES to be implemented in the DHN of that specific case study.

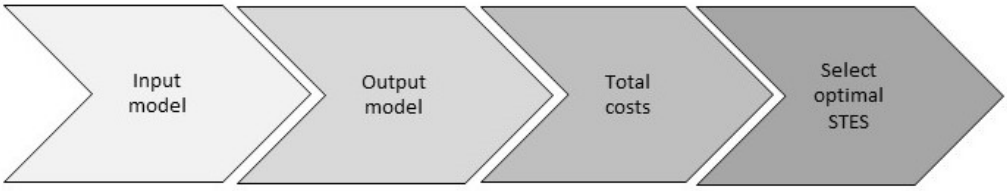

Figure 5.1: *The decision process of selecting the optimal STES using the model developed in this research.*

In this research, the model has been used to determine what STES is most suitable in a DHN with 200 households in the existing built environment with little insulation. The model can be used to determine the STES with the most potential in many other implementations. Furthermore, the model can determine the optimal design of the STES in other implementations.
Recommendations for further research are the implementation of STES in the industry. TCES reaches high temperatures that are not necessary for households connected to a DHN but that can be used for industrial applications. Furthermore, the technology has no losses which are often connected to high-temperature heat storage. The model can be used to determine the design for TCES in industrial applications by calculating the amount of mass reactant that is necessary, the losses in the reactor, and the amount of energy needed to run the reactor.

Another recommendation is to use the model to find an optimal configuration for the implementation of TCES in combination with winter peak load and a heat source available in winter. The model can design a TCES configuration to match the demand and supply during the winter. This will lead to a more compact design compared to seasonal storage, reducing investment costs.
Furthermore, the recommendation is made to use the model to design an optimal STES for houses with higher insulation. The energy label of Dutch households is increasing, meaning the supply temperature of the DHN can be reduced. Different PCMs with lower melting temperatures are suitable for this application. Parameters such as the PCM, and the demand profile of the DHN can be changed to determine the optimal STES for implementation in DHNs with houses with better insulation.
Lastly, the model can be used to determine the optimal design for locations with difficult dimensions. The optimal configuration of the storage tanks is determined in this research, but locations with different dimensions require tanks with different height/diameter ratios. In the model, these ratios can be adjusted in order to find the total energy that can be stored in tanks with other dimensions and the total heat losses throughout the year.

Error Discussion

The model is validated with experiments and the RMSE is calculated for each validation in Section 3.4. The SHS model has small RMSEs during charge and discharge resulting in an accurate model. The validation of the storage mode is more difficult because no experiments of STES in storage mode for longer than a week have been performed. The sensitivity of the error for storage mode is therefore high and can be influenced by the insulation material and thickness, the thermal properties of the ground, and the groundwater flow.
The model for LHS has higher RMSEs during charge and discharge mode compared to SHS. The model follows the ideal situation in which the material first captures all sensible heat after which it stores latent heat. In reality, this happens simultaneously. The total energy stored when the full cycle of heating and cooling is completed is equal to the experiment. However, when the cycle is performed partly multiple times in a row the calculations of the total energy stored and released can start to diverge from reality. When the PCM material heats equally throughout the material and the whole PCM capsule reaches the melting temperature simultaneously, the model is more accurate. Recommendations for improvement of the model entail more accurate modeling of the temperature profile in the PCM model and linking the local PCM temperatures to the heat storage in the model.
The TCES model has small RMSEs and shows accurate results. The drawback of the TCES model is the specific application. The reaction rate is calculated for Potassium Carbonate under ideal conditions. The reaction rate can be adjusted but needs to be calculated for different materials or different operating conditions. The necessary parameters to calculate the reaction rate and the conversion such as the activation energy are not easily available. This makes the model only applicable to a small range of TCES. More research into the calculation of the reaction rate, conversion, and heat transfer coefficient of reactants for TCES is recommended to make the model applicable to more materials.

Environmental Impact

The effect on mitigating global warming can be quantified in the reduction of CO_2 production. STES saves 57,608 kg CO_2 per year during operation delivering the peak load in a

DHN with 200 households compared to the current situation in which gas boilers are used. The CO_2 savings have been calculated with the assumption that electricity for operating TES is delivered by a sustainable energy source. If the electricity is produced with natural gas, the CO_2 production per year during operation for SHS is 1,115 kg. LHS and TCES produce 110% and 36,000% the CO_2 output of SHS. TCES would result in a seven times higher CO_2 output than a gas boiler while SHS and LHS would still produce around 2 % of the CO_2 production of a gas boiler. For the implementation of TCES, sustainable electricity sources are therefore necessary to save CO_2 production. In the current society where sustainable sources only provide around 12% of the electricity, SHS and LHS are more suitable to save CO_2 production.
The environmental impact has currently been evaluated in CO_2 emissions of the TES during operation. The CO_2 emissions during the construction of the TES, heat, and electricity sources have not been taken into account. The CO_2 emissions of the excavation necessary for the SHS are higher than for LHS and TCES. The larger volume and heat losses of SHS also have other environmental impacts such as heating of the ground and loss of biodiversity in that area. TCES does not have heat losses and does not need the insulation of the ground. The inclusion of all environmental impacts in the evaluation is necessary to make a complete comparison.

Continuity of Heat Supply

The continuity of heat supply is also an important factor in the impact on society. The current situation in which gas boilers are used has a continuous supply of heat, except when the supply of gas runs out. With a national gas network, the supply of gas has been guaranteed throughout modern history. Heat in STES in local DHN can run out and discontinuity in the heat supply can be a result. The connection of local DHNs can balance the shortcomings between networks, but shortages in case of extreme weather events will not be covered with this solution because all households will extract more heat from the STES. Therefore, an adequate design for extreme weather events has to be made using a safety factor on the design to prevent discontinuity in heat supply.
However, the combination of STES and DHN will be more vulnerable to discontinuity in heat supply compared to individual gas boilers because the breakdown of a component of STES causes the whole DHN to have a discontinuity in heat supply and the breakdown of one gas boiler causes one household to have a discontinuity in heat supply.

Safety

The implementation of STES in DHN is safe because of the centralized placement outside of the houses. Furthermore, SHS and LHS do not reach high temperatures or include hazardous substances. CTES can reach high temperatures during hydration. However, TCES is theoretically safe when not too large reactants are used to keep the maximum temperature below the melting point of the material. Experiments have to prove whether TCES is also safe in reality. Further research on the safety and the maximum amount of reactant per reactor is recommended.

Costs

With current energy prices and without taking the externalities of CO_2 production into account, SHS is financially competitive with a gas boiler regarding total costs within 15 years. The other technologies will not be competitive within 350 years. Volatile energy prices and the inclusion of externalities in the price of CO_2 production can result in LHS and TCES also becoming financially competitive with gas boilers. The OPEX of SHS and LHS is 99 % determined by the heat to charge the systems. When the heat is supplied by a sustainable source without costs, LHS would become competitive with a gas boiler regarding total costs within 80 years.
TCES has high investment and operation costs. A CO_2 price of 5 €per kg, which is equal to 50 times the current CO_2 price, would make TCES competitive with a gas boiler in total costs in 75 years.
Contradicting current cost calculations, the financial feasibility of TCES can not be ruled out. Volatile energy prices, the projected increase in CO_2 price, and subsidies can make the implementation of TCES financially attractive in the near future.

Implementation in Society

The feasibility of the implementation of STES in society depends on the location and the requirements of the DHN. In urban areas, the volume of SHS and LHS can be too large to find a suitable location. For consumers of the DHN, the heating costs can become too high compared to gas boilers when TCES is installed. Furthermore, TCES is an unknown technique for most people possibly making the innovation difficult to adopt.

The investment costs can be decreased for TCES to make implementation financially more feasible. In Section 4.2 is found that the CAPEX of TCES is dominated by the costs of Potassium Carbonate and the OPEX is dominated by the electricity costs of the humidifiers. Improving the efficiency of the humidifiers and a decrease in the price of the reactant will make the implementation of TCES financially feasible within five years as is shown in Figure 5.2. Research on the reduction of the investment costs in the reactant and the efficiency of humidifiers is therefore recommended.

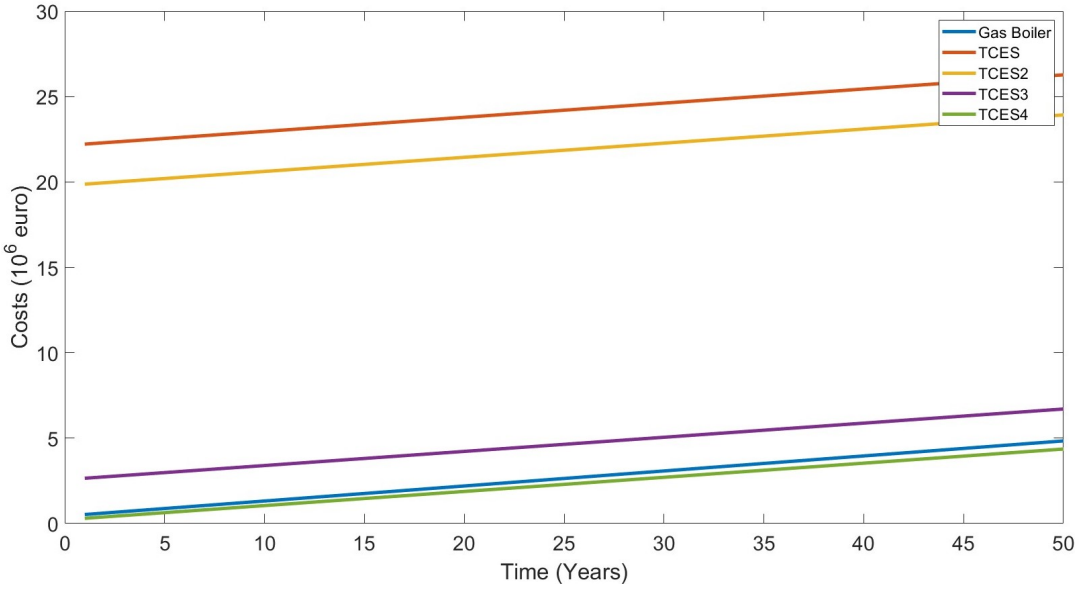

Figure 5.2: *The total costs of a gas boiler versus TCES, TCES with more efficient humidifiers(TCES2), TCES with 100 times cheaper Potassium Carbonate (TCES3) and TCES with more efficient humidifiers and 100 times cheaper Potassium Carbonate (TCES4).*

Efficiency

The total efficiencies of TES are lower than the efficiency of a gas boiler and range from 20% to 87%. TCES has the highest storage efficiency and the lowest total efficiency which is dominated by the energy usage of the humidifier. The humidifier used in this research is a standard humidifier for chemical reactions. The optimization of the humidification of the air with a sustainable source could increase the system efficiency up to 75%. Therefore, further research on the optimization of the humidifier on TCES is recommended.
The total efficiency of LHS (83%) is lower than the total efficiency of SHS (87%), while the storage efficiency is equal (90%). The energy use of the heat pump decreases efficiency for LHS because the energy stored in the phase change is delivered at a temperature below the temperature necessary in the DHN. When a material is used with a melting temperature above the minimum temperature necessary for the DHN the total efficiency of LHS can be increased. Further research into the selection of the PCM for DHN with a minimum temperature of 70 $^\circ$ is recommended to increase the system efficiency of LHS.

Volume

The volumes of TES are 100-500 times larger than the volume of gas boilers. The comparison is made between decentralized gas boilers and centralized storage facilities. Since TCES does not have storage losses, it can be used decentralized resulting in a storage volume of 12 m^3 per household. Apart from a relatively large volume compared to a gas boiler the reaction time of TCES is one hour making decentralized usage inefficient. Longer reaction times lead to delayed and therefore inefficient heating. Reaction times of SHS and LHS are very

small but decentralized usage results in smaller storage facilities which result in relatively higher losses making the system inefficient. Decentralized TES can have potential when TCES reactors are made smaller. Smaller reactors result in smaller reaction times and more flexibility in usage because they can be used separately. Further research on decentralized TCES is therefore recommended.

Heat Source

The research focuses on seasonal storage with heat sources having excess heat in summer. Heat sources with excess heat in winter, for example, waste heat, could also be used to charge TES. TCES has the most potential to be used in combination with a heat source available in winter because the reactors can be charged and discharged simultaneously because of the modular setup. Furthermore, TCES is transportable making the location of the heat source unimportant. The largest drawback of TCES is the investment cost, which can be reduced to less than 1 % when TCES is used in combination with a heat source in winter. Further research on the combination of excess heat sources in winter with TCES is therefore recommended.

Net Congestion

Net congestion, which is a result of the electrification of our society, can lead to the minimization of electrical auxiliary equipment for STES. TCES is not usable without a humidifier, which requires 70% of the electricity input. LHS can be used without a heat pump but latent heat from the PCM can not be used leading to an increase in volume. The most feasible technology in a future with net congestion is SHS where only a water pump is necessary to supply heating demand.

Climate Change

More extreme weather events, caused by climate change can lead to cold waves and higher but shorter peak heating demand. The shorter, but higher peaks in demand require TES with a short reaction time and high power output. LHS reacts instantly but can not deliver high power outputs without the mixing of thermal stratification layers. The PCM material reduces the area of the HTF which increases the absolute velocity of HTF with higher mass flows. Furthermore, the shape of the PCM material increases the likelihood of turbulent flow increasing the mixing of thermal stratification layers as well. Higher mass flows are applicable for SHS compared to LHS, but too high mass flows will also result in the mixing of thermal stratification layers. TCES can deliver high power output without consequences but the reaction time of TCES is higher. Further research on the maximum power output of SHS and LHS without mixing of thermal stratification layers with minimizing the total volume is therefore recommended.

Impact on Society

With 4% of the households in the Netherlands currently connected to a DHN, 6 PJ is needed to supply the heating peak demand per year. 304 $*10^6$ kg CO_2 can be saved by supplying

the peak load in DHN with TES. The share of DHNs and the CO_2 are expected to increase, making the implementation of STES in DHN interesting for Equans.
DHNs work most efficiently in densely populated areas. The volumes of SHS and LHS to supply peak demand of 200 households equate to 3.5 and 2.5 Olympic swimming pools. Buildings can not be placed on top of SHS and LHS tanks, but playgrounds and other building destinations without high weight such as solar panels are possible. Decreasing the diameter and thus increasing the height of the tank is possible without an enormous increase in losses, but excavation costs do increase. Further research on the integration of storage tanks in the existing built environment regarding costs, the effect on biodiversity, and sight and noise pollution is therefore recommended.

6 Conclusion

This research aims to identify the potential of seasonal thermal energy storage to deliver the winter peak load demand in a medium-sized district heating system with houses with little insulation. In this chapter, the conclusion of the study will be presented. The objective of this chapter is to answer the main research question:

- What seasonal thermal energy storage technology is most feasible to be integrated into a small-size district heating network to deliver winter peak load in the existing built environment regarding volume, CO_2 emissions and costs?

The validation of the model has proven that the models developed in this research give a good representation of SHS, LHS, and TCES. A literature review of STES and DHNs has provided the ideal characteristics of SHS, LHS, and TCES for the research conditions. With this model, the trade-off between volume, efficiency, costs, and CO_2 reduction can be made for STES integration in DHN with 200 households in the built environment. Furthermore, different scenarios, including volume or height limitations, or future energy price predictions can be used to determine the most suitable STES per situation.
Lastly, the models developed in the research can be used in specific case studies to determine the necessary volume of the STES, temperature profile throughout the year in the STES, mass flows and temperature of the supply HTF to the DHN, and the total losses of the STES, using the heat demand of the DHN, the HTF, the PCM, the reactant, the shape of the tank, the insulation thickness an material and the heat supply of the source as inputs as is depicted in Table 5.1. With the outputs of the developed models, the costs can be calculated with the method presented in Chapter 3. The maximum volume and costs of the case study can then be used to select the optimal STES to be implemented in the DHN of that specific case study.

The research indicates that SHS is most feasible to be integrated into a small-size district heating network to deliver winter peak load in the existing built environment regarding volume, CO_2 emissions, and costs.
The results show that regarding total costs SHS is competitive with a gas boiler within 10 years with current energy prices and the total volume of the TES is 8760 m^3. LHS and TCES are financially not competitive with a gas boiler within 200 years. The heat losses of the TES are lower than 10 % of the total stored energy.
LHS is technically feasible to be integrated into a DHN to deliver peak load to 200 households. The total volume of LHS is 6000 m^3, corresponding to $\frac{2}{3}$rd of the total volume of SHS. LHS has lower storage losses than SHS but a higher CAPEX and OPEX. With current energy prices, LHS is not financially attractive within 200 years.
TCES has the smallest volume, corresponding to $\frac{1}{4}$th of the volume of SHS. TCES has the highest storage efficiency but the lowest total efficiency which is dominated by the energy necessary for hydration by the humidifier. The CAPEX and OPEX are higher than the CAPEX and OPEX of a gas boiler. In the current energy market, TCES is therefore financially not feasible. However, the energy prices currently are volatile and with changes in energy prices, TCES can become competitive with a gas boiler. Compared to SHS and

LHS, TCES has the advantage of being portable, and separate reactors can be charged and discharged simultaneously, making TCES more flexible in usage. Furthermore, TCES has no storage losses. With a decrease in investment costs which are dominated by the reactant and optimization of the energy efficiency of the humidification for dehydration, TCES has the most potential to be integrated into a small-size district heating network to deliver winter peak load in the existing built environment regarding volume, CO2 emissions and costs with seasonal storage.

In order to answer the main research question the research consists of sub-research questions that will be evaluated in the following sections.

Potential of Seasonable Thermal Energy Storage Categories

From Section 2.2 can be concluded that it is not evident that one SHS, LHS or TCES is most feasible to be integrated into a DH network to deliver winter peak load in the existing built environment regarding volume and costs.

From SHS the most feasible technology to be integrated into a DH network to deliver winter peak load in the existing built environment regarding volume is the hot water storage in the ground because water has high specific heat, density, and thermal conductivity and is not toxic or costly.
From LHS the most feasible PCM is Paraffin because it is safe, reliable, predictable, cheap, and non-corrosive and they have a temperature range between 60 °C and 100 °C which is suitable for DH networks in the built environment.
For TCES the most feasible reactant is Potassium Carbonate because of the low cost of the material, its availability, high capacity for water uptake, and energy storage density. It is also more chemically stable than other salt hydrates, it has low corrosiveness and it is not toxic. The dehydration temperature is below 100 °C making it safe to use in the built environment.

Most Important Characteristics

In order to create a model of the three technologies selected from the three STES categories, the most important characteristics of the STES have been determined in Section 2.2.

For sensible heat storage using water, the most important characteristic of the storage mechanism is thermal stratification caused by buoyancy forces. Thermal stratification ensures optimal performance of the storage technology because heat losses to the environment are minimized and optimal power output can be achieved by extracting the water with the highest temperature at the top. Furthermore discharging with cold water as inflow does not affect the temperature of the water at the top of the tank. Lastly, the maximum storage and thus the charging temperature determines the maximum energy density and is therefore also an important characteristic of the SHS.
Other important characteristics are the height/diameter ratio to optimize thermal stratification and minimize heat losses to the environment. Mass flow is important to optimize power output without causing the mixing of layers. Lastly, insulation is important to minimize heat losses to the environment.
For latent heat storage, the same characteristics are important in the design as for SHS. Furthermore, the characteristics of the PCM material are important. The diameter of the

PCM material is important to minimize thermal resistance between the HTF and the PCM material. Furthermore, the ratio of the HTF and the PCM is important to maximize energy capacity and heat transfer between the PCM material and the HTF.
For the TCES model thermal stratification does not play a role. For TCES the height/diameter ratio and the total volume of the reactor are important to maximize the reaction kinetics. The mass flow of the HTF is important to optimize reaction kinetics and heat transfer through the tank. Furthermore, the melting temperature of the reactants is important in order to determine the maximum temperature the reactor can reach. Lastly, the water vapor pressure is important to optimize reaction kinetics.

Optimal Design per Seasonable Thermal Energy Storage Category

The optimal design is determined by the most important characteristics of STES technologies inSection 3.2. For SHS the optimal design is a hot water storage in the ground with a height equal to the radius, an insulation layer of 0.0025 m on the side, and 0.24 m on top with 0.5 m air between the water and the lid. The insulation material is polyethylene and the maximum storage temperature is 85 °C.
For LHS the optimal design is also storage in the ground with a height equal to the radius, an insulation layer of 0.0025 m on the side, and 0.24 m on top with 0.5 m air between the water and the lid. The PCM material Paraffin is chosen with a ratio of 0.5 to the HTF. The diameter of the PCM material is 0.05 m.
For TCES the reactor has a cylindrical shape with a height of 0.5 m and a diameter of 0.15 m. The mass of the potassium carbonate is 6 kg and the mass flow is 0.05 kg/s. The insulation of the reactor is glass with a thickness of 0.01 m.

The Volumes and Costs of TES to Deliver Peak Load in a DHN with 200 Households

The volumes and costs of TES to deliver peak load in a DHN with 200 households are determined in Section 4.2 using the optimal design per STES category. SHS has the largest volume in comparison to a gas boiler and TCES has the smallest volume. All volumes are at least a hundred times bigger than the volume of the gas boilers.
The investment costs are highest for TCES and lowest for SHS. All investment costs are higher than the investment costs for gas boilers. The operating costs with current gas, CO_2, and electricity prices are lower for all TES technologies than for a gas boiler. The operating costs for TCES are the highest and LHS has the lowest operating costs.
With current prices, the total costs for SHS would be lower than for gas boilers within 15 years. LHS and TCES would not cost less within 100 years. If gas prices double compared to current prices or electricity and heat are generated without costs from a sustainable source, the total costs for SHS and LHS would be lower than for gas boilers within 80 years. If taxes on CO_2 emissions would rise or CO_2 rights would come scarce and the price for CO_2 would rise from 0.1 to 5 €per kg the total costs of all three TES technologies would be lower than for gas boilers within 75 years.

The Influence of different Design Parameters on the Total Volume of Storage Technologies

The results of the influence of different design parameters on the total volume of TES in Section 4.3 indicate lower volumes for SHS and LHS for larger storage volumes. The volume of TCES scales with the demand.
Lower demand results in higher storage volumes relative to the base scenario for SHS and LHS.
From scaling the demand in Section 4.3.1 can be concluded that a decrease in the size of DHN decreases total efficiency and relatively larger volumes are necessary for SHS and LHS.
The results from scaling the height/diameter ratio in Section 4.3.2 suggest higher storage efficiencies for decreasing the height/diameter ratio for SHS when the lid has a sufficient amount of insulation. For LHS maximizing the height/diameter ratio results in higher storage efficiencies and thus relatively smaller storage volumes.
The smallest volumes for TES have been found when interim charging is possible in Section 4.3.3. TCES decreases most in volume and LHS decreases least in volume.
The results from scaling the maximum storage temperature in Section 4.3.4 suggest that a maximum temperature of 95 °C results in the lowest storage volumes for SHS and LHS. The maximum storage temperature does not affect the storage efficiency or volume of TCES.
From Section 4.3.5 can be concluded that thicker insulation results in smaller storage volumes with higher storage efficiency for SHS and LHS. The insulation thickness does not affect the storage efficiency or volume of TCES.
The results in Section 4.3.6 show a significant increase in volume for SHS and LHS when no heat pump is available. The volume of TCES shows a small increase.

The Influence of different Design Parameters on the Total Costs of Storage Technologies

In Section 4.4 the results indicate that the investment costs of TES scale with the volume of STES. The operational costs of TCES scale with the demand.
The operating costs for SHS are lower for higher storage volumes and thicker insulation. Operating costs for SHS are higher for smaller storage volumes, a lower height/diameter ratio, lower storage temperatures, and storage without a heat pump.
The operating costs of LHS are optimal in the standard scenario or when insulation is increased. The operating costs increase for smaller demands, a lower height/diameter ratio, lower and higher storage temperatures and storage without a heat pump.

Bibliography

[1] Ar5 climate change 2013: The physical science basis — ipcc.

[2] Ar5 climate change 2014: The physical science basis — ipcc.

[3] (2016). The paris agreement.

[4] (2019). *het klimaatakkoord*.

[5] (2022). Welke sectoren stoten broeikasgassen uit?

[6] (2023). Humidifier p-series p-series.

[7] Abbassi, Y., Baniasadi, E., and Ahmadikia, H. (2022). Transient energy storage in phase change materials, development and simulation of a new trnsys component. *Journal of Building Engineering*, 50:104188.

[8] Abedin, A. H. and Rosen, M. A. (2012). Closed and open thermochemical energy storage: Energy- and exergy-based comparisons. *Energy*, 41:83–92.

[AG and KG] AG, F. and KG, C. vacuum generator vn-10-l-t3-pq2-vq2-ro1.

[10] Akker, J. H. A. V. D. (2017). Overview of costs of sustainable energy technologies energy production: on-grid, mini-grid and off-grid power generation and supply and heat applications.

[11] Angerer, M., Becker, M., Härzschel, S., Kröper, K., Gleis, S., Vandersickel, A., and Spliethoff, H. (2018). Design of a mw-scale thermo-chemical energy storage reactor. *Energy Reports*, 4:507–519.

[12] Bai, Y., Wang, Z., Fan, J., Yang, M., Li, X., Chen, L., Yuan, G., and Yang, J. (2020). Numerical and experimental study of an underground water pit for seasonal heat storage. *Renewable Energy*, 150:487–508.

[13] Basciotti, D. and Pol, O. (2011). A theoretical study of the impact of using small scale thermo chemical storage units in district heating networks. *iea-shc.org*.

[14] Bastida, H., Ugalde-Loo, C. E., Abeysekera, M., Qadrdan, M., Wu, J., and Jenkins, N. (2019). Dynamic modelling and control of thermal energy storage. *Energy Procedia*, 158:2890–2895.

[15] Bland, A., Khzouz, M., Statheros, T., and Gkanas, E. (2017). buildings pcms for residential building applications: A short review focused on disadvantages and proposals for future development. *Buildings*, 7:78.

[16] Carslaw, H. S. and Jaeger, J. C. (1947). Conduction of heat in solids. *Conduction of heat in solids*.

[17] Chu, J. (2014). Evaluation of a dual tank indirect solar-assisted heat pump system for a high performance house.

[Dahash et al.] Dahash, A., Janetti, M. B., and Ochs, F. Numerical analysis and evaluation of large-scale hot water tanks and pits in district heating systems.

[19] Dahash, A., Ochs, F., Janetti, M. B., and Streicher, W. (2019). Advances in seasonal thermal energy storage for solar district heating applications: A critical review on large-scale hot-water tank and pit thermal energy storage systems. *Applied Energy*, 239:296–315.

[20] Dahash, A., Ochs, F., and Tosatto, A. (2021). Techno-economic and exergy analysis of tank and pit thermal energy storage for renewables district heating systems.

[21] Dalenbäck, J.-O. and Mangold, D. (2007). Prospects for large-scale solar heating systems in europe. In *3rd European Solar Thermal Energy Conference*, page 243.

[22] Demirel, Y. (2012). *Energy: production, conversion, storage, conservation, and coupling*. Springer Science & Business Media.

[23] Desai, F., Prasad, J. S., Muthukumar, P., and Rahman, M. M. (2021). Thermochemical energy storage system for cooling and process heating applications: A review. *Energy Conversion and Management*, 229:113617.

[24] Dijkstra, H., Dinkelman, D., Hanegraaf, M., Veldkamp, H., and Wees, J.-D. V. (2020). Duurzaamheid van geothermie in warmtenetten.

[25] Dincer, I. (2002). On thermal energy storage systems and applications in buildings. *Energy and Buildings*, 34:377–388.

[26] Dincer, I. and Rosen, M. (2002). Thermal energy storage: systems and applications.

[27] Enescu, D., Chicco, G., Porumb, R., Energies, G. S., and undefined 2020 (2020). Thermal energy storage for grid applications: Current status and emerging trends. *mdpi.com*, 13.

[28] Fabrizio, E. and Monetti, V. (2015). Methodologies and advancements in the calibration of building energy models. *Energies 2015, Vol. 8, Pages 2548-2574*, 8:2548–2574.

[29] Faninger, G. (2000). Combined solar–biomass district heating in austria. *Solar Energy*, 69:425–435.

[30] Gaeini, M., Shaik, S., and Rindt, C. (2019). Characterization of potassium carbonate salt hydrate for thermochemical energy storage in buildings. *Energy and Buildings*, 196:178–193.

[31] Georgious, R., Refaat, R., Garcia, J., and Daoud, A. A. (2021). Review on energy storage systems in microgrids. *Electronics*, 10(17):2134.

[32] Geyer, P., Buchholz, M., Buchholz, R., and Provost, M. (2017). Hybrid thermo-chemical district networks – principles and technology. *Applied Energy*, 186:480–491.

[GmbH] GmbH, h. Lucht-water-warmtewisselaar.

[34] Guelpa, E. (2021). Impact of thermal masses on the peak load in district heating systems. *Energy*, 214:118849.

[35] Guelpa, E. and Verda, V. (2019). Thermal energy storage in district heating and cooling systems: A review. *Applied Energy*, 252:113474.

[36] Gustafsson, J., Delsing, J., and van Deventer, J. (2010). Improved district heating substation efficiency with a new control strategy. *Applied Energy*, 87:1996–2004.

[37] Haller, M. Y., Cruickshank, C. A., Streicher, W., Harrison, S. J., Andersen, E., and Furbo, S. (2009). Methods to determine stratification efficiency of thermal energy storage processes – review and theoretical comparison. *Solar Energy*, 83:1847–1860.

[38] IEA (2022). Tracking sdg7: The energy progress report. *International Energy Agency*, 135.

[39] Kalaiselvam, S. and Parameshwaran, R. (2014). Thermochemical energy storage. *Thermal Energy Storage Technologies for Sustainability*, pages 127–144.

[40] Liu, W., Klip, D., Zappa, W., Jelles, S., Kramer, G. J., and van den Broek, M. (2019). The marginal-cost pricing for a competitive wholesale district heating market: A case study in the netherlands. *Energy*, 189:116367.

[41] Lund, H., Möller, B., Mathiesen, B. V., and Dyrelund, A. (2010). The role of district heating in future renewable energy systems. *Energy*, 35:1381–1390.

[42] Lunghi, P. and Burzacca, R. (2004). Energy recovery from industrial waste of a confectionery plant by means of bigfc plant. *Energy*, 29:2601–2617.

[43] Ma, Z., Knotzer, A., Billanes, J. D., and Jørgensen, B. N. (2020). A literature review of energy flexibility in district heating with a survey of the stakeholders' participation. *Renewable and Sustainable Energy Reviews*, 123:109750.

[44] Mette, B., Kerskes, H., and Drück, H. (2011). Process and reactor design for thermochemical energy stores. *30th ISES Biennial Solar World Congress 2011, SWC 2011*, 6:4846–4857.

[45] Nallusamy, N., Sampath, S., and Velraj, R. (2007). Experimental investigation on a combined sensible and latent heat storage system integrated with constant/varying (solar) heat sources. *Renewable Energy*, 32:1206–1227.

[46] Nelson, J. E., Balakrishnan, A. R., and Murthy, S. S. (1999). Parametric studies on thermally stratified chilled water storage systems. *Applied Thermal Engineering*, 19:89–115.

[47] Newton, B. (1995). Modeling of solar storage tanks.

[48] Novo, A. V., Bayon, J. R., Castro-Fresno, D., and Rodriguez-Hernandez, J. (2010). Review of seasonal heat storage in large basins: Water tanks and gravel–water pits. *Applied Energy*, 87:390–397.

[49] N'Tsoukpoe, K. E., Liu, H., Pierrès, N. L., and Luo, L. (2009). A review on long-term sorption solar energy storage. *Renewable and Sustainable Energy Reviews*, 13:2385–2396.

[50] Outlook, S. A. E. (2015). World energy outlook special report. *International Energy Agency*, 135.

[51] Panthalookaran, V., El-Amin, M. F., Heidemann, W., and Müller-Steinhagen, H. (2008). Calibrated models for simulation of stratified hot water heat stores. *International Journal of Energy Research*, 32:661–676.

[52] Raccanello, J., Rech, S., and Lazzaretto, A. (2019). Simplified dynamic modeling of single-tank thermal energy storage systems. *Energy*, 182:1154–1172.

[53] Recktenwald, G. W. (2004). Finite-difference approximations to the heat equation. *Mechanical Engineering*, 10(01).

[54] Remmelts, J., Tensen, S., and Ferreira, C. I. (2021). Seasonal thermal energy storage for large scale district heating. *Proceedings of the 13th IEA Heat Pump Conference (HPC2020)*.

[55] Rezaie, B. and Rosen, M. A. (2012). District heating and cooling: Review of technology and potential enhancements. *Applied Energy*, 93:2–10.

[56] Rosen, M. A., Le, M. N., and Dincer, I. (2005). Efficiency analysis of a cogeneration and district energy system. *Applied Thermal Engineering*, 25:147–159.

[57] Sarbu, I. and Sebarchievici, C. (2018). A comprehensive review of thermal energy storage. *Sustainability 2018, Vol. 10, Page 191*, 10:191.

[58] Sayegh, M. A., Jadwiszczak, P., Axcell, B. P., Niemierka, E., Bryś, K., and Jouhara, H. (2018). Heat pump placement, connection and operational modes in european district heating. *Energy and Buildings*, 166:122–144.

[59] Schleussner, C.-F., Lissner, T., Fischer, E., Wohland, J., Perrette, M., Golly, A., Rogelj, J., Childers, K., Schewe, J., Frieler, K., Mengel, M., Hare, B., and Schaeffer, M. (2015). Differential climate impacts for policy-relevant limits to global warming: The case of 1.5 c and 2 c. *Earth System Dynamics Discussions*, 6:2447–2505.

[60] Sharma, A., Tyagi, V. V., Chen, C. R., and Buddhi, D. (2009). Review on thermal energy storage with phase change materials and applications. *Renewable and Sustainable Energy Reviews*, 13:318–345.

[61] Sifnaios, I., Gauthier, G., Trier, D., Fan, J., and Jensen, A. R. (2023). Dronninglund water pit thermal energy storage dataset. *Solar Energy*, 251:68–76.

[62] Sinclair, C. and Unkaya, G. (2020). Potential sources of waste heat for heat networks in scotland.

[63] Sun, B., Liu, Z., Ji, X., Gao, L., and Che, D. (2022). Thermal energy storage characteristics of packed bed encapsulating spherical capsules with composite phase change materials. *Applied Thermal Engineering*, 201:117659.

[64] Teräsvirta, A., Syri, S., and Hiltunen, P. (2020). Small nuclear reactor—nordic district heating case study. *Energies 2020, Vol. 13, Page 3782*, 13:3782.

[65] Ucar, A. and Inalli, M. (2008). Thermal and economic comparisons of solar heating systems with seasonal storage used in building heating. *Renewable Energy*, 33:2532–2539.

[66] Unrau, C. (2017). Numerical investigation of one-dimensional storage tank models and the development of analytical modelling techniques.

[67] van Egmond, R. J. (2020). Warmtenetten topsector energie.

[68] Weber, R. and Dorer, V. (2008). Long-term heat storage with naoh. *Vacuum*, 82:708–716.

[69] Wetterlund, E. and Söderström, M. (2010). Biomass gasification in district heating systems – the effect of economic energy policies. *Applied Energy*, 87:2914–2922.

[70] Xiang, Y., Xie, Z., Furbo, S., Wang, D., Gao, M., and Fan, J. (2022). A comprehensive review on pit thermal energy storage: Technical elements, numerical approaches and recent applications. *Journal of Energy Storage*, 55.

[71] Yang, T., Liu, W., Kramer, G. J., and Sun, Q. (2021). Seasonal thermal energy storage: A techno-economic literature review. *Renewable and Sustainable Energy Reviews*, 139:110732.

Colophon

This document was typeset using LaTeX, using the KOMA-Script class `scrbook`. The main font is Palatino.